

**FOR
REFERENCE ONLY**

Cross Layer Ultrasound Video Streaming over Mobile WiMAX and HSUPA Networks

Ali Alinejad

A THESIS SUBMITTED IN PARTIAL FULFILLMENT OF
THE REQUIREMENTS OF KINGSTON UNIVERSITY
FOR THE DEGREE OF DOCTOR OF PHILOSOPHY

Faculty of Science, Engineering and Computing
Kingston University, London



MAY 2012

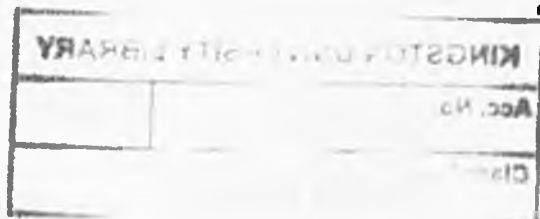


Cross Layer Ultrasound Video Streaming over Mobile WiMAX and HSUPA Networks

Ali Alinejad

PhD

2012



Acknowledgement

First I would like to express my sincere appreciation and gratitude to my supervisors, Professor Robert S. H. Istepanian and Dr. Nada Philip. Their continuous guidance, encouragement, and support have been truly remarkable throughout the duration of my studies. They provided invaluable support in every aspect of my research.

I would also like to thank the Faculty of Science, Engineering and Computing, Kingston University, London for providing me with this opportunity to fulfil this research. My thanks go to the Faculty staff and IT staff for helping me in all the thesis requirements.

I would like to express my thanks to Professor N. Amso from Cardiff University Medical School for his medical advice and for providing the relevant medical images and ultrasound video data.

I am also grateful to Vodafone R&D UK, Mr. Nigel Jefferies, and Rinicom Ltd UK for their equipment support to this work.

This thesis could not have been accomplished without the love, support and patient of my family, my parents, my parents-in-law, my lovely wife Nazli, and my gorgeous little princess Nika. Thanks for their support, their understanding and endless love, through the duration of this work. I love them.

Last, but certainly not least, I would like to thank all my friends who have generously and unconditionally supported me with their love.

Abstract

It is well known that the evolution of 4G-based mobile multimedia network systems will contribute significantly to future m-health applications that require high bandwidth and fast data rates. Central to the success of such emerging applications is the compatibility of broadband networks such as mobile WiMAX (IEEE 802.16e) and HSUPA, and especially their rate adaption issues combined with the acceptable real time medical quality of service requirements.

The design of effective broadband mobile healthcare systems using emerging WiMAX and HSxPA networks is important from the medical perspective especially in applications such as remote medical ultrasound diagnostic systems.

In this thesis, we introduce a new cross layer design approach for medical video streaming over mobile WiMAX and HSUPA networks. In particular, we propose an approach based on optimising medical Quality of Service (m-QoS) in mobile WiMAX network environments described in this work.

Preliminary performance analysis of the proposed cross layer algorithm has been evaluated via simulation studies. These results show that the proposed cross layer optimizer achieves improved performance compatible with the necessary medical QoS requirements and constraints for the relevant clinical application.

Furthermore, this work addresses the relevant challenges of cross layer design requirements for real time rate adaptation of ultrasound video streaming in Mobile WiMAX and HSUPA networks. The comparative performance analysis of such approach is validated in two experimental m-health testbed systems for both Mobile WiMAX and HSUPA networks. The experimental results show an improved performance of Mobile WiMAX compared to the HSUPA using the same cross layer optimisation approach.

Additionally, we map the medical QoS to typical WiMAX QoS parameters in order to optimise the performance of these parameters in typical m-health scenarios. Preliminary performance analysis of the proposed multiparametric scenarios is evaluated to provide essential information for future medical QoS requirements and constraints.

Contents

CONTENTSI

LIST OF ABBREVIATIONSIV

LIST OF TABLES VII

LIST OF FIGURES VIII

CHAPTER 1 1

 INTRODUCTION 1

 1.1 M-HEALTH 1

 1.1.1 *m-health wireless broadband systems*..... 3

 1.1.2 *Real-time ultrasound video streaming* 6

 1.2 MEDICAL QUALITY OF SERVICE AND CROSS LAYER DESIGN ISSUES..... 8

 1.3 RESEARCH CONTRIBUTION..... 11

 1.4 STRUCTURE OF THE THESIS 12

CHAPTER 2..... 14

 LITERATURE REVIEW 14

 2.1 INTRODUCTION 14

 2.2 CROSS LAYER DESIGN APPROACHES 14

 2.2.1 *Cross layer models*..... 14

 2.2.2 *Cross layer design in m-health applications*..... 18

 2.2.3 *Cross layer optimiser* 18

 2.3 WIRELESS BROADBAND M-HEALTH SYSTEMS 20

 2.3.1 *Mobile m-health system over WiMAX networks* 22

 2.3.2 *Mobile m-health system over HSxPA networks*..... 24

 2.4 MEDICAL VIDEO STREAMING IN WIRELESS ENVIRONMENTS 25

 2.5 QUALITY OF SERVICE IN MULTIPARAMETRIC M-HEALTH APPLICATIONS..... 27

 2.6 SUMMARY 29

CHAPTER 3 31

 MOBILE WiMAX AND HSUPA NETWORKS..... 31

 3.1 INTRODUCTION 31

 3.2 MOBILE WiMAX NETWORK 31

 3.2.1 *Technology specifications* 32

 3.2.2 *Physical layer*..... 35

 3.2.3 *Data link layer* 38

 3.3 HSXPA NETWORK 43

 3.3.1 *Technology Specifications*..... 45

 3.3.2 *Physical layer*..... 49

 3.3.3 *Transport channel processing*..... 51

 3.4 QoS IN MOBILE WiMAX AND HSXPA NETWORKS 54

3.4.1 <i>QoS in Mobile WiMAX</i>	54
3.4.2 <i>QoS in HSxPA network</i>	59
3.4.3 <i>QoS mapping issues</i>	60
3.5 SUMMARY	64
CHAPTER 4	65
OPTIMISED CROSS LAYER APPROACH FOR MEDICAL VIDEO STREAMING	65
4.1 INTRODUCTION	65
4.2 CROSS LAYER ARCHITECTURE AND DESIGN	65
4.2.1 <i>Cross layer optimizer and Reinforcement algorithm</i>	68
4.2.1.1 Reinforcement Algorithm	70
4.2.1.2 Data abstraction	75
4.3 IMPLEMENTATION OF PROPOSED CROSS LAYER	78
4.3.1 <i>OPNET implementation</i>	82
4.3.1.1 Network domain scenarios and parameter settings	85
4.3.1.2 OPNET node model design	87
4.3.1.3 OPNET process model implementation	89
4.4 SUMMARY	93
CHAPTER 5	94
PERFORMANCE ANALYSIS OF MEDICAL VIDEO STREAMING OVER WiMAX	94
5.1 INTRODUCTION	94
5.2 CROSS LAYER MEDICAL VIDEO STREAMING OVER WiMAX NETWORKS	94
5.2.1 <i>Simulation set-up</i>	95
5.2.2 <i>Optimisation results</i>	97
5.3 MULTIPLE PARAMETER M-HEALTH SCENARIOS	101
5.3.1 <i>Simulation set-up</i>	101
5.3.2 <i>Optimisation results</i>	103
5.4 OBJECTIVE AND SUBJECTIVE ANALYSIS OF ULTRASOUND MEDICAL DATA	105
5.4.1 <i>Simulation set-up</i>	106
5.4.2 <i>Performance results</i>	107
5.5 SUMMARY	113
CHAPTER 6	115
EXPERIMENTAL SET-UP AND RESULTS	115
6.1 INTRODUCTION	115
6.2 EXPERIMENTAL SET-UP	115
6.2.1 <i>Experimental WiMAX system set-up</i>	117
6.2.2 <i>HSUPA system set-up</i>	118
6.3 PERFORMANCE ANALYSIS AND RESULTS	119
6.4 SUMMARY	124
CHAPTER 7	126
CONCLUSIONS AND FUTURE WORK	126

7.1 INTRODUCTION	126
7.2 CONCLUSIONS	126
7.3 FUTURE WORK	129
AUTHOR’S PUBLICATIONS	131
REFERENCES.....	133
APPENDIX – A	142
APPENDIX – B	146
APPENDIX – C	149
APPENDIX – D	150

List of Abbreviations

16QAM	16-Quadrature Amplitude Modulation
3G	Third Generation
3GPP2	Third Generation Partnership Project2
4CIF	4 × Common Intermediate Format
4G	Fourth Generation
64QAM	64-Quadrature Amplitude Modulation
AAS	Adaptive Antenna System
AMC	Adaptive Modulation and Coding
APA	Adaptive Power Allocation
ARQ	Automatic Repeat Request
BE	Best Effort
BER	Bit Error Rate
CAC	Call Admission Control
CQI	Channel Quality Information
CS	Circuit Switched
CID	Connection Identifier
CIF	Common Intermediate Format
CINR	Carrier To Interference Plus Noise Ratio
CLD	Cross Layer Design
CLO	Cross Layer Optimiser
CN	Core Network
CPS	Common Part Sublayer
CQICH	Channel Quality Information Channel
CRC	Cyclic Redundancy Check
CS	Convergence Sublayer
CSD-RR	Channel State Dependent Round Robin
DCH	Dedicated Channel
DPCCH	Dedicated Physical Control Channel
DL	Downlink
DSA	Dynamic Service Activate
DSC	Dynamic Service Change
DSD	Dynamic Service Delete
DT	Directly Tuneable

ertPS	Extended Real Time Polling Service
EV-DO	Evolution Data Optimized
FDD	Frequency Division Duplexing
FEDD	Feasible Earliest Due Date
FTP	File Transfer Protocol
FEC	Forward Error Correction
GBR	Guaranteed Bit Rate
GGSN	Gateway GPRS Service Node
GPRS	General Packet Radio Service
HARQ	Hybrid Automatic Repeat Request
HS-DSCH	High-Speed Downlink Shared Channel
HS-DPCCH	High-Speed Dedicated Physical Control Channel
HSPA	High Speed Packet Access
HSxPA	High Speed Uplink/ Downlink Packet Access
HS-SCCH	High Speed Shared Control Channel
HSDPA	High Speed Downlink Packet Access
HSUPA	High Speed Uplink Packet Access
HVS	Human Visual System
ICMP	Internet Control Message Protocol
IP	Internet Protocol
IT	Indirectly Tuneable
LAN	Local Area Network
m-health	Mobile Healthcare
m-QoS	Medical Quality Of Service
MAC	Medium Access Control
MDP	Markov Decision Process
ME	Mobile Equipment
MIMO	Multiple Input Multiple Output
MOS	Mean Opinion Score
MSE	Mean Squared Error
MVS	Medical Video Streaming
nrtPS	Non Real Time Polling Service
PSNR	Peak Signal To Noise Ratio
QCIF	Quarter Common Intermediate Format
QoS	Quality Of Service

QPSK	Quadrature Phase Shift Keying
QS	Quantization Step
PKM	Privacy Key Management
PS	Packet Switched
RACH	Random Access Channel
RAN	Radio Access Network
RL	Reinforcement Learning
RLC	Radio Link Control
RNC	Radio Network Control
ROI	Region Of Interest
RTP	Real Time Transport Protocol
rtPS	Real Time Polling Service
RTT	Round Trip Time
SC	Single Carrier
SF	Spreading Factor
SFID	Service Flow ID
SGSN	Serving GPRS Service Node
SNR	Signal To Noise Ratio
SPI	Scheduling Priority Indicator
SSIM	Structural Similarity
TCP	Transmission Control Protocol
TTI	Transmission Time Interval
UDP	User Datagram Protocol
UE	User Equipment
UGS	Unsolicited Grant Scheme
UL	Uplink
UMTS	Universal Mobile Telecommunications System
US	Ultrasound Streaming
UTRAN	Universal Terrestrial Radio Access Network
VOIP	Voice Over IP
WiMAX	Worldwide Interoperability For Microwave Access
WirelessHUMAN TM	Wireless High Speed Unlicensed Metropolitan Area Network
WCDMA	Wideband Code Division Multiple Access

List of Tables

Table 1.1 Comparison between WiMAX and HSPA [21] 5

Table 2.1 QoS Mechanisms and parameters in 3 layers architecture [42] 16

Table 2.2 m-health QoS requirements [57-60, 112] 21

Table 3.1 Modulation and coding schemes [71] 38

Table 3.2 Type field in MAC header [74]..... 43

Table 3.3 DCH, HSDPA, and HSUPA comparison [79, 80]..... 46

Table 3.4 HSDPA and HSUPA technical specifications [79, 80] 47

Table 3.5 E-DPDCH main features [79]..... 51

Table 3.6 E-DPDCH channel bit rates [79]..... 51

Table 3.7 HSUPA categories 53

Table 3.8 Comparison of different WiMAX QoS classes [23, 39] 57

Table 3.9 WiMAX QoS parameters [23, 39] 58

Table 3.10 UMTS QoS classes and requirements [81] 60

Table 3.11 m-QoS for ultrasound video streaming [91, 94-96] 63

Table 4.1 Cross layer QoS parameters 75

Table 4.2 Segments of the State in RL algorithm 77

Table 4.3 Segments of the Action in RL algorithm 77

Table 4.4 Simulation parameters 87

Table 4.5 The WiMAX statistics wires in node model design..... 88

Table 5.1 Traffic specification of cross layer scenario..... 97

Table 5.2 WiMAX end-to-end delay simulation results comparison (with and without cross layer) 100

Table 5.3 Mobile broadband m-health service QoS mapping [112] 102

Table 5.4 Mean delay results for m-health services [32, 57] 105

Table 5.5 Objective quality indices summary 112

5.6 Mean opinion score evaluation indices 112

Table 6.1 WiMAX settings 117

Table 6.2 Comparative performance results over mobile WiMAX and HSUPA 123

List of Figures

Figure 1.1 Evolution timeline of beyond 3G network [13] 4

Figure 1.2 General cross Layer architecture 11

Figure 2.1 General cross layer functionality [40, 44] 17

Figure 2.2 Typical m-health scenarios over mobile WiMAX network..... 24

Figure 3.1 General WiMAX network [39]..... 32

Figure 3.2 WiMAX standards evolution line [74, 75] 33

Figure 3.3 IEEE 802.16-2009 standard contents [74]..... 34

Figure 3.4 WiMAX layer architecture [21, 72] 35

Figure 3.5 Functional stages of WiMAX physical layer [18, 39, 76] 36

Figure 3.6 WiMAX modulation schemes [78] 37

Figure 3.7 CID and QoS class in MAC layer [39] 39

Figure 3.8 WiMAX frame structure [21, 39, 73, 74]..... 40

Figure 3.9 WiMAX generic MAC header format [74, 77] 41

Figure 3.10 MAC signalling header type I format [74] 42

Figure 3.11 UMTS migration path [79] 44

Figure 3.12 HSUPA network [80] 44

Figure 3.13 Serving and controlling RNC [80] 48

Figure 3.14 HSUPA protocol architecture [79, 81]..... 49

Figure 3.15 Channels needed for HSUPA [79, 80]..... 50

Figure 3.16 Transport channel processing [79] 52

Figure 3.17 WiMAX QoS envelope model [74] 56

Figure 3.18 Model diagram of WiMAX BS and SS [39, 73]..... 59

Figure 3.19 Medical QoS mapping for WiMAX and HSxPA networks..... 63

Figure 4.1 Different cross layer approaches: (a) Top-down; (b) Bottom-up; (c) Application-centric; (d) MAC-centric; (e) Integrated [40, 97] 66

Figure 4.2 General wireless video streaming system [83] 69

Figure 4.3 A sample MDP diagram..... 71

Figure 4.4 The basic RL model [104] 72

Figure 4.5 Schematic diagram of implemented cross layer approach..... 76

Figure 4.6 Schematisation of the CRL algorithmic approach 79

Figure 4.7 (a) Reinforcement algorithm (b) Cross layer optimizer using the reinforcement algorithm..... 81

Figure 4.8 OPNET workflow 83

Figure 4.9 OPNET Modeler® hierarchy 85

Figure 4.10 OPNET network model of the implementation 86

Figure 4.11 Node model of the implementation 88

Figure 4.12 OPNET process model of the implementation	90
Figure 4.13 Definition list of function block.....	91
Figure 4.14 State variables of gna_clsvr_mgr process.....	92
Figure 4.15 Temporary variables gna_clsvr_mgr process	93
Figure 5.1 Typical remote ultrasound video streaming scenario	95
Figure 5.2 Extraction of ultrasound video data specifications.....	96
Figure 5.3 Cross layer simulation results. (a) PSNR vs. simulation time (b) Application response time vs. simulation time (c) Uplink SNR vs. simulation time	99
Figure 5.4 Reward matrix optimization	101
Figure 5.5 OPNET simulation set-up of the multiparametric m-health WiMAX network [112]	103
Figure 5.6 Probability density function of ultrasound video streaming and blood pressure latency.....	104
Figure 5.7 Jitter of ultrasound video streaming in clinic, homecare, and ambulance scenarios	105
Figure 5.8 WiMAX ultrasound streaming system and emulation model [21, 91]	107
Figure 5.9 Performance of video1_PSNR vs. packet loss probability	108
Figure 5.10 Performance of video2_PSNR vs. packet loss probability	109
Figure 5.11 Experimental test ultrasound images (a), (c) Packet loss =0.00% Average PSNR=38.61dB Average SSIM=0.966 Average MSE =9.43 (b) Packet loss =0.10% Average PSNR=35.37dB Average SSIM = 0.944 Average MSE =20.00 (d) Packet loss =0.18% Average PSNR=34.97dB Average SSIM = 0.941.	110
Figure 5.12 SSIM vs. packet loss	111
Figure 5.13 MSE vs. packet loss	111
5.14 MOS vs. packet loss probability for the tested ultrasound video data.....	113
Figure 6.1 Remote mobile ultrasound video streaming over HSUPA and Mobile WiMAX networks	115
Figure 6.2 Testbed setup of the WiMAX and HSUPA networks.....	116
Figure 6.3 WiMAX experimental testbed. (a) Mobile WiMAX base station and ultrasound video streaming node; (b) CPE and ultrasound video receiver node	117
Figure 6.4 HSUPA experimental testbed. (a) HSUPA card and ultrasound video streaming node; (b) Ultrasound video receiver node	118
Figure 6.5 Coverage of the testbed Vodafone HSUPA cellular link [109]	119
Figure 6.6 Mean throughput vs PSNR.....	120
Figure 6.7 Ultrasound images PSNR 38.86. (a) Original image. (b) Received image over HSUPA network. (c) Received image over Mobile WiMAX network	121
Figure 6.8 RTT results of different ultrasound video stream packet sizes over WiMAX	122
Figure 6.9 RTT results of different ultrasound video stream packet sizes over HSUPA	122
Figure 6.10 PSNR comparison of optimised WiMAX and HSUPA	123
Figure 6.11 Frame rate comparison of optimised WiMAX and HSUPA networks	124
Figure A. 1 Cross layer emulator's user interface.....	142

Figure B. 1 WiMAX device set-up.....	146
Figure B. 2 Gdb Browser.....	147
Figure B. 3 RCMS control panel.....	148
Figure C. 1 Vodafone ExpressCard.....	149
Figure D. 1 OPNET Modeler 15.0 start up.....	150

Chapter 1

Introduction

1.1 m-health

m-health can be defined as ‘mobile computing, medical sensor, and communications technologies for healthcare’. m-health is an evolving concept that was first introduced initially in 2000 as ‘unwired e-med’ in. In general, this emerging concept represents the evolution of e-health systems from traditional desktop “telemedicine” platforms to wireless and mobile configurations [1, 2].

In recent years and with current advances in mobile broadband networks numerous m-health scenarios have been deployed successfully worldwide. For example, with current wireless technologies, healthcare professionals and experts can access to patient records remotely by connection to the institution’s information system using iphone, ipad, and other portable devices. Patient history reports, laboratory results, pharmaceutical data, insurance information, and medical resources can be accessed by physicians with enhance of mobile technology, thereby improving the quality of patient care. Also there have been major research initiatives on m-health systems using current broadband wireless access technologies [3-9]. However, there are some restrictions to existing broadband wireless technologies and their strategies for health care services which hindered the wider applications of m-health technologies across healthcare systems. These factors can be summarized as follows [2, 10]:

- 1) The limitation of existing practical wireless data rates combined with the non-availability of robust secure mobile internet connectivity and information

access.

- 2) The lack of linkage between integrated “m-Health-on-demand” system and different mobile telecommunication technologies for healthcare services which is caused by deficiency of compatibility between different mobile communication standards, devices, and relevant protocols.
- 3) A standard method for payments and reimbursements is required to be defined and developed for e-health and m-health services.
- 4) There is a need to change some aspects of health-care industry but due to its complexity changes are very difficult. At the same time, health-care institutions often need to apply organizational changes in order to benefit from e-health and m-health services.
- 5) There is a need to adapt the existing m-health service with existing integrated information systems e.g., ordering systems, medical records, appointment systems, etc.

Further the above restrictions, there are two other critical issues that have not yet been addressed adequately and are the main focus of the work in this thesis:

- 1) Future m-health systems are required to provide effective and accurate clinical diagnosis and remote analysis, especially with bandwidth demanding m-health services such as in real-time tele-ultrasonography applications. It is well known that the evolution of mobile telecommunication systems from 3G to 4G will facilitate the provision of such faster data rates and higher quality medical video streaming. However, to date few studies have addressed these challenges from the m-health perspective.
- 2) The Quality of Service (QoS) issues and their guarantee to provide robust m-healthcare services with clinically acceptable quality. In order to future 4G-based

m-health systems to be clinically acceptable. These services must provide the end users (patients, healthcare provider) with an acceptable medical quality of service (m-QoS) from the doctors and clinical end perspective.

The main research focus of this thesis is to address particularly the above two research challenges.

1.1.1 m-health wireless broadband systems

The evolution of m-health systems is tightly coupled with computing and network technologies [11]. A decade ago, wireless broadband systems were introduced to substitute wired broadband systems with high speed wireless data transfer. These days, 4G networks are planned to be deployed in near future which can be a significant growth in m-health area [11].

It is well known that 4G systems aims to provide such high speed, high capacity, low cost, IP based services for nomadic and mobile wireless environment [12]. In general, mobile multimedia service, mobile ubiquitous network, and AAA (Anytime, Anywhere, and Always on) access are main targets of beyond 3G (3rd Generation) networks [13, 14].

HSUPA and WiMAX are the two significant broadband standards that were introduced by 3G partnership project (3GPP) and WiMAX forum respectively. Figure 1.1 illustrates summary of beyond 3G network evolution [13].

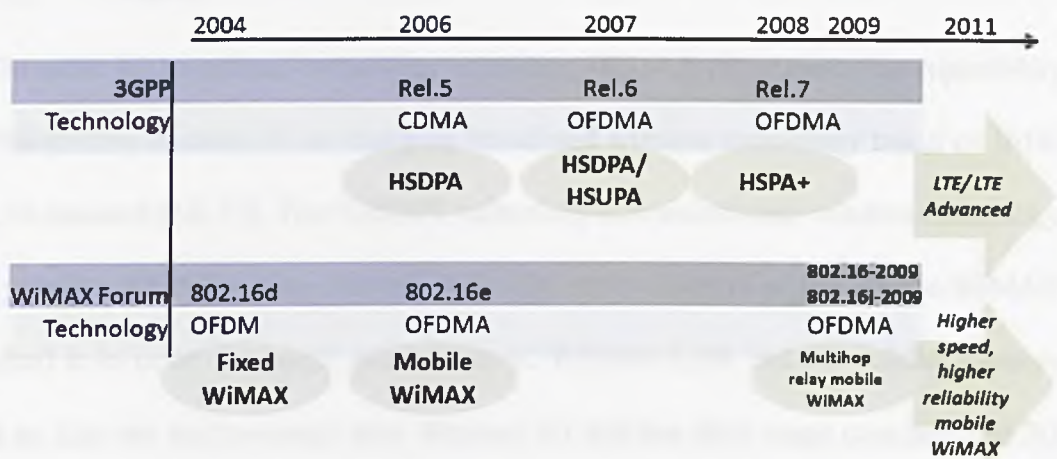


Figure 1.1 Evolution timeline of beyond 3G network [13]

In the following section, we introduce a brief description of the most relevant technologies used in this work for completeness:

(i) HSPA

The introduction of 3.5G or High Speed Downlink Packet Access (HSDPA) represented the enhancement of W-CDMA (Wideband Code Division Multiple Access) networks with higher data transfer speeds, improved spectral efficiency, and greater system capacity with a theoretical downlink peak of 14.4 Mbps (typically around 1.4 Mbps) and an uplink of 384 kbps[15]. Emerging m-health systems can benefit from these downlink data transfer speeds that were previously only feasible on wired communication networks. However, the uplink data rate was low. HSUPA is the 3GPP’s release 6, introduced in 2006 to improve the uplink data rate of HSDPA, and offers an enhanced data rate, fast packet retransmission mechanisms, and reduced packet latencies with an uplink data rate up to a theoretical maximum of 5.6 Mb/s (typically around 1.5 Mbps).

(ii) WiMAX

The other 4G broadband technology candidate, WiMAX (Worldwide Interoperability for Microwave Access), is an emerging broadband wireless technology based on IEEE 802.16 standard [16, 17]. The WiMAX technology is a mainstream wireless technology that provides BWA for mass markets [18]. The main objective of the Mobile WiMAX standard is to cover the major weaknesses of Wireless LAN and 3G cellular systems such as data rate and coverage area. Because WLAN has short range coverage and 3G networks cannot support high data rate despite of their long range coverage. To this aim, this standard deploys a specification that supports a mobile broadband access system and high data rate [19].

Mobile WiMAX is next release of fixed WiMAX introduced by WiMAX forum with optimization in communication technology to overcome the mobility and coverage issues.

	Fixed WiMAX	Mobile WiMAX	HSxPA
Standards	IEEE 802.16_2004	IEEE 802.16e_2005	3GPP Release6
Bandwidth	3.5 MHz and 7 MHz in 3.5 GHz band; 10 MHz in 5.8 GHz band	5 -25 MHZ	5MHz
Peak downlink/ Uplink data rate	9.4Mbps/3.3 Mbps	46Mbps/7Mbps	14.4Mbps/ 1.4Mbps
Modulation	QPSK, 16QAM, 64 QAM	QPSK, 16QAM, 64QAM	QPSK, 16QAM
Coverage(typical)	3–5miles	< 2miles	1–3miles
Mobility	Not applicable	Mid	High

Table 1.1 Comparison between WiMAX and HSPA [21]

WiMAX operates at radio frequencies between 2 GHz and 11 GHz for non-line-of-sight (N-LOS) operation and between 10 GHz and 66 GHz for line-of-sight (LOS) operation [20].

Table 1.1 shows a comparison between fixed/mobile WiMAX and HSPA technologies in terms of coverage area, data rate, supported modulation, and bandwidth.

It is well known that the BWA (Broadband Wireless Access) provides high data rate wireless communication between a fixed access point and multiple mobile or fixed stations. This technology was initially proposed to support interactive video service to homes but then shifted to providing high speed data networks for homes, businesses, public organizations, education, and health [20].

The evolution of BWA and mobile technologies can be a major driving force for future development in m-health systems [2]. With advances in m-health technologies, the BWA can substantially contribute to improve the daily activities with enabling to exchange real-time medical information and clinical data between different elements of the healthcare chain to introduce new care delivery models [22].

The increased availability, miniaturization, performance, enhanced data rates, and the expected convergence of future wireless communication and network technologies around mobile health systems will accelerate the deployment of m-health systems and services within the next decade. The improvement in telecommunication technology and introducing high speed broadband technology present paradigm shift in m-health technology.

1.1.2 Real-time ultrasound video streaming

As explained earlier, the main focus of this thesis will be on broadband m-health services and especially on medical video streaming and applications using wireless

broadband technologies described earlier. In this section, we briefly introduce some of the relevant issues in this area. It is well known that there is a growing demand for remote ultrasonography services which require remote expert opinion, since specialist experts are not available in scenarios such as isolated or remote areas. In these scenarios, medical specialists have no or limited access of data (ultrasound video data, radiology) to assess the level of the clinical symptoms in order to make vital decisions to whether resume treatment at home or send the patient, by ambulance, helicopter to the closest hospital. For example, recent studies report almost 50% of the diagnostic cases, patients are transferred to the hospital centre for just a few hours to receive an ultrasound examination, and are sent back home afterwards [115]. A study in Finland investigated the impact of teleradiology consultation on saving opportunity and treatment costs by reducing unnecessary patient transportation [114]. The outcomes show that teleradiology enhanced to avoid unnecessary transportation by 81%, and only 19% of the patients have been transported to hospitals. 75% of these patients who transported to a central hospital were operated on, immediately on arrival without further radiological testing [114].

There has been a study in mid 1990s, which reported transmitting of the ultrasound video images via a communication link of 1.5 Mbps T-1 leased line [25]. In the proposed system, the medical expert could communicate with the technician remotely and real time so as to supervise the image acquisition. Real-time and high demanded traffic nature of ultrasound video streaming introduce the need for BWA QoS provisioning concept. Quick delivery and reliable service are extremely important for ultrasound video streaming [26]. Different medical scenario and services require their specific quality of service parameters.

Streaming video can be in real-time or pre-encoded (stored video). Real-time video

streaming may be interactive as in videoconferencing or not interactive e.g. broadcast of a sport event. In the real-time case the time constraints are an important factor. In particular for m-health applications most medical video applications require specific time delay bounds and other specific QoS constraints, these issues will be discussed in details in the subsequent chapters.

In general videoconferencing is used increasingly in many m-health applications, including medical personnel education, peer consultation, patient education, and patient care [27]. In the recent years, the methods used to stream the ultrasound images is general video conferencing systems that are based on standard video codecs e.g. H263, MPEG4, M_JPEG etc [28]. However, these video streaming codec systems have been carefully designed and developed over the years towards achieving good communication QoS for the general video conference users [29]. In m-health applications, there are additional requirements of medical quality of service, especially in limited and variable wireless conditions that affect the quality of the video streaming and hence diagnostic decision making process.

1.2 Medical quality of service and cross layer design issues

In this section, we describe briefly the concept of Medical Quality of Service (m-QoS) for medical video streaming (MVS). Further details on this topic are described in chapter 2.

It is well known that traditional Quality of Service can be defined as a set of specific requirements for a particular service provided to its users by a network technology. In general, the QoS can be divided into two levels [10, 30]:

- (i) Network QoS: the QoS that the network and technology can offer to the user,

e.g. bandwidth, time delay and reliability.

- (ii) Application QoS: the quality of the perceived services by the user; different users have different translation for QoS.

More recently the concept of “Quality of Experience” has been introduced in conjunction with QoS studies. The QoE metrics are usually used to estimate the user perception [31]. However, this concept is not within the research topic of this thesis and is left for future work. In m-health environments providing the necessary QoS in uncertain wireless environments is a challenge that requires further research. In the ultrasound medical streaming application, the following important user QoS requirements in the application layer are used in deciding the resulting throughput. These are summarized as:

- (i) Image quality (e.g. PSNR, SSIM, or subjective analysis)
- (ii) Image size (e.g. QCIF, CIF)
- (iii) Frame rate of the received images
- (iv) Jitter
- (v) End-to-end delay

The aforementioned QoS indices are dependent to network QoS parameters; in order to match the required resources with the available network resources, there must be a tradeoff between these QoS requirements to satisfy the medical (clinical) requirements and the required bounds with relevant metrics. The concept of m-QoS which can be defined as a sub category of QoS from the m-health perspective that represents: *'augmented requirements of critical mobile health care applications and the traditional wireless Quality of Service requirements'* [32]. Improving multimedia QoS in broadband wireless networks is an active research area [31]. In this work, we propose new tradeoff to meet the m-QoS requirements considering the different network layers'

parameters.

Recently relevant studies on QoS in m-health applications have been reported, these are reviewed in details in chapter 2. However, no study to-date addressed the m-QoS issues with existing cross layer design approaches.

In this thesis, we focus on the application of m-QoS to cross layer design architecture for broadband m-health applications.

In general, cross layer design (CLD) refers to protocol and model architecture design, which is exploiting the dependence between layers to obtain optimum gains [33]. Since making a decision in one layer affects QoS parameters in other layers, a suitable approach is used for the decision making process that fulfills the required QoS requirements. Cross layer algorithm can combine the parameters and mechanisms at different layers to optimally find a solution for providing a better QoS support at a given network dynamics and resources [34].

In general, cross layer systems perform three major tasks; these are data abstracting, optimizing, and reconfiguration. Abstraction and reconfiguration strictly depend on the system model and the interaction between the layers. And the optimization algorithms and protocols are used for allocating the optimal solution. Figure 1.2 illustrates a general cross layer architecture [34].

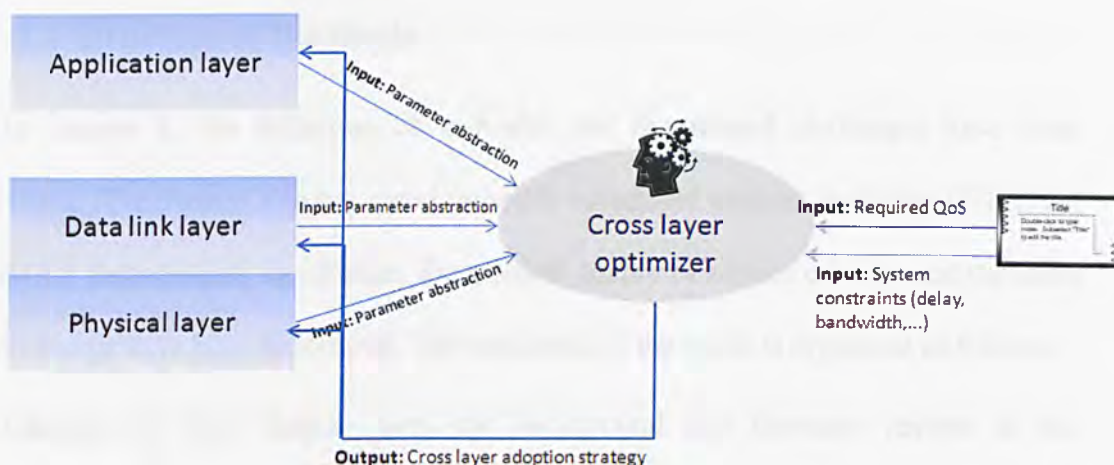


Figure 1.2 General cross Layer architecture

Cross layer systems use different models and algorithms that depend on the specific architecture that is being used in such implementation. These are described in details in chapter 4.

1.3 Research contribution

The major contributions of this thesis can be summarized in the following objectives:

- 1) The study and comparative performance analysis of medical video streaming over mobile WiMAX and HSUPA networks
- 2) Design and development of a complete broadband m-health model. The model is based on OPNET Modeler[®] 15.0 that assesses the performance of the system under different medical quality of service constraints.
- 3) Optimal design and performance analysis of a cross layer architecture for wireless broadband m-health systems.
- 4) Experimental performance analysis of the optimised cross layer architecture using mobile WiMAX (802.16e) and HSUPA testbeds.

1.4 Structure of the thesis

In chapter 1, the definition of m-health and the related challenges have been reviewed. The chapter also presented m-health broadband systems including HSPA and WiMAX technologies. In addition, the medical quality of service concept and the cross layer design have been introduced. The remainder of the thesis is organised as follows:

Chapter 2: This chapter gives the background and literature review of the multidisciplinary issues relevant to the thesis's work. It starts with a background and brief review on cross layer design and different cross layer approaches. This is followed by reviewing of existing m-health applications over wireless broadband access networks. We also review some of the earlier work and research in ultrasound medical streaming and QoS requirements for different m-health applications.

Chapter 3: This chapter presents an overview of mobile WiMAX and HSUPA networks used in this work with focus on the technology specifications, physical layer, and data link layer specifications. In addition the details of quality of service parameters considered in these networks will also be discussed.

Chapter 4: This chapter describes briefly the existing cross layer design approaches used in wireless video streaming. The chapter also presents the Q-Learning approach used in the cross layer design and applied to the medical video streaming. It also presents the proposed cross layer optimiser designed specifically for ultrasound video streaming using OPNET Modeler[®] developed for this purpose. Also a complete simulation model of this approach using the OPNET Modeler[®] is presented.

Chapter 5: This chapter presents performance analysis results of the proposed cross layer design. It also discusses the medical QoS mapping to typical WiMAX QoS parameters to optimise the performance of these parameters in a typical m-health scenario. Preliminary performance analysis of the proposed multiparametric scenarios is

evaluated. Also objective and subjective analysis will be preformed over ultrasound video streaming. The effects of packet loss on the medical image quality in terms of objective and subjective indices are also presented.

Chapter 6: This chapter shows the experimental set-up of the mobile WiMAX and HSUPA networks. The experimental performance analysis and results are presented.

Chapter 7: This chapter concludes the thesis and summarises the contributions of this work. In addition, suggestion and future research direction are presented.

Chapter 2

Literature Review

2.1 Introduction

This chapter presents the background and literature review of the multidisciplinary issues relevant to the thesis's work. These are summarised as follows:

1. An introduction to cross layer design and cross layer approaches. This is followed by related work on existing cross layer optimization issues.
2. A review of existing m-health applications over wireless broadband networks.
3. A review of the related work on the medical video streaming in wireless environments.
4. A summary of the relevant quality of service issues and challenges in m-health applications.

2.2 Cross layer design approaches

This section presents an introduction to the cross layer design and some of the previous works in this area.

2.2.1 Cross layer models

During the last decade the advances in wireless broadband systems have been increasing significantly. Simultaneously, demand for high bandwidth application with specific QoS has kept increasing. Wireless networks usually deploy standard protocol

stack to ensure interoperability between layers. Due to the fact that wireless nature is highly variable and resource poor, the functionality of layered model in mobile environment does not have enough efficiency in terms of QoS and performance. Therefore there has been increasing interest in approaches that rely on interaction between different layers [35-37].

In general, the cross layer refers to the protocols and models that allocate specific strategies across multiple layers to improve interlayer operation and system performance [38, 39]. The exchange of information across protocol stack boundaries is allowed by cross layer approach [10]. This is not against the typical layering concepts; but it is a complementary model to the traditional Open System Interconnection (OSI) concept.

The cross layer design approaches can be classified as follows [40]:

- 1) Top-down approach
- 2) Bottom-up approach
- 3) Application-centric approach
- 4) MAC-centric approach
- 5) Integrated approach

However, there are other categorisations that are based on “loosely coupled” or “tightly coupled” cross layer design [41]. In the loosely coupled cross layer design, optimisation is focused on optimising one protocol layer by data abstracting from the other layers. In the tightly coupled cross layer design, optimisation is carried out in the different layers.

Different types of cross layer management entities are categorized as follows [42]: Internal intralayer cross entities, internal interlayer entities, external centralised entities,

and external decentralised entities. The internal entity models deploy CLO inside each network element. In the interlayer model, the CLO is located in any protocol stack layer. But intralayer model is based on jointly optimise of multiple protocol stack layers by abstracted layer parameters. The external entity models use CLO in an external station such as BS that can be distributed or centralised implementation.

Layer	Mechanism
Application	Modifying perceived QoS e.g. frame rate adaption, video /voice quality manipulation
Data link	Scheduling strategies, retransmission policies, error control system (FEC, coding rate control)
Physical	Adaption modulation, power management, interference control, hand over strategies

Table 2.1 QoS Mechanisms and parameters in 3 layers architecture [42]

A list of layered mechanisms and parameters are involved in CLD that are shown in Table 2.1 with the relevant QoS mechanisms in the application, data link, and physical layers respectively.

Furthermore, cross layer design refers to protocol design that exploits the dependence between layers to obtain optimum gain and performance through deploying layers’ QoS mechanisms [38]. The general functionality of the cross layer optimiser is illustrated in Figure 2.1. These include three main tasks [40, 44]:

- i) Layer abstraction
- ii) Optimisation or finding the optimal solution
- iii) Layer reconfiguration

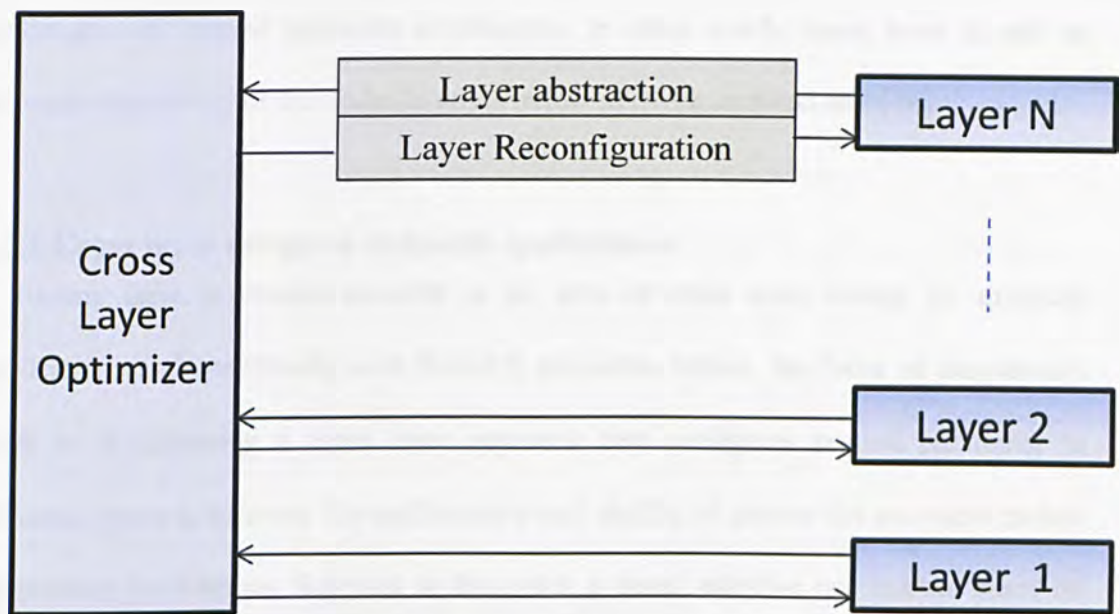


Figure 2.1 General cross layer functionality [40, 44]

Most of the current cross layer approaches focus on lower layers. In [35], several cross layer proposals referring to physical and data link layers are reviewed. In [45], cross layer interaction with physical and data link layers to optimize MIMO (multiple-input and multiple-output) smart antenna through minimizing packet losses rate and maximizing the average throughput and spectral efficiency is introduced.

In [46], different cross layer parameters include DT (Directly Tunable), IT (Indirectly Tunable), D (Descriptive), and A (Abstracted) are described. Details of these will be explained further in chapter 4.

Further details on the advantages and disadvantages on each of the existing cross layer approaches are beyond the scope of this thesis and can be found in [36] and [41].

As mentioned in the first chapter, the work of this thesis focuses on the wireless video streaming application with considerations on distortion profiles, relevant elements of video streaming, and radio link performance. The main research challenges in mobile multimedia remain on resource allocating and adapting to the dynamically changing wireless environments. Cross layer design approaches can provide the solution for such

challenges via layered networks architecture. In other words, cross layer is able to increase adaptability of the nodes in any wireless network architectures [46].

2.2.2 Cross layer design in m-health applications

To-date there is limited research in the area of cross layer design for m-health applications and specifically over WiMAX networks. Hence, the focus of this thesis's work is in proposing a cross layer approach that configures several parameter in different layers to increase the performance and quality of service for real-time mobile diagnostics applications. Relevant to this work, a novel adaptive rate control based on reinforcement learning algorithm with feedback from lower layers to reconfigure application layer is presented in [47]. This method proposes a rate control approach for medical video streaming to match optimally the rate of video application to the available network bandwidth resources.

Similarly, a multilayer controller including application and data layers to optimise system throughput in medical applications over 802.11e wireless standard is presented in [48]. The critical issue that differentiate this work from these is that the existing wireless networks do not necessarily guarantee the required QoS parameter optimally, especially for real-time mobile diagnostic applications. Therefore, a new architecture is required to address and optimise the relevant QoS issues.

2.2.3 Cross layer optimiser

Cross layer optimiser is the kernel of the cross layer architecture that makes decision to take an optimal solution with minimum impact on different layers' functionalities. For example changing the transmission power or modulation type can implicitly have an effect on routing protocols [49].

The work [50] includes an example of cross layer optimiser that deploys a “Marking Algorithm” within the optimiser structure to differentiate the H.264 partitions over IEEE 802.11e standard. In this work NALUs (Network Abstraction Layer Units) are encapsulated into a QoS data frame, and the traffic is mapped to different ACs (Access Categories). The proposed optimiser algorithm is designed specifically for IEEE 802.11 standard. This concept can be used in WiMAX scheduler part as an extension. The work [51] presents a cross layer approach between application and MAC layers. This approach deploys WiMAX MAC management messages to adapt the video streaming parameters to network conditions and resource availability.

In [52], a cross layer optimiser has been formulated for OFDM wireless networks to configure the lower layers. This work uses joint dynamic subcarrier assignment (DSA) and adaptive power allocation (APA) with considering utility function that is used to balance the efficiency and fairness. The work uses “Maximal Match (MM)” approach in optimiser to compute the scheduling at each time for multihop wireless networks.

In [53], several optimiser structures are presented, these include: Convex programming, Lagrange duality, stochastic stability, and learning methods. In general, cross layer optimiser can add computation complexity for finding the optimal QoS strategy. And some of these methods are suitable for the real-time applications.

In this work, the learning approach is adopted as this approach is best suited for the real-time medical diagnostic applications. This method can work as a background process and uses an initial optimization table to decrease real-time computational processing time [54].

2.3 Wireless broadband m-health systems

Historically, the first generation of wireless communication technology aimed to provide analogue voice services, the second generation aimed to provide digital voice services, the third generation aimed to provide robust mobile services, and the fourth generation aims to provide high data rate services with reliable broadband communication systems [55]. More recently, the advances in WiMAX and HSxPA networks triggered a new area of research to address the relevant medical broadband challenges in the different m-health applications. In work [62], an integrated WiMAX, 3G, and WLAN m-health network model is proposed that includes a wireless network of hospitals, clinics, drugstores, mobile ambulances, mobile experts, information management data base, and mobile/fixed patients.

In [56], the medical services are categorised to: active and passive medical services. The traditional medical services are introduced as passive. The active medical services deploy different portable physiological measurement devices to monitor patients.

In [57], a general m-health system architecture categorising different medical traffic to four types with their relevant QoS requirements:

- (i) Audio applications
- (ii) Video applications
- (iii) Bio-signal applications
- (iv) File transfer applications

In general, m-health applications can be categorised as real time applications and non real-time applications; real-time applications include applications such as the transfer of electrocardiography (ECG), blood pressure, oxygen saturation, medical images and medical video data. Non real time m-health applications include access to administrative

files and electronic health records (EHRs), access to drug store data bases, and queries to medical report warehouses, etc.

Different m-health scenarios such as emergency m-health, mobile patient monitoring, mobile medical data, mobile robotic system, post-hospital care, teleconsultation collaborative, and medical information management services need specific QoS indices. These applications and their corresponding QoS indices are shown in Table 2.2 [57-59, 112].

m-health service	Real-time application	Non real-time application	Data rate/size	QoS indices	Reference
Electrocardiography (ECG) monitoring	√		24 kb/s/12 channels	Delay	57
Blood pressure monitoring (Sphygmomanometer)	√		< 10 kb/s	Delay	59
Heart sound (Digital audio stethoscope)	√		~ 120 kb/s	Packet loss, Delay	59
Region of Interest JPEG Image	√		15- 19 MBytes	PSNR, Frame size, Packet loss,	57
Radiology		√	~ 6 MBytes	PSNR, Frame size, Packet loss	57
Magnetic resonance imaging (MRI)		√	< 1MBytes	PSNR, Frame size, Packet loss	59
Ultrasound video streaming	√		250 kb/s – 1.544 Mb/s (WMV2)	PSNR, Frame Rate, Frame size, Packet loss, Delay	59, 112
Wireless medical consultation (e.g. Accessing to patient records)		√	~ 10 Mb/s	Packet loss	60
Video/Audio conference	√		~ 1 Mb/s	Packet loss, Delay	60
Remote control applications (e.g. Robotic control)	√		~ 1 kb/s	Packet loss, Delay	60

Table 2.2 m-health QoS requirements [57-60, 112]

Work [62] presents potential m-health applications and scenarios as follows:

- (i) Emergency telemedicine: this includes remote access to the experts from an emergency site through transmitting vital bio-signal, ultrasound images, video and voice communications.
- (ii) Mobile patient monitoring and healthcare provider: these provide remote and real-time patient monitoring that include wearable and smart sensors.
- (iii) Mobile medical data: this includes medical data, patient's records, and medical data bases.
- (iv) Mobile robotic systems: This refers to systems that enable experts to control medical devices remotely for instance OTELO (Mobile Tele-Echography System Using an Ultra-light Robot) project.
- (v) Pre-hospital care: it includes ambulances that able to send and receive vital medical information to/from hospital before arriving to hospital.

2.3.1 Mobile m-health system over WiMAX networks

The advantages of WiMAX technology for m-health scenarios include: High bandwidth, integrated services, QoS support, and security [57, 61, 62]. As a result, this technology is a suitable choice for different m-health applications and scenarios. In [63], a WiMAX based m-health system for remote diagnosis from an ambulance is described. This work also presents a list of different m-health applications such as remote diagnosis, remote follow-up, remote monitoring, and remote assistance that can be used over WiMAX network. However, no research to date has addressed the issues of the optimised cross layer design for medical video streaming over mobile WiMAX network.

Work [56] describes a WiMAX based emergency medical service system that consists of healthcare service center, emergency medical service hospital, and ambulance. This work believes that the WiMAX can be a suitable choice for m-health applications. A general telemedicine architecture is described in [57]. This work reviews different m-health scenarios such as:

- (i) Ambulance scenario includes ECG, voice, video, and file transfer traffic
- (ii) Clinic scenario of transmitting simultaneous ECG, voice, video, medical file transfer, and etc
- (iii) Follow-up scenario includes ECG, blood pressure, heart rate, ROI, ultrasound video streaming, video conference, and voice conference.

Furthermore, different categorisations of m-health scenarios are presented:

- (i) Emergency services in case of accidents
- (ii) Follow-up services
- (iii) Patient telemonitoring
- (iv) Homecare services
- (v) Intrahospital services
- (vi) Medical information management services.

This work deploys a “Water filling” flow chart to manage bandwidth allocation for the different m-health scenarios.

Figure 2.2 shows typical m-health scenarios over mobile WiMAX network. All these categories necessitate the need for an alternative multiple medical parametric networking architectures that provide high bandwidth requirements with cost effective route compare to the cellular approach.

Different m-health applications such as emergency telemedicine, mobile patient monitoring, mobile medical data, mobile robotic system, post-hospital care, teleconsultation collaborative, and medical information management services all require specific data rates and QoS indices. These were summarised in table 2.2 and the details of these applications are described elsewhere [59]. In the chapter 5, we will briefly present this approach and discuss the relevant challenges of such mapping process.

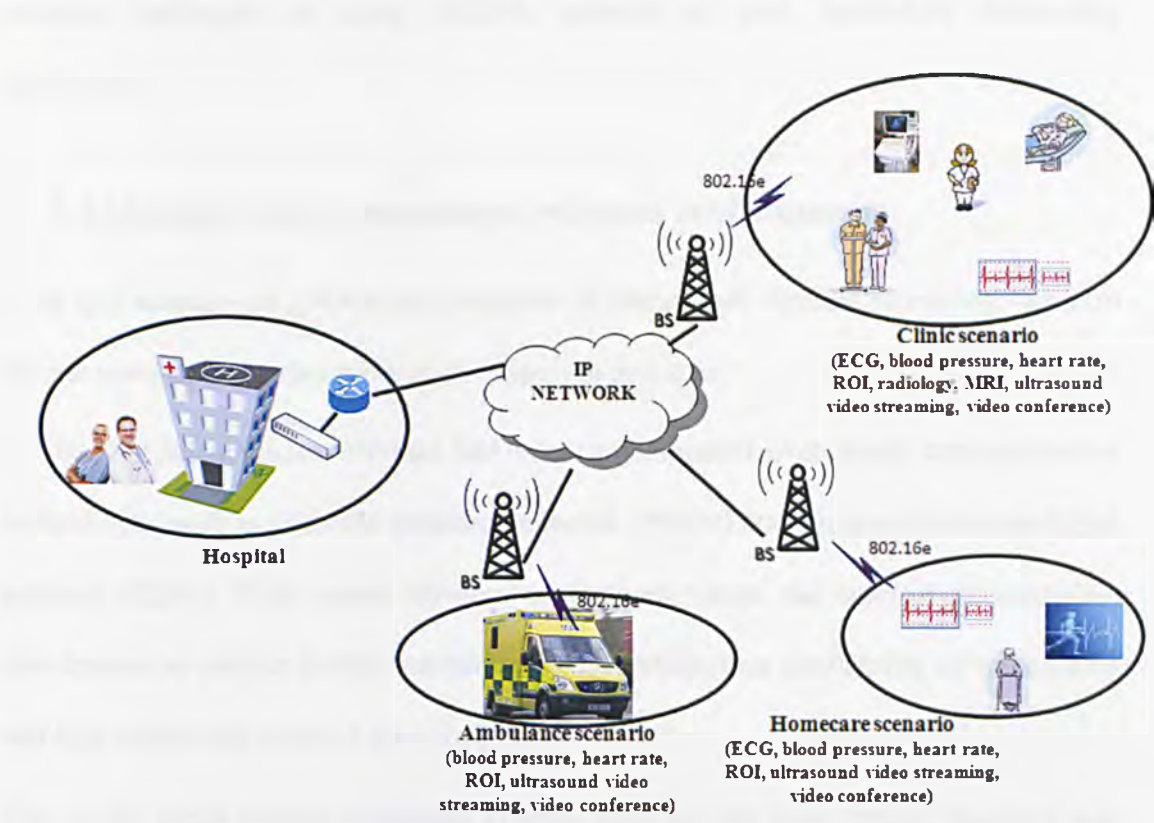


Figure 2.2 Typical m-health scenarios over mobile WiMAX network

2.3.2 Mobile m-health system over HSxPA networks

The performance of HSPA networks for delivering emergency m-health applications is studied in a recent work [64]. In this work a joint transmission of voice, real time data, medical data and file transfer is performed in both uplink and downlink using simulated network environment. The performance of data rates and QoS requirements of different real-time and non real-time m-health applications such as digital blood

pressure, digital thermometer, scanned X-ray, and electrocardiogram ECG monitoring were presented.

The performance of an advanced medical robotic system that uses a fully integrated end-to-end mobile tele-echography system for remote areas over 3.5G/HSDPA communication network is studied in [32]. The results provide a complete performance analysis of HSDPA networks in conjunction remote robotic ultrasound system and the relevant challenges in using HSDPA network in such bandwidth demanding applications.

2.4 Medical video streaming in wireless environments

In this section, we present an overview of ultrasound medical streaming; we also review some of the earlier work and research in this area.

The first telemedicine services had been implemented over wired communication technologies such as plain old telephone network (POTN) and integrated services digital network (ISDN). With recent wireless network evolution, the wireless telemedicine, also known as mobile health, started to provide ubiquitous availability of multimedia and high bandwidth medical services [62].

One of the initial remote ultrasound systems used for real time remote diagnosis was reported in 1995 [65]. This work used a digital image capture and distribution system that supports remote ultrasound examinations and real-time diagnosis over wired broadband system. This work used a colour plane 8 bits per pixel (256-colour) image with resolution of 640×480 pixels sent over dedicated land line communication link of data rate 1.5 Mbit/s [65]. At the receiver end the arrived frames were decompressed and displayed. For reliable transmission of each frame Xpress Transport Protocol (XTP) was used.

In 1998, the Multimedia Interactive DemonStrator Tele-Presence (MIDSTEP) was introduced [66]. The project had the objective of realizing two telesurgery demonstration systems; one for local telemanipulation over LAN (Local Area Network) and one for remote telemanipulation over WAN (Wide Area Network). Both utilized remote robotic manipulation of an ultrasound probe, controlled by an expert ultrasonographer, to guide a surgeon at the patient site in performing simple invasive surgical tasks. The ultrasound images were acquired at a 384×288 resolution and compressed using 10:1 M-JPEG video coder and then Asynchronous Transfer Mode (ATM) communication technology is used to transmit the video data to the expert side. In this system, a User Datagram Protocol (UDP) was used to transmit video packets with a rate control system to maintain a frame rate of better than 15 fps. This application required 10 fixed lines with total of 100Mbps data rates and fixed location for both expert and remote stations [67].

In 2000, another European project 'TeleInVivo' was developed with a similar approach: a clinical expert standing next to the patient was performing the echography service. ultrasound data being sent using satellite to a data base station and processed to reconstruct a 3D representation of anatomical region of interest. A wavelet-based images compression algorithm was implemented for the size reduction of the image data sets to be transferred. The compression was lossy but very efficient in cases where bandwidth is the crucial issue. However this system still lacks the ability of two way interaction during the consultation process, and did not solve the problem of the presence of the specialist in the remote area.

A telerobotic system was introduced in [68]. In this system, the internet user could access and command a 2 DoF (degrees of freedom) robot in a real time closed loop over the Internet, receiving both visual and force feedback. A Java Based Interface for

Telerobotics (JBIT) system was developed to demonstrate the feasibility of the internet based telerobotics equipment. The real video was realized using the H.263 compression technique with a rate of 4 frames/sec performance over 28.8 Kbps modem connection, and the obtained results confirmed that real time closed loop operation over the Internet is possible. The system provided poor image quality with the 4 frames/sec transmitted over a 28.8 Kbps channel [67].

A remote diagnosis system which controls an Echographic Diagnosis Robot (EDR), has been evaluated by a group of researchers in the Department of Medical Informatics at Ehime University in Japan [69]. Two wireless local area network bridges SB-1100 connected Ehime University to a temporal examination room at a distant of 1.4Km from the hospital. The PCS-1600, Sony videoconference systems were used in this experiment to stream the ultrasound images captured by the ultrasound probe. This videoconference system uses H.263 video coding technologies [67]. The time delay was less than 1sec when the image size was Common Intermediate Format (CIF) (352×288 pixels). This work was based on a wireless LAN, carried over a short distance.

From these studies, it can be seen that to-date no work has been carried out using both WiMAX and HSUPA networks based on cross layer optimizer for real-time mobile ultrasound diagnostic applications and to study the performance of both networks in real-time robotic ultrasonography diagnostics.

2.5 Quality of Service in multiparametric m-health applications

As explained in section 1.2, the concept of medical Quality of Service (m-QoS) was first introduced in [47]. This concept is defined as the *'augmented requirements of*

critical mobile healthcare applications with respect to traditional wireless quality of service requirements'.

In general, different m-health scenarios require different sets and levels of QoS requirements as shown in table 2.2. The QoS metrics discussed in this table are generally categorised for bandwidth, timeliness and reliability. Specifically for bandwidth metrics the generated data rate of the application is considered in addition to packet loss and network delay. QoS optimisers can consider the following data transmission categories that can be deployed in m-health scenarios [32, 57, 67, 70]:

- (i) **Real-time diagnostic applications** – This category includes real time ultrasound video streaming, video/voice conference for remote consultations, and VOIP (Voice over Internet Protocol). These applications are delay sensitive. In terms of data loss, these applications can tolerate some packet loss. But it can affect the service quality. In real-time ultrasound image streaming the tolerable data impairment is less than that for ambient video conference applications. this category of application usually requires the high bandwidth compared to other categories. However, the VOIP doesn't require high bandwidth.
- (ii) **Real-time critical applications** – This category includes remote monitoring of patients physiological functions such as hear rate, blood pressure monitoring. These applications cannot tolerate any delay and packet loss. And they require continuous small bandwidth.
- (iii) **Mobile web-based medical consultation** – In general, this category is used in medical information and consultation scenario in GP offices, such as interactive access to patients' information and records, web browsing, file sharing, and download of medical data (documents, images, or videos).

These applications require high bandwidth. This type of applications can tolerate some delay, but cannot tolerate packet loss.

- (iv) **Remote control applications** – This category includes the remote control of medical equipment, such as robotic control signals. These applications require a continuous but very low bandwidth and cannot tolerate delay and data loss.

In general, m-health scenarios can be categorized as accident, clinical care and home care scenarios [57, 59]. The accident and emergency (A&E) category include transmission of multiparametric data such as blood pressure, heart rate, ROI (region of interest), ultrasound video streaming, video conference, and voice conference. Future ambulance units can be equipped with mobile WiMAX systems that have wireless connection to WiMAX base station and provide instant clinical diagnostics on the move. The clinical care category refers to the local/remote clinic scenario where specialist experts are not available. This scenario includes multiple medical data and parameters such as ECG (electrocardiography), blood pressure, heart rate, ROI, radiology, MRI (magnetic resonance imaging), ultrasound video streaming, video conference, and voice conference from supported applications. The home care follow-up category provides medical/health services to especially elderly people to be monitored without the need to travel to the hospital. This scenario includes multiple medical applications such as transmitting simultaneous ECG, blood pressure, heart rate, ROI, ultrasound video streaming, video conference, and voice conference.

2.6 Summary

In this chapter, we presented a detailed literature review of the multidisciplinary areas covered by this work. This included literature review on the different cross layer design approaches and optimisation methods that will be

deployed to the proposed cross layer model. Based on the literature review, we will extract the cross layer optimiser design. As discussed earlier, the cross layer optimiser makes decision to take an optimal solution with minimum impact on different layers' functionalities. The reinforcement learning approach is adopted as this approach is best suited for the real-time medical diagnostic applications. This method can work as a background process and uses an initial optimization table to decrease real-time computational processing time

The chapter also presented the relevant studies of mobile broadband m-health application over WiMAX and HSPA networks together with their relevant quality of service issues and their requirements for real-time and non real-time medical applications that will be used to design and implement a complete m-health model with considering multiparametric m-health services.

Chapter 3

Mobile WiMAX and HSUPA Networks

3.1 Introduction

In this chapter, we introduce some of the details of the mobile WiMAX and HSxPA networks. This chapter presents an overview and relevant data of mobile WiMAX (IEEE 802.16e) and HSUPA network architectures relevant to this work. The chapter also presents some of the necessary technical specifications, physical layer, and data link layer standards used in this work. This is followed by the quality of service parameters adopted in the two network technologies.

3.2 Mobile WiMAX network

The IEEE 802.16 family standards that have been commercialized under the name WiMAX (Worldwide Interoperability for Microwave Access), is officially called WirelessMAN (Wireless Metropolitan Area Networks). The WiMAX is a wireless broadband system that includes fixed and mobile standards which are based on IEEE 802.16-2004 and IEEE 802.16e-2005 respectively. In particular, the IEEE 802.16e (Mobile WiMAX) standard aims to provide broadband connectivity to mobile users in wireless metropolitan area network (WMAN) environments [39] which provides specifications of MAC and physical layers.

Figure 3.1 shows an example of WiMAX network [71]. WiMAX cell consists of one base station (BS) and one or more subscriber stations (SS) either fixed or mobile located in the coverage area. WiMAX network includes a group of WiMAX cells that BSs are

connected to core network (CN). The BS is in charge of managing wireless access for SSs in each coverage area [39].

In the following sections, a brief introduction of WiMAX architecture and its specification will be explained. Further details can be cited in [21, 71-73].

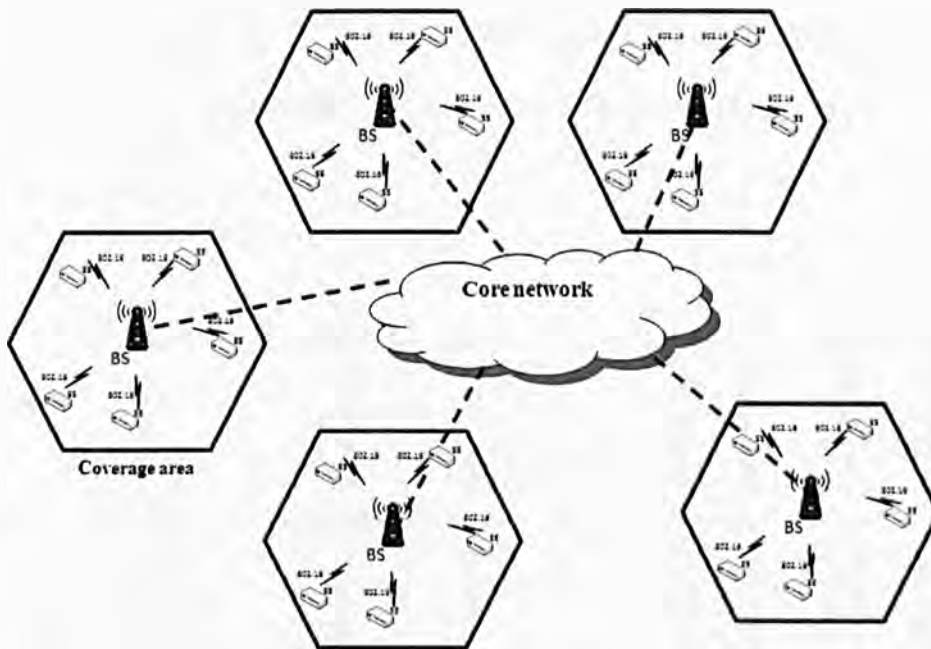


Figure 3.1 General WiMAX network [39]

3.2.1 Technology specifications

The first version of WiMAX standards was approved by the IEEE in 2001 that known as fixed WiMAX. In 2004, the fixed WiMAX standard has been improved as 802.16-2004.

Mobile WirelessMAN standard has been presented in 2005 as 802.16e-2005. According to the WiMAX forum this version was the most popular implementation of WiMAX standards. Then 802.16-2009 is presented by rolling up several predecessor standards as improvement of 802.16e. The IEEE 802.16-2009 standard embraces both fixed and mobile point-to-multipoint broadband wireless networks and standardizes the air interface and related functions for broadband wireless access systems. Figure 3.2

illustrates the WiMAX standard evolution history. This standard includes the IEEE 802.16e and enhancement of fixed WiMAX standard (IEEE 802.16-2004). The IEEE 802.16-2009 is also called Mobile WiMAX™.

Figure 3.3 shows the IEEE 80.16-2009 contents that includes a revision of IEEE Std 802.16-2004, and consolidates material from IEEE standard 802.16e-2005, IEEE 802.16-2004/Cor1-2005, IEEE 802.16f-2005, and IEEE Std 802.16g-2007, along with additional maintenance items and enhancements to the management information base specifications [74].

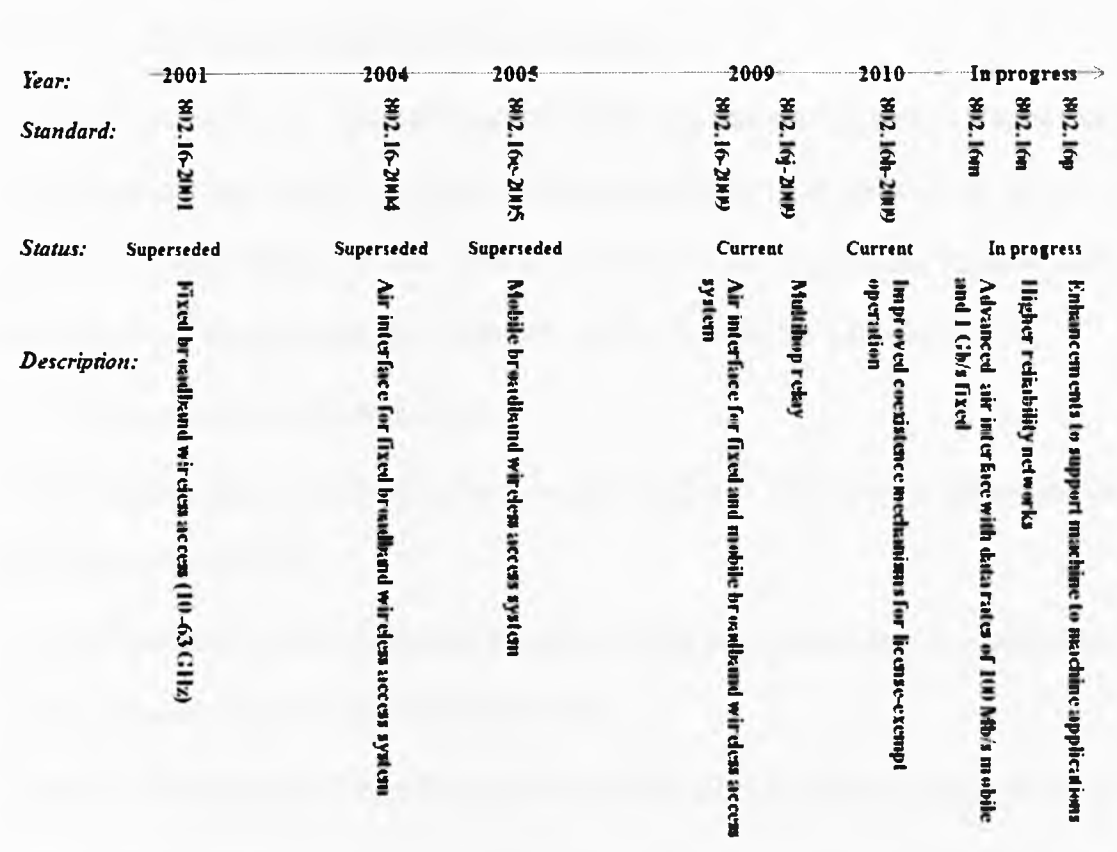


Figure 3.2 WiMAX standards evolution line [74, 75]

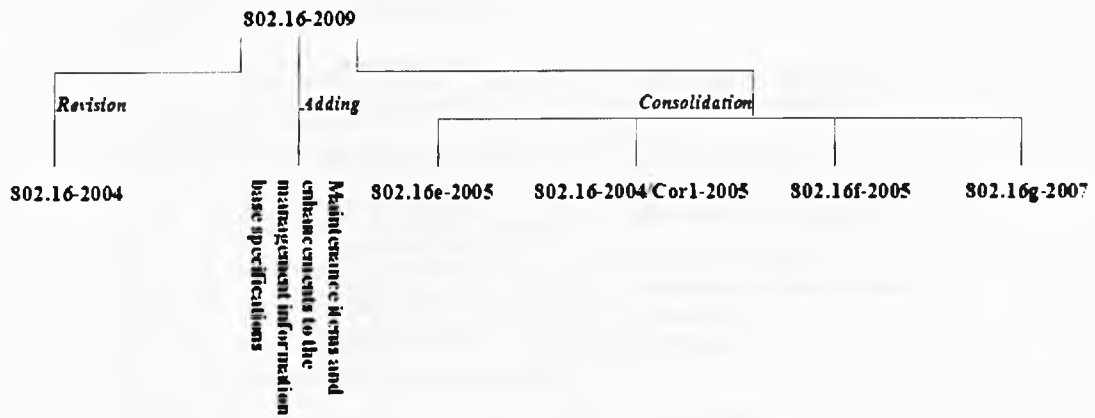


Figure 3.3 IEEE 802.16-2009 standard contents [74]

In this work, we use both mobile WiMAX and WiMAX terminology instead of 802.16e and 802.16-2009 standards for convenience.

Mobile WiMAX is a connection oriented technology and the Subscriber Station (SS) cannot transmit data until base station allocates channel to it. In other words, BS is in charge of channel allocation and admission control based on available resources and traffic policy. The communication links between MS and BS are followed as [76]:

- A) SS requests a bandwidth allocation
- B) BS takes decision about the allocation and decides if it has the enough resources, and registers the MS/SS
- C) BS assigns 16-bits connection identifier (CID) to a connection or a subscriber which is usually shared for uplink and downlink

Figure 3.4 shows the reference model of this standard and sublayers' main duties. In next two sections, we present a general overview of this reference model most relevant to the current research work. The standard specifies medium access control (MAC) and physical layer features. The MAC layer includes following sublayers: service specific convergence (CS) sublayer, MAC common part sublayer (MAC CPS), and security sublayer that will be discussed in more details in the next sections.

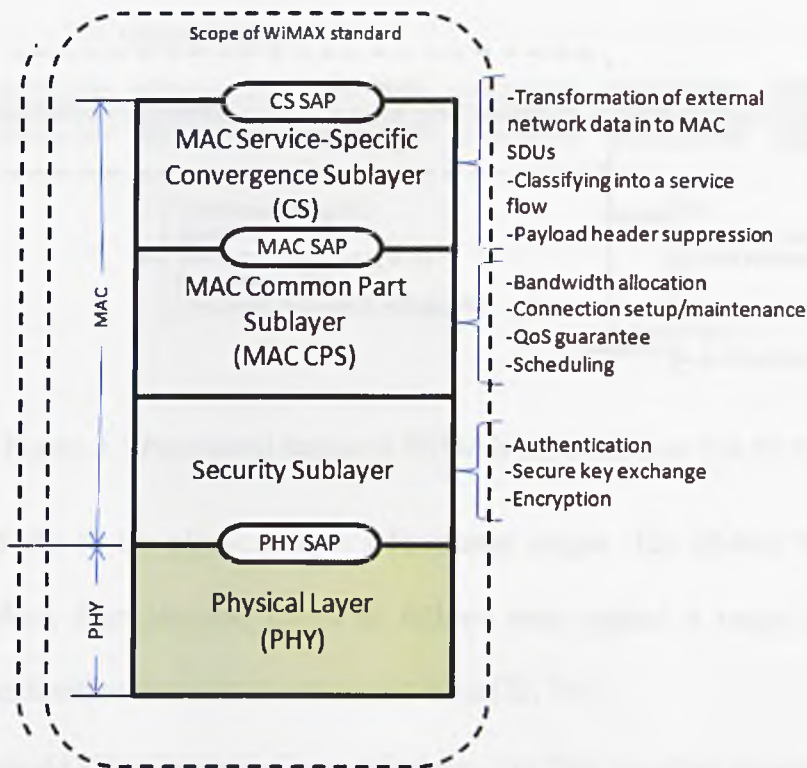


Figure 3.4 WiMAX layer architecture [21, 72]

3.2.2 Physical layer

In general, the basic functionalities of WiMAX Physical layer are summarized as follows [21, 76, 77]:

- Encoding / decoding of signals
- Preamble generation / removal
- Bit transmission / reception
- Frequency bands and channelization
- High Order Modulation techniques (QPSK, 16QAM, 64QAM)
- Advanced Error Correcting Codes (e.g., Turbo Codes and LDPC codes)
- Synchronization
- Duplexing (TDD/FDD)
- Power Control

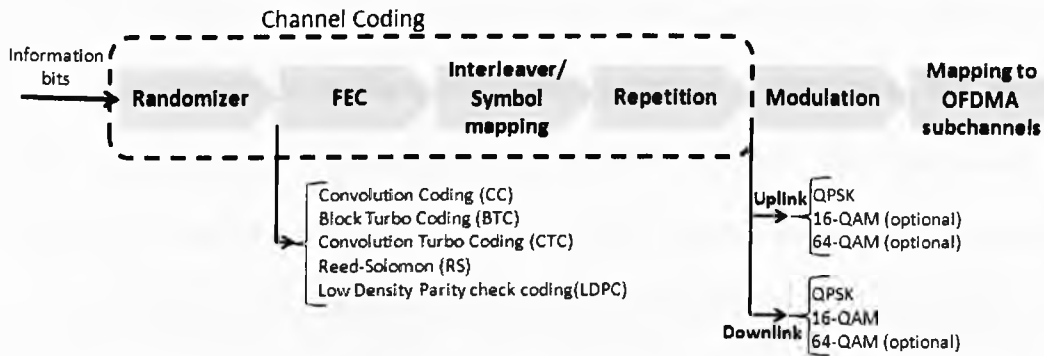


Figure 3.5 Functional stages of WiMAX physical layer [18, 39, 76]

Figure 3.5 shows the physical layer's functional stages. The Mobile WiMAX air interface defines four physical layers as follows that support a range of different frequency bands either licensed or unlicensed band [72, 74]:

1) **WirelessMAN-SC (Single Carrier) Release 1.0:** This interface is based on single carrier modulation and it is designed to operate for 10 to 66 GHz spectrum in line of sight (LOS) communication. Rain attenuation and multipath affect reliability of the network at these frequencies.

2) **Fixed WirelessMAN-OFDMTM:** This interface, known as IEEE 802.16d, uses spectrum below 11 GHz licensed bands. It is designed for fixed stations. In this PHY, multiple subscribers use a time division multiple access (TDMA) to share the media. Thousands of subcarriers are transmitted and each user is given complete control of all subcarriers.

3) **Fixed WirelessMAN-OFDMA:** The combination of time division and frequency division multiple access in conjunction with OFDM is called OFDMA. It uses spectrum below 11 GHz licensed bands.

4) **WirelessMAN-OFDMA:** This interface uses licensed bands below 11 GHz. it is deployed for NLOS point to multi point for mobile WiMAX.

5) **WirelessHUMANTM:** Wireless High-Speed Unlicensed MAN is similar to OFDM PHY, this interface uses spectrum below 11 GHz license-exempt bands.

Figure 3.6 illustrates a schematic view of SC, OFDM, and OFDMA concepts. In the single carrier physical layer, the entire frequency channel is given to the MS and time division multiplexing is considered. In the OFDM-TDMA, the subchannels are modulated, the time domain concept is used and one user has access to the channel at a certain time period. And OFDM-FDMA is similar OFDM-TDM, but frequency division multiplexing is used instead of time division multiplexing. OFDMA deploys both time and frequency division multiplexing and the subsets of subcarriers are assigned to the MSs [78].

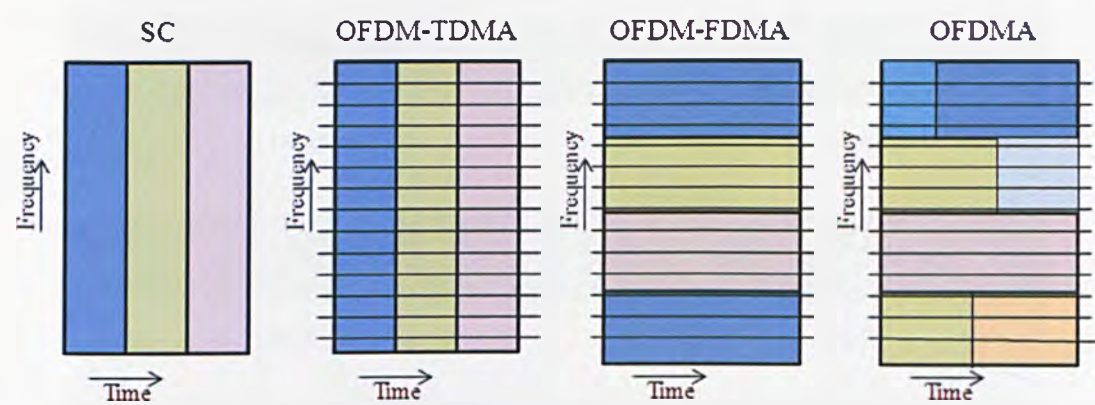


Figure 3.6 WiMAX modulation schemes [78]

The mobile WiMAX PHY provides different type of modulation and coding depends on signal-to-noise (SNR) ratio. It also supports channel bandwidth of between 1.25 MHz and 20 MHz. The BS is able to dynamically adapt the bandwidth, modulation, and coding schemes to overcome the varying SNR. These are summarized in Table 3.1 [71].

Mobile WiMAX uses adaptive antenna system (AAS), multiple input multiple out (MIMO), and adaptive modulation abilities to improve the system capacity, coverage, or throughput.

AAS is a multiantenna technique that includes the antenna array and signal processing modules to adjust antenna radiation pattern dynamically.

MIMO is another signal processing technique that includes at least two transmitter antennas and two receiver antennas to increase the system capacity [72, 74].

Rate ID	Modulation level (Coding)	Information (Bits/Symbol)	Min Required SNR
0	BPSK (1/2)	0.5	6.4
1	QPSK (1/2)	1	9.4
2	QPSK (3/4)	1.5	11.2
3	16QAM (1/2)	2	16.4
4	16QAM (3/4)	3	18.2
5	64QAM (2/3)	4	22.7
6	64QAM (3/4)	4.5	24.4

Table 3.1 Modulation and coding schemes [71]

3.2.3 Data link layer

WiMAX data link layer supports point to multi point system. The Media Access Control (MAC) comprises of three sub-layers as follows:

- (i) Service Specific Convergence sublayer (CS)
- (ii) Common Part Sublayer (CPS)
- (iii) Security Sublayer (SS)

The service specific convergence sublayer (CS) which provides all transformation and mapping of external network data that comes from upper layers, received by the CS Service Access Point (CS-SAP), and converted into MAC Service Data Units (SDUs), then MAC-SDU will be passed to the MAC common part sublayer (CPS) through the MAC SAP and MAC SDUs will be associated to the proper MAC service flow

identifier (SFID) and connection identifier (CID) which is shown in Figure 3.7. Multiple CS specifications are provided for interfacing with various upper layer protocols.

The internal format of the CS payload is unique to the CS, and the MAC CPS does not require understanding the format or parsing any information from the CS payload [76].

The convergence sublayer handles the higher layer protocols and is classifying external network service data units (SDU) and associating them to the proper service flow identified by the CID. The CS is also called the kernel of MAC layer which prepares a connection oriented communication. The common part sublayer provides channel allocating, connection establishing and connection maintaining. In other words, the QoS and scheduling parameters can be implemented in this sublayer.

The security sublayer's duties are authentication, secure key exchange and encryption. The below protocols are used by the security sublayer:

- A) Encapsulation protocol
- B) Privacy key management (PKM)

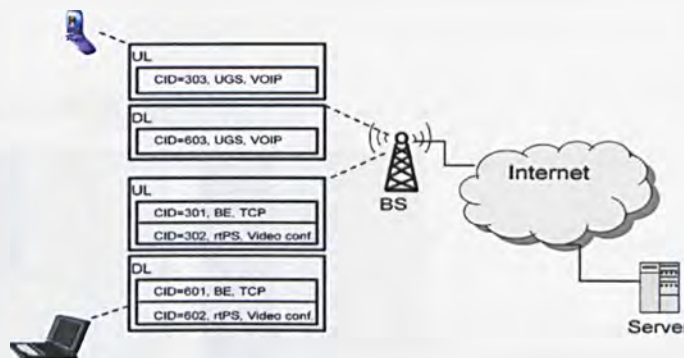


Figure 3.7 CID and QoS class in MAC layer [39]

A WiMAX frame structure is divided into two subframes:

- (i) Downlink subframe
- (ii) Uplink subframe

The downlink subframe is used by the BS to send data and control information which is provided to the SSs and the uplink subframe is shared by all SSs for data transmission. Figure 3.8 shows the WiMAX frame structure [8, 9, 76]. This figure

illustrates WiMAX MAC frame, transmit/receive transition gap (TTG), and receive/transmit transition gap (RTG) concepts.

Duplexing scheme in WiMAX is provided by Frequency Division Duplexing (FDD) or Time Division Duplexing (TDD). In each FDD frame, both Uplink and Downlink subframes simultaneously exist on separate frequency but in the TDD frame the Uplink subframe follows the downlink subframe with specified timing gap.

Each burst frame includes several MAC frames. And the maximum length of the MAC PDU is 2048 bytes. MAC packet data unit (MPDU) consists of MAC service data units (MSDUs) which are received from upper OSI layers by convergence sublayer, and then the MAC common part sublayer is sending the MPDUs to PHY layer. Each MPDU begins with a fixed length generic MAC header which may be followed by a payload. The MPDU may also contain a cyclic redundancy check (CRC), as shown in Figure 3.8 [21, 76].

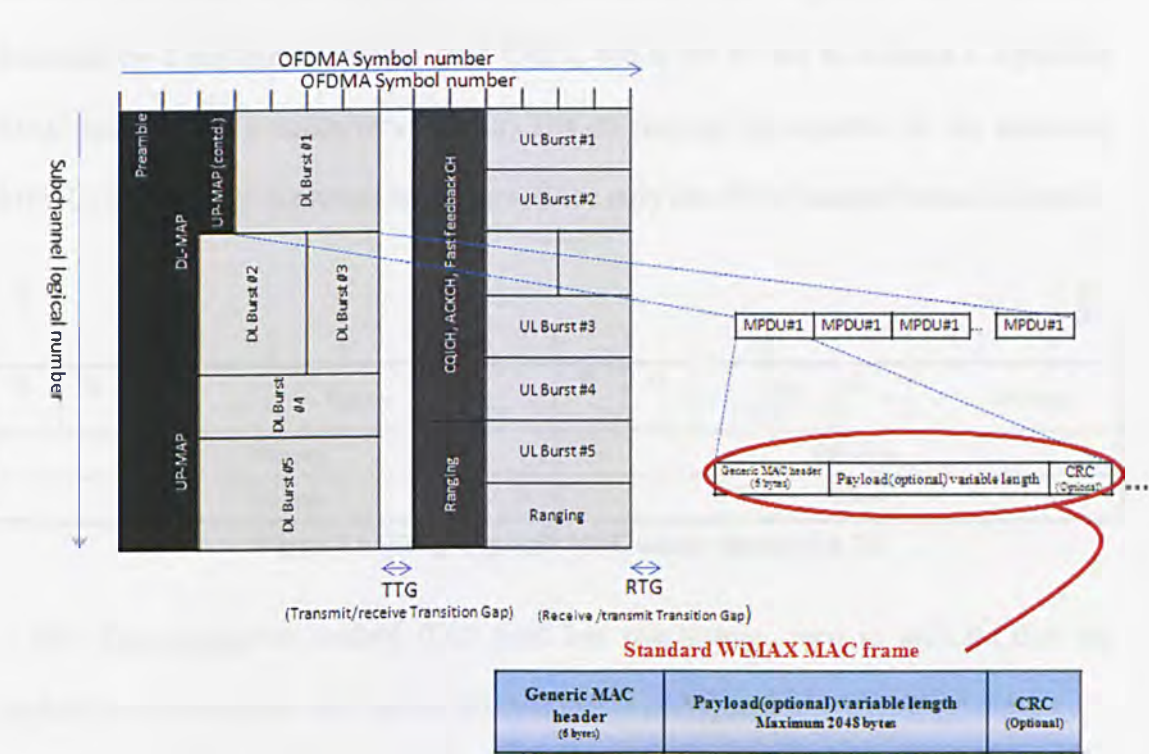


Figure 3.8 WiMAX frame structure [21, 39, 73, 74]

The MPDU can have subheader which follows the generic MAC header; there are seven types of subheaders for different usages as follows:

- 1) Grant management subheader (GMSH)
- 2) Fragmentation subheader (FSH)
- 3) ARQ feedback subheader
- 4) Packing subheader (PSH)
- 5) Fast feedback allocation subheader (FFSH)
- 6) Extended subheader
- 7) Reserved

The generic MAC header includes the following information, shown in Figure 3.9 [39, 76].

HT: The header type (HT) field is used to distinguish the two types of uplink MAC headers. The value of the HT is set to zero to indicate that the generic MAC header is followed by a payload subheader (and CRC), and is set to one to indicate a signalling MAC header (e.g. a bandwidth request) and no payload is required. In the downlink MPDU, the HT field is always set to zero, since only one MAC header format is used.

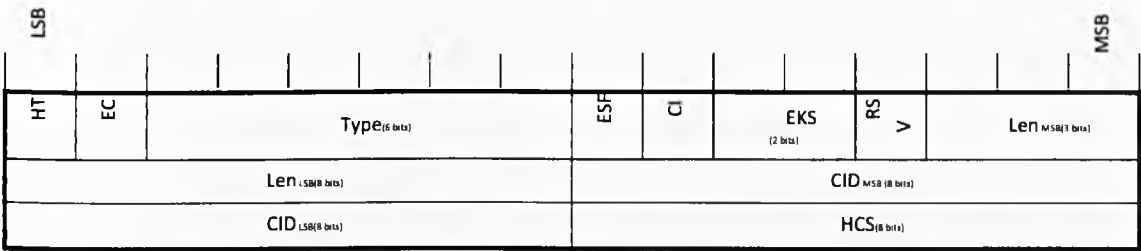


Figure 3.9 WiMAX generic MAC header format [74, 77]

EC: The encryption control (EC) field has two values; zero to indicate that the payload is not encrypted and one to indicate that is encrypted.

Type: This field gives information about the subheaders and special payload types in the payload part.

ESF: The extended subheader field (ESF) is applicable in both the DL and the UL. The ESF indicates if the extended subheader is present or not. If the ESF is zero, the extended subheader is absent. If the ESF is one, the extended subheader is present and will immediately follow the generic MAC header.

EKS: The encryption key sequence (EKS) represents the method of encryption used to encrypt the payload data. It is meaningful only if the EC field is set to one. It should be mentioned here that extended subheaders are not encrypted.

LEN: The length (LEN) field indicates the total length of the MAC PDU in bytes (including the MAC header and CRC data).

CID: The CID is the unique connection identifier assigned to each connection by the BS.

HCS: The header check sequence (HCS) is an eight-bit field used to detect errors in the header. The generating polynomial is given as $x^8 + x^2 + x + 1$.

Figure 3.10 shows another MAC header format which is used for bandwidth request and signal allocation.

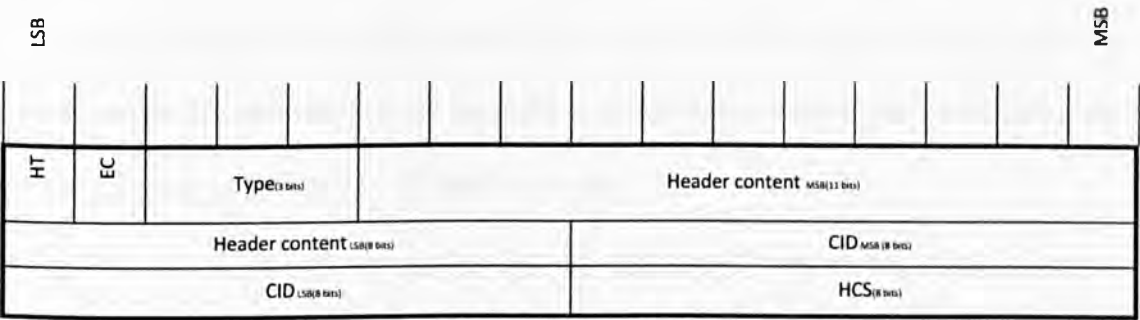


Figure 3.10 MAC signalling header type I format [74]

In this header format, 3 bits-type field define MAC header type that summarises in table 3.2.

<i>Type Field (three bits)</i>	<i>MAC Header Type</i>
000	BR incremental
001	BR aggregate
010	PHY channel report
011	BR with UL Tx power report
100	Bandwidth request and CINR report
101	BR with UL sleep control
110	SN report
111	CQICH allocation request

Table 3.2 Type field in MAC header [74]

3.3 HSxPA network

With the introducing of HSDPA, the significant aspects of the management of the air interface have been moved from the radio network controller (RNC) down into the base station or Node B in 3G terminology. Moving this functionality closer to the air interface means that the 3G system can react more quickly to changes in the quality of the wireless link between the user and the Node B and to the user's data requirements. In turn, this efficient and reactive control allows for higher data throughput and greater cell capacity. High-Speed Uplink Packet Access (HSUPA), sometimes termed Enhanced Uplink, represents the latest 3GPP Release 6 technology and aims to provide optimized packet data support in the uplink. HSUPA provides higher peak data rate, better capacity, low latency, and better coverage [113].

Figure 3.11 shows the evolution line of Universal Mobile Telecommunications System (UMTS) networks. HSUPA is deployed on the top of the WCDMA network either on the same carrier or using another carrier [79].

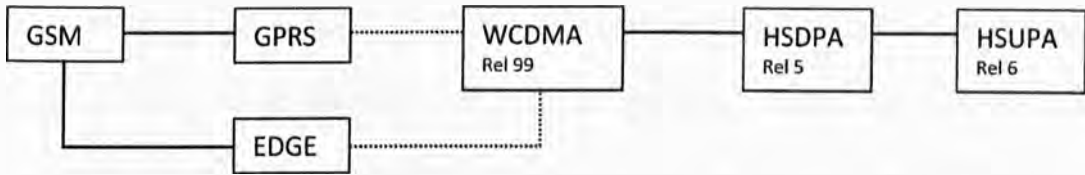


Figure 3.11 UMTS migration path [79]

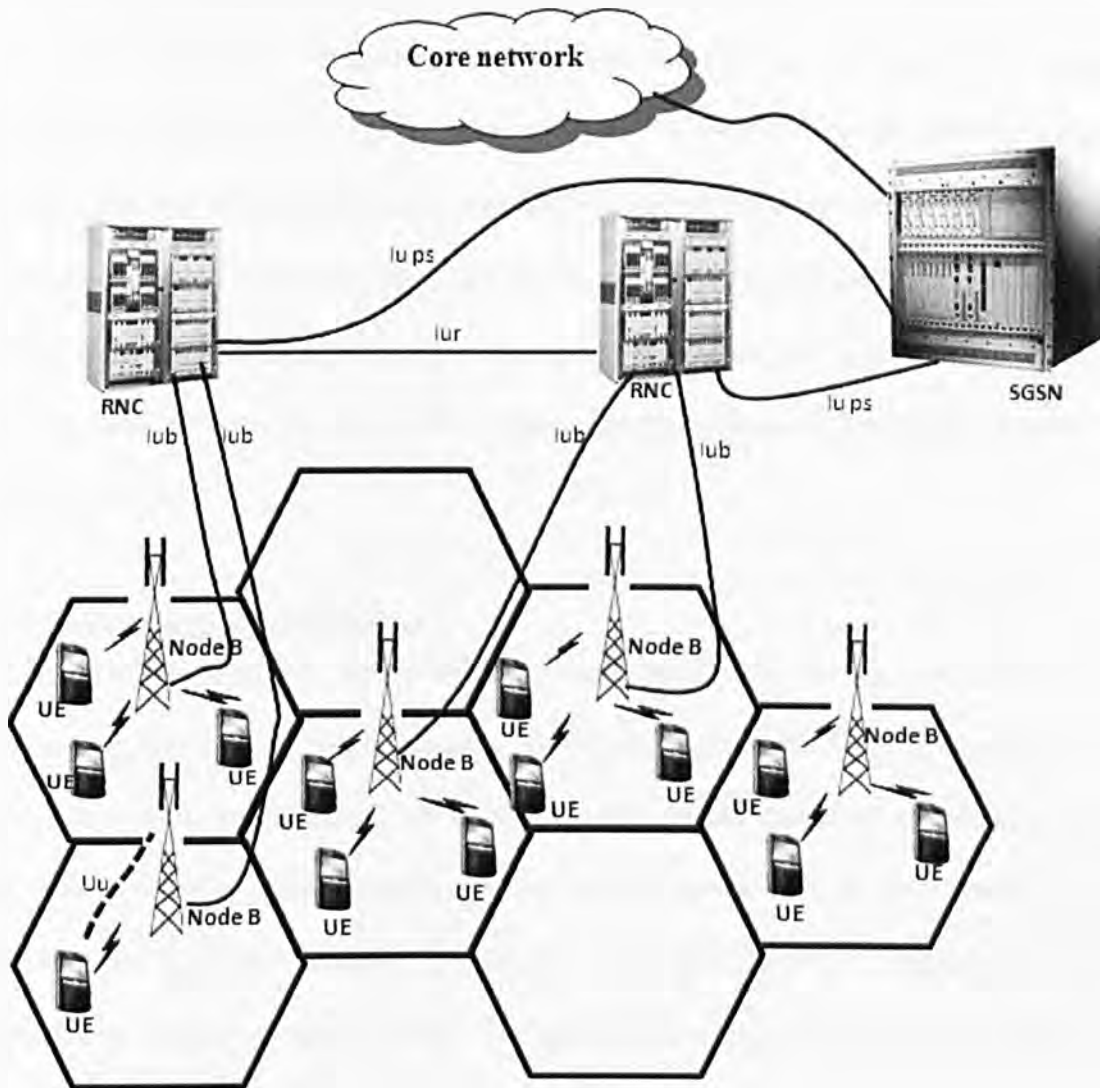


Figure 3.12 HSUPA network [80]

Figure 3.12 illustrates the HSUPA network architecture. The HSUPA includes user equipment (UE), Node B, radio network controller (RNC), and serving GPRS support node (SGSN) [80].

The UMTS core network consists of two domains: the Circuit Switched (CS) service domain and the Packet Switched (PS) service domain. These two domains are responsible for providing appropriate services to the circuit switched traffic such as voice and the packet switched traffic such as web and other Internet Protocol related applications, respectively.

The Node B provides wireless coverage for UEs, the interface between the UE and the Node B is known as Uu. One or more Node Bs are controlled by the RNC through Iub interface, and finally RNCs communicate with core network through the SGSN with Iu-ps interface [80]. A set of RNCs and Node Bs make up a Universal Terrestrial Radio Access Network (UTRAN). The Iu-cs and Iu-ps interfaces are used to connect the UTRAN to the circuit switched service domain and the packet switched service domain respectively.

3.3.1 Technology Specifications

Like HSDPA, HSUPA offers enhanced data rates, fast packet retransmission mechanisms, and reduced packet latencies. The uplink data rate for HSUPA is increased up to a theoretical maximum of 5.76 Mb/s. One of the techniques used to achieve this data rate is adaptive channel coding which adjusts the amount of error correction according to load and channel conditions. And Hybrid ARQ (HARQ) packet transmission techniques and the 2-ms TTI (transmission time interval) also are copied from HSDPA.

HSUPA is the next logical step for improving the throughputs and reducing latency in the 3G networks. Because of the use of dedicated channel per user, HSUPA is more often called as the Enhanced Uplink Dedicated Channel (E-DCH). The traffic scheduling is rather random in HSUPA since all data users are not synchronized with each other, and therefore a common pipe cannot be established by the network for all

users as it does for downlink. The only common resource the system can control is the uplink noise rise.

In a typical UMTS network, under interference limited condition, the downlink is a bottleneck. However, with the introduction of E-DCH, the uplink performance and capacity have been improved especially under conditions with mixed voice and data services on one carrier.

In table 3.3, we compare DCH, HSDPA and HSUPA.

Feature	DCH	HSDPA(HS-DSCH)	HSUPA (E-DCH)
Variable spreading factor	Yes	No	Yes
Fast power control	Yes	No	Yes
Adaptive modulation	No	Yes	No
BTS based scheduling	No	Yes	Yes
Fast LI HARQ	No	Yes	Yes
Soft handover	Yes	No	Yes
TTI length [ms]	80, 40, 20, 10	2	10, 2

Table 3.3 DCH, HSDPA, and HSUPA comparison [79, 80]

It is clear that there are some similarities between HSDPA and HSUPA that can be listed as follows:

- HARQ
- Shorter TTI
- Multiple parallel codes
- Node B scheduling

And the main differences are:

- (i) In HSDPA, all data users share a common traffic channel (HS-DSCH) but in HSUPA, there is a dedicated channel for each user (E-DCH).
- (ii) HSDPA applies link adaptation to control the throughput while HSUPA still uses power control for each individual link.

(iii) In HSUPA the traffic scheduling is rather random since all data users are not synchronized with each other the only common resource that system can control is the uplink noise.

HSUPA supports fast Node B scheduling for uplink, fast HARQs with incremental redundancy, short transmission time interval, and multi code transmission [79]. Table 3.4 lists the important technical features of HSUPA and HSDPA networks.

Technology	HSDPA	HSUPA
Description	High-Speed Downlink Packet Access	High-Speed Uplink Packet Access
Geography	U.S., Europe and Japan initially	U.S., Europe and Japan initially
First commercial deployment	2006	2007
Frequency range	Band VII: 2620 to 2690 MHz Band VIII: 925 to 960 MHz Band IX: 1844.9 to 1879.9 MHz Band II is the same as PCS 1900 Band III is the same as DCS 1800 Band VIII is the same as E-GSM	Band VII: 2500 to 2570 MHz Band VIII: 880 to 915 MHz Band IX: 1749.9 to 1784.9 MHz Band II is the same as PCS 1900 Band III is the same as DCS 1800 Band VIII is the same as E-GSM
Multiple access technology	TDMA/CDMA	TDMA/CDMA
Modulation and filter type	QPSK and 16QAM with RRC filter ($\alpha=0.22$)	BPSK with RRC filter ($\alpha=0.22$)
Channel spacing	5 MHz	5 MHz
Peak single user data rate	Up to 13.976 Mbps	Up to 5.76 Mbps
Primary service	High-mobility cellular High-speed packet data	High-mobility cellular High-speed packet data
Packet switched or circuit switched	Packet switched	Packet switched
Standards development organization	3GPP	3GPP
Reference web site	www.3gpp.org	www.3gpp.org

Table 3.4 HSDPA and HSUPA technical specifications [79, 80]

HSUPA achieves its high performance through more efficient uplink scheduling in the base station and faster retransmission control. The important features of HSUPA can be listed as:

- Maximum transmission rate of 5.76Mbps
- BPSK modulation
- No adaptive modulation
- Multicode transmission
- Spreading Factor either 2 or 4
- 10ms and 2ms TTI but initially only 10ms TTI to be used.
- Hybrid ARQ (HARQ)
- Fast Packet Scheduling in the uplink
- Soft Handover supported

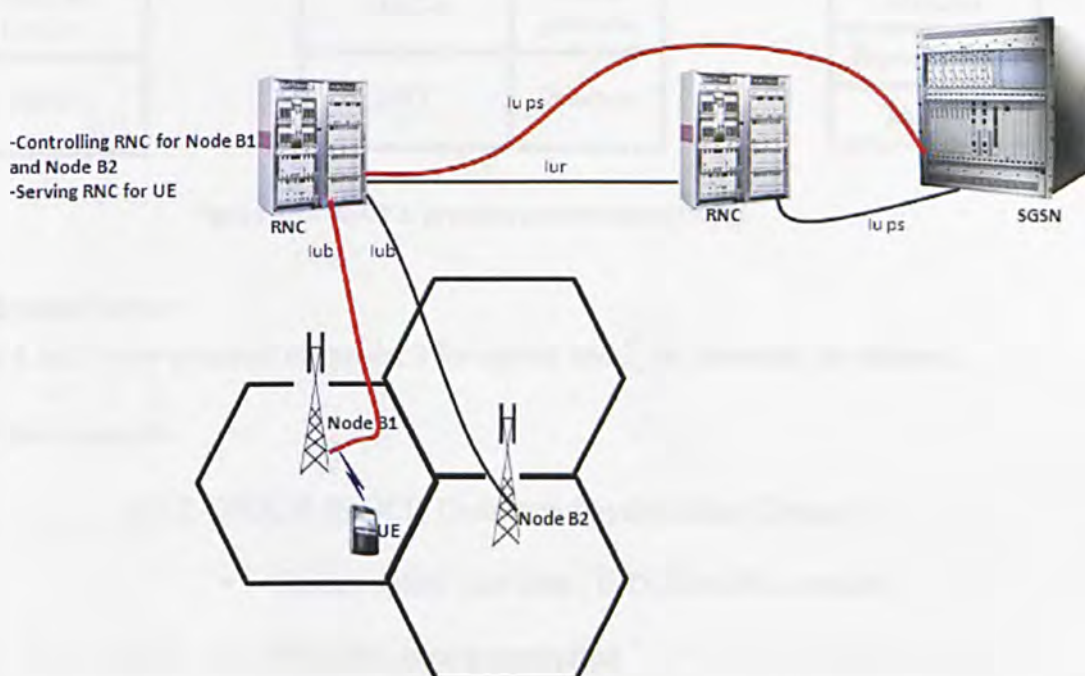


Figure 3.13 Serving and controlling RNC [80]

There are two types of RNC: controlling RNC and serving RNC. The controlling and serving RNC can be different nodes. The controlling RNC is the node that connects to Node B through Iub. The serving RNC is the RNC that provided Iu interface for UE to the core network [80]. Figure 3.13 shows the serving and controlling RNC concept. In

the HSUPA technology, each Node B has a controlling RNC to manage the Node B. And each UE has a serving RNC to manage its UE connection. Figure 3.14 shows HSUPA protocol stack that will be discussed briefly in next sections.

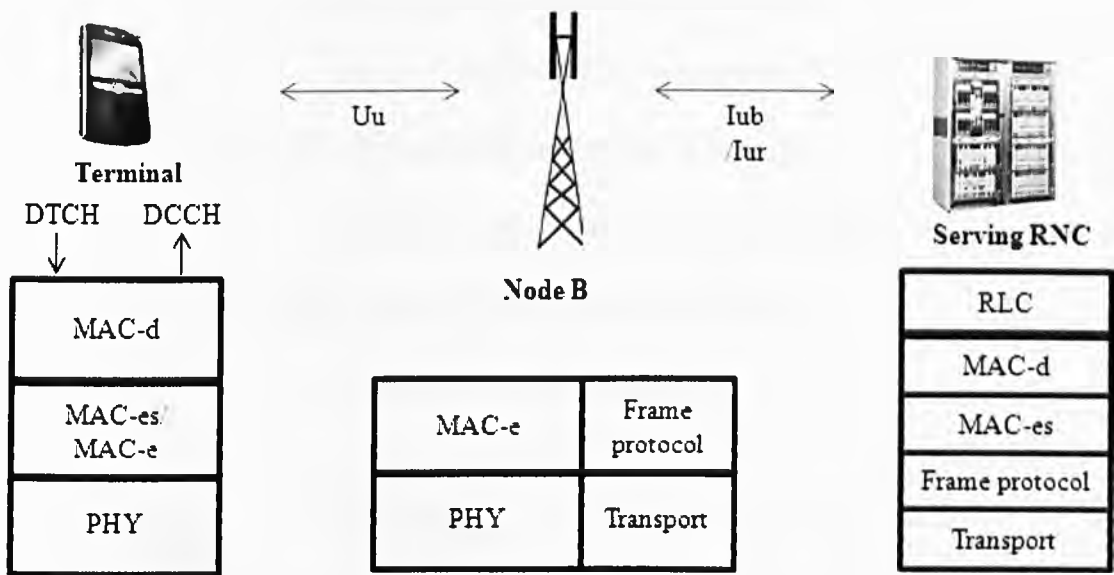


Figure 3.14 HSUPA protocol architecture [79, 81]

3.3.2 Physical layer

HSUPA has 5 new physical channels, 2 for uplink and 3 for downlink as follows:

A) Uplink channels

(1) E-DPDCH (E-DCH Dedicated Physical Data Channel)

- Carries uplink user data / E-DCH traffic channel
- SF 2-256, power controlled
- Number of parallel E-DPDCHs is 1-4

(2) E-DPCCH (E-DCH Dedicated Physical Control Channel)

- Carries uplink control information
- SF 256, power controlled

- Carries E-DCH Transport Format Combination Identifier (E-TFCI), Retransmission Sequence Number (RSN) and a single bit called “happy bit”

B) Downlink channels

(1) E-AGCH (E-DCH Absolute Grant Channel)

- Carries absolute scheduling grants, SF 256

(2) E-RGCH (E-DCH Relative Grant Channel)

- Carries relative scheduling grants, SF 128

(3) E-HICH (E-DCH HARQ Indicator Channel)

- Carries ACKs/NACKs, SF 256

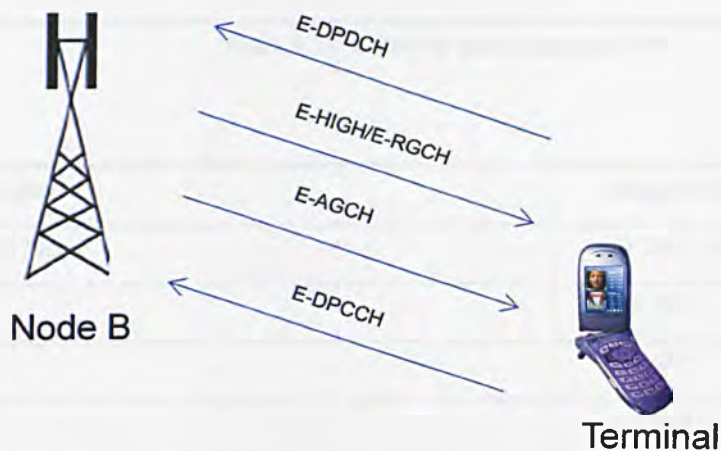


Figure 3.15 Channels needed for HSUPA [79, 80]

Figure 3.15 illustrates different HSUPA channels. The E-DPDCH and E-DPCCH are new uplink physical channels for transmitting data and control signals in 3GPP release 6. E-DPDCH supports OVSFs (orthogonal variable spreading factors) to adjust the number of channels bits to the amount of data. The minimum spreading factor that supports is 2. Table 3.5 summarizes the main features of E-DPDCH channel [79].

The E-DPDCH supports the transmission of two SF2 and two SF4 simultaneously. In other words, it supports 5.76 Mbps bit rate. Table 3.6 presents different combination of SF and channel bit rate in HSUPA.

E-DPDCH features	
Maximum SF	256
Minimum channel data rate	15 kbps
Minimum SF	2
Maximum channel data rate	1920 kbps
TTI length	10 ms , 2 ms
Modulation	BPSK
Maximum number of parallel codes	$2 \times \text{SF2} + 2 \times \text{SF4}$

Table 3.5 E-DPDCH main features [79]

Channel bit rates	Supported SF
15 kbps – 1.92 Mbps	SF256 – SF2
1.92 Mbps	$2 \times \text{SF4}$
3.840 Mbps	$2 \times \text{SF2}$
5.760 Mbps	$2 \times \text{SF4} + 2 \times \text{SF2}$

Table 3.6 E-DPDCH channel bit rates [79]

3.3.3 Transport channel processing

The transport channel processing refers to transform the transport block delivered to the MAC layer to bits on the physical layer. Figure 3.16 shows the function blocks of transport channel processing that the main functions can be listed as follows [79]:

- (i) CRC attachment: A 24-bit CRC is attached to transport data block.
- (ii) Code block segmentation: The transport block is split to equal size of code block.
- (iii)Channel coding: Turbo coding with code rate of 1/3 is used.

- (iv)Physical layer HARQ: produces different redundancy version for incremental redundancy by matching the channel code output bits to the available physical channel bits.
- (v) Physical channel segmentation: distributes channel bits to more than one E-DPDCH if needed.
- (vi)Interleaving and physical mapping: interleaves and maps bits to radio frame.

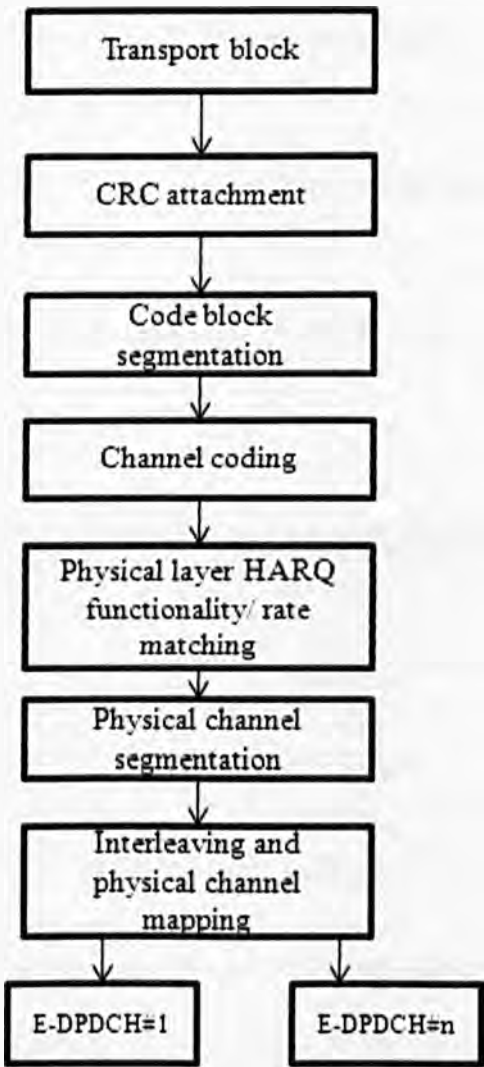


Figure 3.16 Transport channel processing [79]

The HSUPA standard doesn't support adaptive modulation, because the data rate is high enough and the higher order modulation needs more energy per bit. Therefore, the HSUPA supports BPSK (bit shift keying) modulation with multicode transmission.

However, in the downlink, the usage of higher modulation can provide higher data rate with no extra transmitted power of HSDPA [79].

This standard supports fast L1 HARQ, with the similar concept of HARQ in HSDPA, but the main difference between HARQ with HSUPA and HARQ with HSDPA is that HSUPA HARQ is fully synchronized with incremental redundancy [79].

HSUPA includes three MAC-layer protocols as follows [79, 81]:

- (i) MAC-e: Controls HARQs and scheduling between UE and Node B,
- (ii) MAC-es: Reorders PDUs and provides in-sequence delivery in case of soft handover between UE and SRNC.
- (iii) MAC-d: Multiplexes different services into a single transport channel in UE and SRNC

Table 3.7 shows the different categories of HSUPA and the corresponded uplink speed.

HSUPA Category	Max uplink speed
Category 1	0.73 Mbit/s
Category 2	1.46 Mbit/s
Category 3	1.46 Mbit/s
Category 4	2.93 Mbit/s
Category 5	2.00 Mbit/s
Category 6	5.76 Mbit/s

Table 3.7 HSUPA categories

The HSUPA scheduler at the node B is request-grant based. The UE sends a request for transmission, and the scheduler decides when and how many UEs are allowed at the scheduling turn, and how much power is allocated to each of them.

There are two types of grant as follows:

- (i) Absolute grant: will provide a fixed uplink budget that the user can utilize

(ii) Relative grant: will notify the user to increase or decrease its current uplink power

The overall performance of HSUPA will be highly dependent on how effectively the scheduler manages the traffic flow while minimizing the uplink interference at the same time.

3.4 QoS in Mobile WiMAX and HSxPA networks

In this section, we provide a summary of the QoS in both mobile WiMAX and HSxPA networks in conjunction with the relevant m-QoS issues discussed in section 2.3. In general, QoS refers to different parameters that present different types of network traffic, network status, and the quality of experience which a user will encounter. QoS variables depend on specific application, the required thresholds, and traffic specifications. Most of the applications use bit error rate, jitter, latency, PSNR, and throughput as basic QoS variables. To meet these QoS requirements, BS, Node-b, or RNC should have a suitable mechanism for resource allocation, resource management, and network configuration. In the following sections, we describe briefly the QoS features of both Mobile WiMAX and HSxPA networks.

3.4.1 QoS in Mobile WiMAX

The IEEE.802.16/WiMAX standard does not specify any specific resource allocation algorithm and the equipment suppliers have their own mechanisms and relevant algorithms to adapt. There are examples such as Fair Scheduling, Distributed Fair Scheduling, Max Min Fair Scheduling, Energy Efficient Scheduling, Feasible Earliest Due Date (FEDD), and Channel State Dependent Round Robin (CSD-RR) [78].

The WiMAX QoS control mechanisms include scheduling, bandwidth request, admission control, and bandwidth control [73].

The WiMAX technology is designed to support QoS. However, it is difficult to guarantee QoS in wireless networks. This is due to variable and unpredictable characteristics of wireless networks [39]. To this aim, the WiMAX standard specifies following QoS related concepts: service flow QoS scheduling, dynamic service establishing, and two-phase activation model.

The service flow provides unidirectional packet transport either in uplink or downlink that includes a set of the QoS indices such as latency, jitter, minimum and maximum traffic, and traffic priority. A 32 bit SFID (service flow ID) and the flow direction (uplink or downlink) are assigned to each service flow. The standard defines three types of service flows as follows [74]:

- (i) Provisioned service flow
- (ii) Admitted service flow
- (iii) Active service flow

The provisioned service flow is defined by, for example, network management system and the standard assigns a 32-bit SFID to it. In the admitted service flow, the BS reserves the required resources and this type of service flow has a 32-bit SFID and a 16-bit CID. And finally, in the active service flow, the reserved resources are committed. This service flow also has both 32-bit SFID and 16-bit CID. Figure 3.17 illustrates above concept in an *envelope model* [74]. The 802.16e standard provides the management frames for creating, changing, or deleting service flows known as dynamic service activate (DSA), dynamic service change (DSC), and dynamic service delete (DSD) respectively [39, 74].

In general, mobile WiMAX is a connection oriented system where the base station assigns the 16-bits connection identifier (CID) to each connection or subscriber which is usually shared for the uplink and the downlink connectivity [76].

IEEE 802.16 has five QoS classes that are assigned to each SFID. These QoS classes are classified as follows [23, 39]:

(I) UGS (Unsolicited Grant Scheme): This service class supports constant bit rate. In other words, it has a fixed periodic bandwidth allocation whenever the connection is established. The requirement grant size is calculated by the BS without any further requests or polls. It is suitable for applications with fixed periodic packet size such as VOIP without silence suppression.

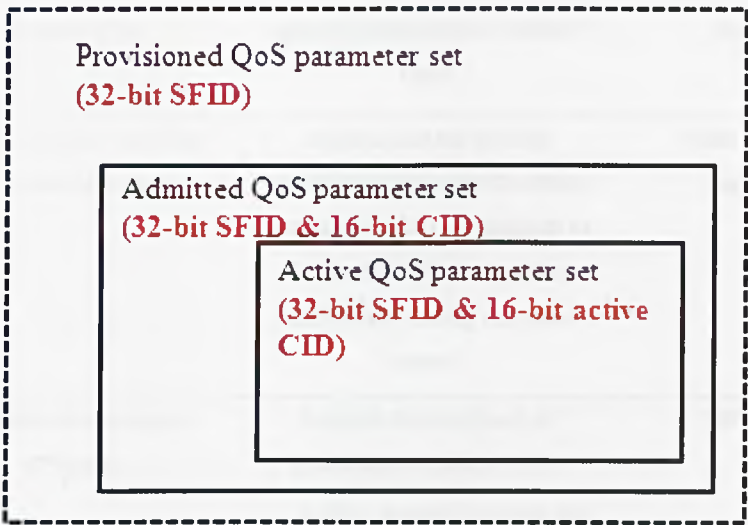


Figure 3.17 WiMAX QoS envelope model [74]

(II) rtPS (Real Time Polling Service): This service class is for real time variable bit rate (VBR) traffic at periodic interval such as MPEG video. The bandwidth is allocated based on the required QoS parameters such as delay or traffic arrival rates. Since the traffic is variable, the BS needs to regularly poll each MS to determine what allocations need to be made.

(III) ertPS (Extended Real Time Polling Service): This service class is based on UGS and rtPS, it is suitable for VOIP with silent period. Unlike the UGS, BS should poll the MS during the silent periods to determine when the traffic will be started.

(IV) nrtPS (Non Real Time Polling Service): This service class is designed for non-real time variable bit rate traffic which the delay is not important. However, minimum band width is guaranteed. This class is usually used for FTP traffic.

(V) BE (Best Effort): This service class is used for data stream with no support for delay or throughput. The telnet and web browser data use this class.

QoS	Pros	Cons	Possible application
UGS	No overhead. Meet guaranteed latency for real-time service	Bandwidth may not be utilized fully since allocations are granted regardless of current need.	CBR voice (no silence submission), circuit emulation
ertPS	Optimal latency and data overhead efficiency	Need to use the polling mechanism (to meet the delay guarantee) and a mechanism to let the BS know when the traffic starts during the silent period.	Voice with silence suppression
rtPS	Optimal data transport efficiency	Require the overhead of bandwidth request and the polling latency (to meet the delay guarantee)	MPEG video
nrtPS	Provide efficient service for non-real-time traffic with minimum reserved rate	N/A	Data application with minimum rate requirements, e.g. FTP
BE	Provide efficient service for BE traffic	No service guarantee; some connections may starve for long period of time.	Data applications with no minimum rate requirements

Table 3.8 Comparison of different WiMAX QoS classes [23, 39]

Table 3.8 shows a comparison of the WiMAX QoS service classes and pros and cons of each service class. In summary, UGS class has a static allocation and ertPS class is a combination of UGS class and rtPS class. Both UGS and ertPS classes can reserve the bandwidth during setup. Unlike UGS class, ertPS allows all kinds of bandwidth request

including contention resolution. rtPS cannot participate in contention resolution. nrtPS and BE classes use several types of bandwidth requests such as piggybacking, bandwidth stealing, unicast polling, and contention resolution.

Table 3.9 shows the QoS parameters which exist in different WiMAX QoS classes. All these parameters become important especially in different m-health applications described earlier in chapter 2. The WiMAX QoS parameters are listed as follows [61, 73, 74]:

- (i) Maximum sustained traffic rate: This parameter defines a maximum bound for the traffic (bits/s) coming from higher layer to WiMAX MAC layer that does not include the MAC overhead.
- (ii) Minimum reserved traffic rate: This parameter defines minimum guaranteed data rate (bits/s) for a service flow. If this parameter is set to zero, it means there is no need for the minimum guaranteed traffic rate.
- (iii) Maximum latency: This specifies the maximum delay of the reception of a packet by BS or SS and forwarding it on the air.
- (iv) Tolerated jitter: This parameter specifies the maximum delay variation of a service flow.

	UGS	ertPS	rtPS	nrtPS	BE
Maximum sustained traffic rate	√	√	√	√	√
Minimum reserved traffic rate			√	√	
Maximum latency	√	√	√		
Tolerated jitter	√	√			

Table 3.9 WiMAX QoS parameters [23, 39]

The traffic priority can be added to these service classes to differentiate the subscribers or the connections even within the same service class.

Figure 3.18 illustrates a model diagram of BS and SS implementation in terms of data traffic and the QoS classes. Each connection associated with a service flow which has its own QoS requirements.

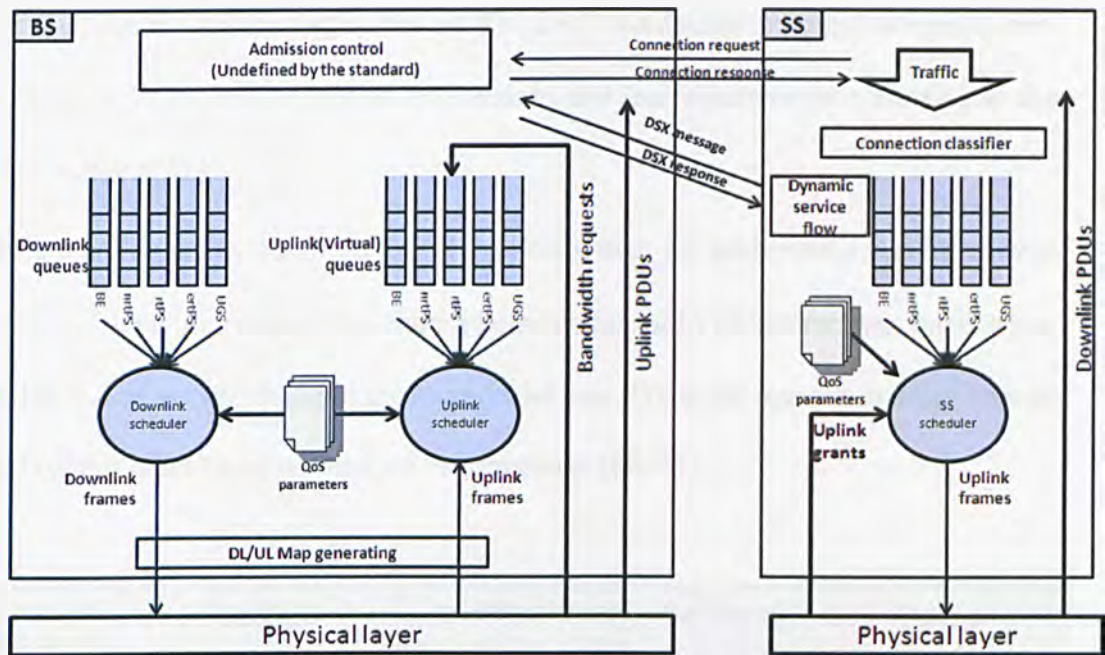


Figure 3.18 Model diagram of WiMAX BS and SS [39, 73]

The BS assigns up to three dedicated connection Identifier (CID) to every MS in initializing phase, the CIDs belong to different quality of service and also allocates the band width according to the MS requirements and its policy. And the MS uses the channel quality information channel (CQICH) to report the DL carrier-to-interference-plus-noise ratio (CINR). In other words, the CQICH is allocated to the MS for transmitting the CINR [76, 78, 82].

3.4.2 QoS in HSxPA network

HSUPA technology is able to achieve the increased individual connection throughputs, increased total cell throughputs, and reduced round trip times that help to improve quality of service experienced by the end-user [80].

The 3GPP defines four general QoS classes [79, 83]: conversational, streaming, background, and interactive. The main QoS parameters that are considered in HSPA networks are GBR (Guaranteed Bit Rate), SPI (Scheduling Priority Indicator), and DT (Discard Timer). Call admission control (CAC) has been located inside the RNC to ensure the desired QoS for traffic classes. The CAC can decide to accept or reject a new flow. Table 3.10 presents different QoS classes and the requirements according to the UMTS standard [81].

The streaming traffic class has a higher priority than the background and interactive classes; all streaming connections should be served prior to all interactive connections, and GBR can be set according to the required bit rate. DT is the maximum delay time in Node-B and it is set based on the QoS requirements [80, 83].

QoS classes	Real-time application	Quality of service requirements		Sample application
		Delay	Packet ordering	
Conversational	Yes	Low	Strict	Voice
Streaming	Yes	Modest	Strict	Video
Interactive	No	Modest	Modest	Web browsing
Background	No	No	No	Data transfer

Table 3.10 UMTS QoS classes and requirements [81]

3.4.3 QoS mapping issues

The effective QoS mapping across different layers is one of the key issues for QoS provisioning. More specifically, end-to-end QoS mapping considers QoS parameters at different layers and provides a cross relation between these parameters. In this work, we focus on QoS of m-health applications specifically on ultrasound video streaming QoS to satisfy the clinical and diagnostic requirements.

Several research works have been reported in the literature to evaluate the current communication technologies' capabilities to provide the required medical QoS by the

telemedicine applications and point out the importance of QoS managements in telemedicine application [84-88]. In all these studies the argument was around three important QoS factors which are the time, the bandwidth, and the quality. And it is well known that in telemedicine application, medical data (especially real time data and emergency data) need to be delivered to the remote end in a timely manner within the available network bandwidth and within the end user required quality (e.g. image quality in video streaming applications).

The classification of the m-health applications can be categorized to the three major traffic classes will be presented in section (5.3). Different m-health scenarios require different sets and levels of m-QoS requirements. In chapter 2, we provided some example of m-health applications and defined its important m-QoS requirements when implemented in an integrated environment [89]. These QoS metrics presented in table 2.2 are bandwidth, timeliness and reliability. In particular for bandwidth metrics the generated data rate of the specific application is considered. For timeliness metrics, the delay element is considered. And finally for reliability the packet loss element is chosen as the most common measurable element for reliability [70]. Next, we present the relevant objective image quality assessment methods selected as applied on the received ultrasound streaming images. These are defined as follows:

1. **Peak signal-to-noise ratio (PSNR)** index which can be defined as following equation [90, 91].

$$PSNR = 10 \cdot \log \left[\frac{255^2}{\frac{1}{NM} \sum_{i=0}^{N-1} \sum_{j=0}^{M-1} (x(i, j) - y(i, j))^2} \right] \quad (3.1)$$

Where $x(i, j)$ refers to the pixel (i, j) in the original image and $y(i, j)$ to the pixel (i, j) in the test image. Both images are size of $N \times M$.

2. **Structural SIMilarity (SSIM)** index which can be defined as in the following equation [91, 92]:

$$SSIM(x, y) = \frac{2(\mu_x \mu_y + c1)(2\sigma_{xy} + c2)}{(\mu_x^2 + \mu_y^2 + c1)(\sigma_x^2 + \sigma_y^2 + c2)}, \quad -1 < Q < 1 \quad (3.2)$$

Where

$$\begin{aligned} \mu_x &= \frac{1}{L} \sum_{i=1}^L x_i, & \mu_y &= \frac{1}{L} \sum_{i=1}^L y_i, \\ \sigma_x^2 &= \frac{1}{L-1} \sum_{i=1}^L (x_i - \mu_x)^2, & \sigma_y^2 &= \frac{1}{L-1} \sum_{i=1}^L (y_i - \mu_y)^2, \\ \sigma_{xy} &= \frac{1}{L-1} \sum_{i=1}^L (x_i - \mu_x)(y_i - \mu_y), \end{aligned}$$

x , y and L represent the original image, the test image and the number of pixels in the portion of the image under processing respectively.

$c1$ and $c2$ are constant values used to calculate the SSIM metric which are equivalent to 6.5025 and 58.5225 respectively. The mean value of the proper number of image subwindows is then calculated (Istepanian et al., 2008). The dynamic range of SSIM is $[-1, 1]$. The best value 1 is achieved if and only if $x=y$.

3. **Mean squared error (MSE)** index that can be defined as following equation:

$$MSE = \frac{1}{NM} \sum_{i=0}^{N-1} \sum_{j=0}^{M-1} (x(i, j) - y(i, j))^2 \quad (3.3)$$

Where $x(i, j)$ refers to the pixel (i, j) in the original image and $y(i, j)$ to the pixel (i, j) in the test image [91]. Both images are size of $N \times M$.

Table 3.11 summarizes the ultrasound video streaming QoS requirements. The m-QoS metrics and functional bounds shown in the table are specified by the earlier

clinical evaluation [91, 94-96].

m-QoS index	Acceptable value
Ultrasound frame size	QCIF (176×144), CIF (352×288), 4CIF (704×576)
PSNR	>35 dB
SSIM	>0.959
MSE	<14.07
Frames per Second:	>5
End-to-end delay	<350ms

Table 3.11 m-QoS for ultrasound video streaming [91, 94-96]

Furthermore, the main quality of service metrics in video streaming is summarized in terms of utilization, packet loss, end-to-end delay and delay jitter. These parameters need to be guaranteed by the network in order to provide a satisfactory video streaming service [30].

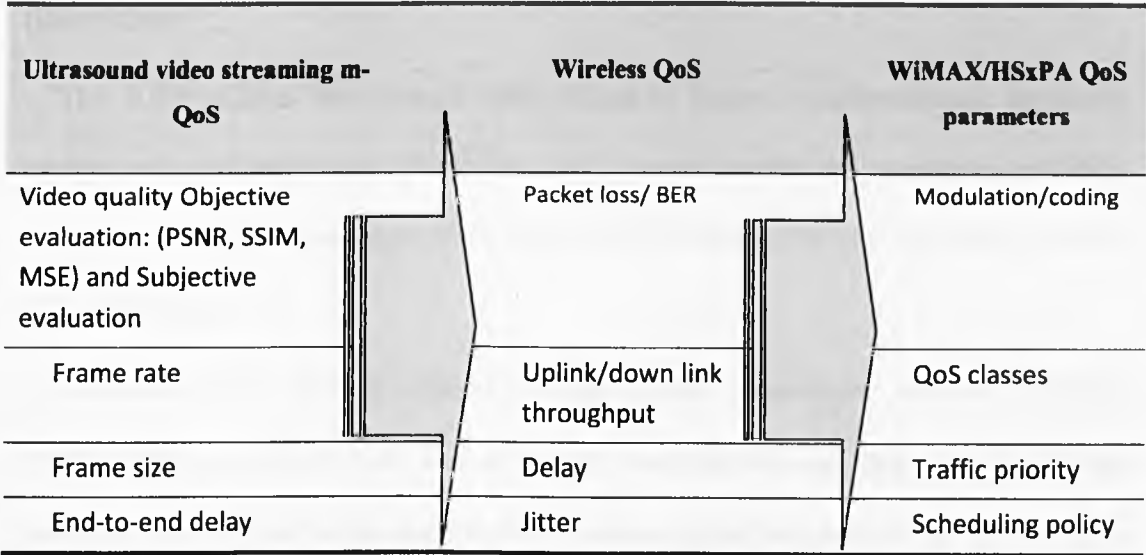


Figure 3.19 Medical QoS mapping for WiMAX and HSxPA networks

From this discussion, it can be concluded that the QoS issues of both network architectures (mobile WiMAX and HSxPA) require different QoS indices that can be matched or cross-mapped with the earlier defined m-QoS. Figure 3.19 illustrates the relevant QoS mapping for both networks. The detailed of parameters will be explained

further in chapter 5.

3.5 Summary

In this chapter, we presented an overview of mobile WiMAX and HSUPA network architectures used in this work. The detailed WiMAX network architecture was introduced that includes the WiMAX physical and data link layer standards. The HSUPA network was also explained in terms of the standard development and layer architecture. The WiMAX and HSPA QoS control mechanisms/features were discussed.

The WiMAX QoS control mechanisms include scheduling, bandwidth request, admission control, and bandwidth control. This technology has five QoS classes as follows: UGS (Unsolicited Grant Scheme), rtPS (Real Time Polling Service), ertPS (Extended Real Time Polling Service), nrtPS (Non Real Time Polling Service), BE (Best Effort).

The 3GPP defines four general QoS classes as follows: conversational, streaming, background, and interactive. The main QoS parameters that are considered in HSPA networks are GBR (Guaranteed Bit Rate), SPI (Scheduling Priority Indicator), and DT (Discard Timer).

In addition, the relevant objective image quality assessment methods including PSNR, SSIM, and MSE have been discussed. And the relevant QoS mapping of both networks were studied in details. Finally, a cross-mapped structure of the QoS of these networks with m-QoS indices was also introduced.

Chapter 4

Optimised Cross Layer Approach for Medical Video Streaming

4.1 Introduction

This chapter presents the optimised cross layer approach designed specifically for ultrasound video streaming application. A complete simulation model of this approach using the OPNET Modeler® is also presented.

The chapter also presents the Q-Learning approach used in the cross layer design approach applied to the medical video streaming.

4.2 Cross layer architecture and design

The most significant cross layer models are shown as follows [40]:

(1) Top-down approach

Figure 4.1 (a) shows a top-down approach: in this model, the upper layers dictate the QoS strategy to the lower layers. In other words, the optimiser takes a decision based upon the application's QoS requirements to reconfigure the MAC layer, and consequently, the optimiser reconfigures the physical layer to provide the required service to the MAC layer. However, this model has been used in the most existing systems and the implementation is relatively simple; it cannot guarantee finding the best solution.

(2) Bottom-up approach

This model is shown in Figure 4.1 (b): In this approach, the optimiser is trying to insulate the upper layers from the lower layers' service variations. The optimiser configures the upper layers based on lower layer states to minimise the side effect of lower layer variations. For example, the application's parameters will be set according to the MAC layer status.

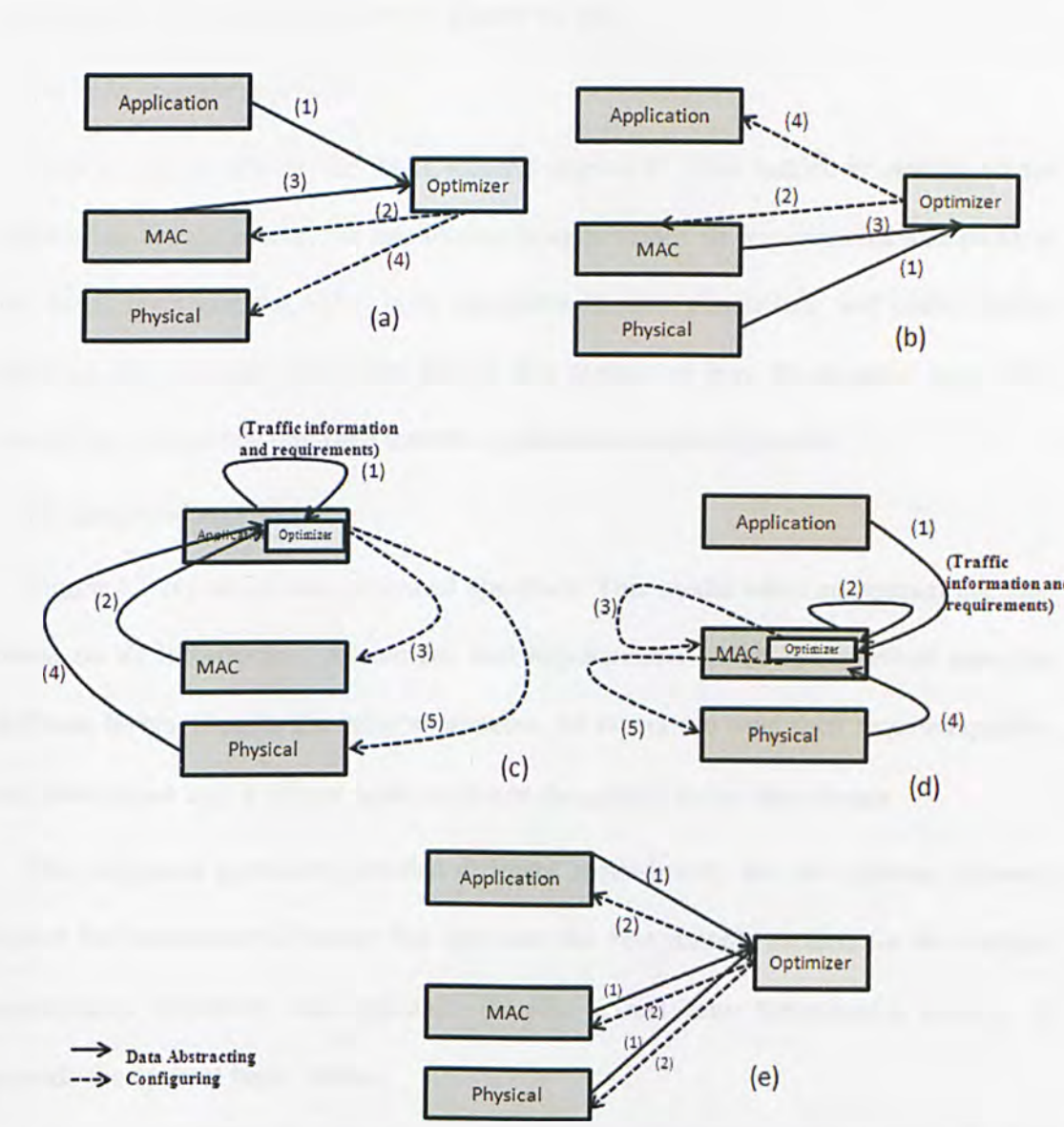


Figure 4.1 Different cross layer approaches: (a) Top-down; (b) Bottom-up; (c) Application-centric; (d) MAC-centric; (e) Integrated [40, 97]

(3) Application-centric approach

In this model, the optimiser which is located in the application layer, reconfigures layers in a top-down (or bottom-up) manner, based on the application layer requirements. However, this model, due to the slower rate of changes in the upper layers rather than the lower-layers, cannot be adapted for the real time changes within the lower layers. This model is shown in Figure 4.1 (c).

(4) MAC-centric approach

Figure 4.1 (d) shows the MAC-centric approach: This model is similar to the application-centric model; the application layer provides its requirements and states to the MAC layer and the MAC layer optimises its own parameters, and consequently, optimises the physical layer according to data abstracted from the physical layer. This model has a faster reaction time than the application-centric approach.

(5) Integrated approach

Figure 4.1 (e) shows the integrated approach: This model takes an optimal decision based on all information, parameters, and requirements which are received from the different layers. Despite the other approaches, all layers can send their required quality, and there is not only a unique layer to dictate the quality to the other layers.

The integrated approach provides different requirements for the different network layers; this characteristic makes this approach the best suitable method for the medical applications. However, this approach requires a real time optimisation method to provide the optimal layer values.

In general, a cross layer can add computation complexities for finding the optimal QoS strategy, because the number of QoS strategies is increasing in comparison to layer architecture. Formulas (4.1), (4.2) and (4.3) show this fact [53].

$$S_{\text{Layerd}} = \sum_{L_i \in L} S_{L_i} \quad (4.1)$$

$$S_{\text{CL}} = \prod_{L_i \in L} S_{L_i} \quad (4.2)$$

Then:

$$S_{\text{Layerd}} \leq S_{\text{CL}} \quad (4.3)$$

Where S_{Layerd} and S_{CL} are QoS strategies in layered and cross layer architecture respectively, and L is set of the layers and L_i is i^{th} layer. In this work, we adopt the reinforcement learning algorithm that requires less computational complexity and suitable for real time m-health applications.

Since the final output which is perceived by users is within the application layer, the CLO for the best solution gives the priority to this layer. However, the optimizing of the other layer also are important.

4.2.1 Cross layer optimizer and Reinforcement algorithm

From the earlier section, it can be seen that the cross layer models require real-time optimization methods especially for wireless broadband medical application. In particular, the key challenge in mobile multimedia streaming optimisation is QoS provisioning with efficient resource utilization [98] whereby video quality is changed in terms of frames per second, frame size and PSNR to optimise the quality of service against varying wireless conditions. Figure 4.2 shows the functional block diagram of a typical wireless video streaming system and the relevant layers. The lower layer is the link layer that includes the MAC layer and physical layer; these depend on the type of wireless QoS classes with supported modulation and coding schemes. Layer 2 and layer 3 prepare end-to-end connectivity and extra error resilience approaches. The upper layer

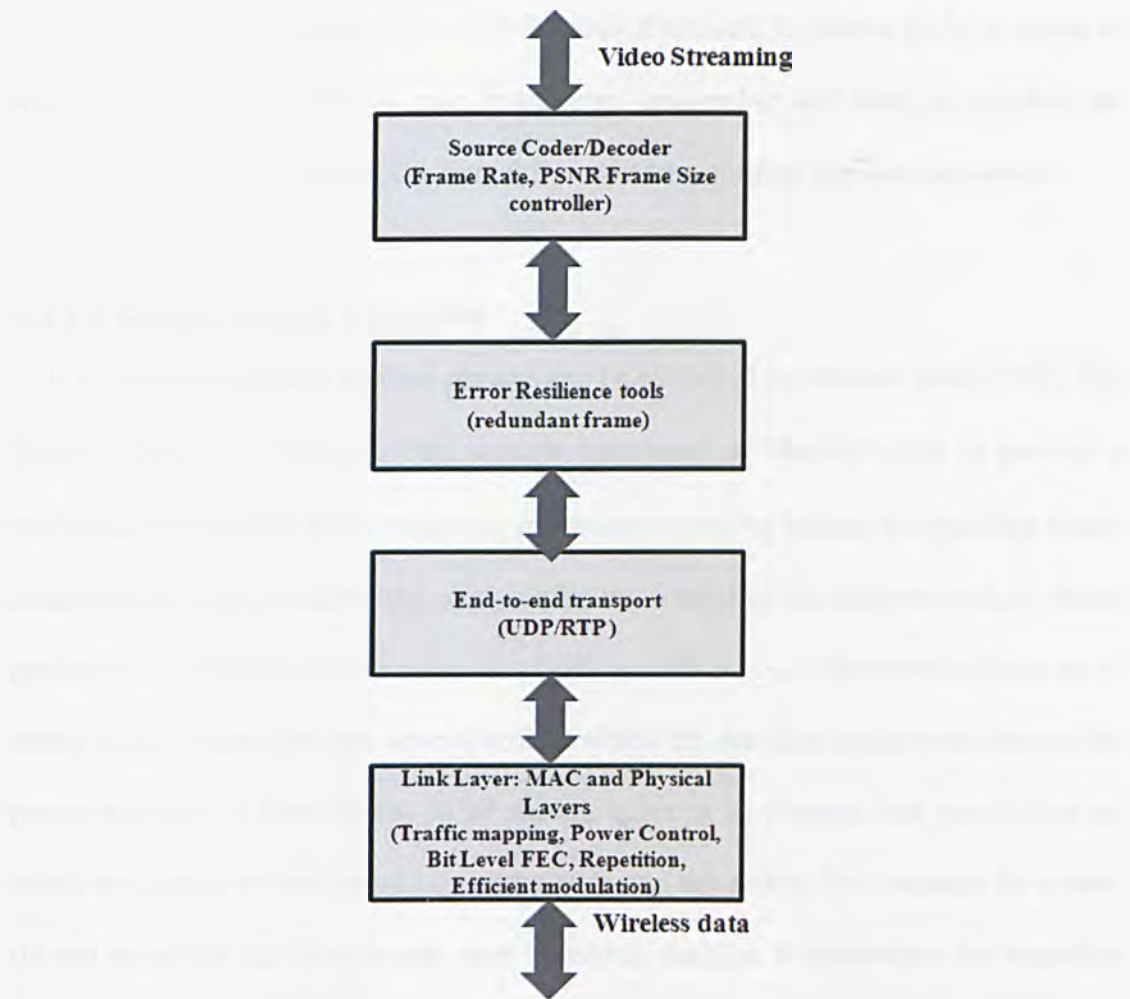


Figure 4.2 General wireless video streaming system [83]

is used to decode/encode video streaming and has rate control to provide optimal video traffic [99, 100]. Since making a decision in one layer sometimes affects QoS parameters in other layers, a cross layer approach is required to consider a complement QoS control approach. Hence the cross layer approach is used to combine the parameters and mechanisms at different layers optimally to find a solution for improved QoS support at given network dynamics and limited resources [34]. A summary of the different cross layer approaches used in mobile multimedia systems was presented in chapter 2.

In this work, we consider the m-QoS issues discussed in section (2.3) in terms of image quality (PSNR), frame rate, frame size, and end-to-end delay to validate the performance of the two networks from the perspective of these relevant parameters.

4.2.1.1 Reinforcement Algorithm

It is well known that a random process can be modelled by Markov chain [101]. The Markov Decision Process (MDP) deploys transitions of Markov chain to provide a mathematical framework for modelling the decision-making process in situations where outcomes are partly random and partly under the control of the decision maker. More precisely, the MDP is a discrete time stochastic control process characterized by a set of states; in each state there are several actions which the decision maker must choose the proper action(s) at time. In the MDP model, agent is an element that can choose an action and gets a reward based on current state and the action. For example for a state (s) and an action (a), the relevant state transition function P determines the transition probabilities to the next state. The decision maker earns a reward (r) (or a penalty) for each state visited. This means that if the current state of the MDP at time step k is known, transitions to a new state at time step $k + 1$ are independent of all previous states. Figure 4.3 illustrates a MDP diagram.

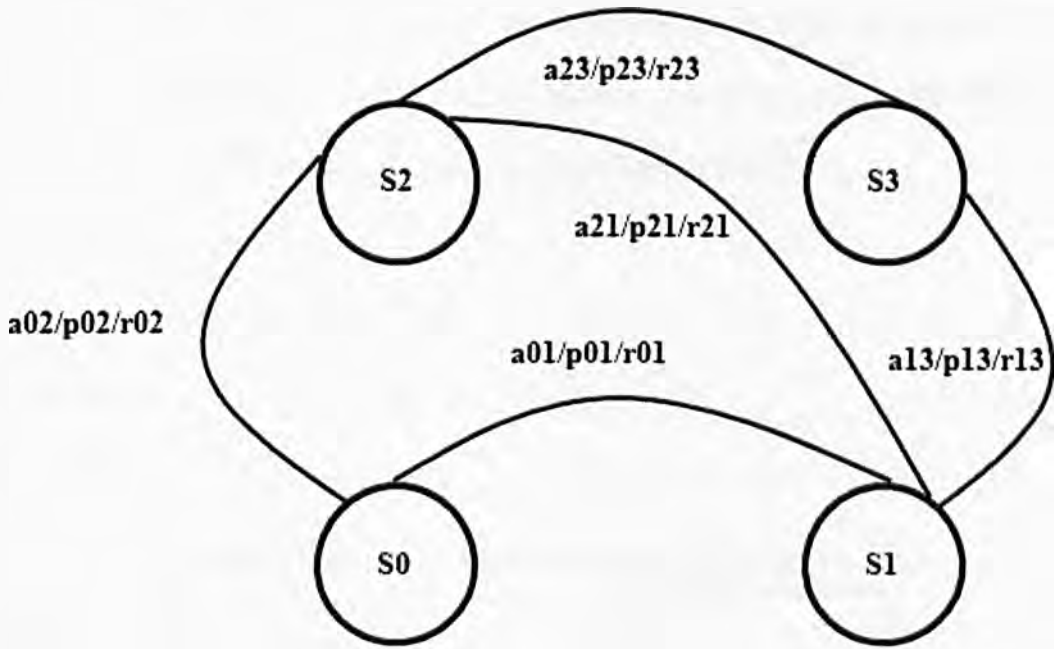


Figure 4.3 A sample MDP diagram

This methodology has been deployed to solve network control problems; but the main issue of deploying this method in the cross layer optimiser is that this model needs an enormously large state space to model the wireless network environment [102]. Consequently, the resultant numerical computation is high due to the problem of dimensionality. In addition it requires a priori knowledge of state-transition probabilities. Therefore, many researchers use Reinforcement Learning (RL) algorithms to ameliorate the large state space problems [102]. The most obvious advantage of the (RL) algorithm is that it can approach an optimal solution in real-time operation if the RL algorithm is convergent. One of these real-time (RL) algorithms is the Q-learning approach. The principle of the Q-learning approach is based on a trial agent that tries an action at a particular state, and evaluates its consequences in terms of the immediate rewards or costs that receives and its estimation of the value of the state to which it is taken [103]. By trying all actions in all states repeatedly, it learns the overall best actions, judged by long term discounted return and without knowing the state-transition probability.

The RL includes an agent to interact with the environment, algorithm to learn the status, and analyse their performance. The RL agent is in charge of solving the Markov decision problem (MDP) which includes following elements [101]:

- (i) States
- (ii) Actions
- (iii) Transition
- (iv) Reward

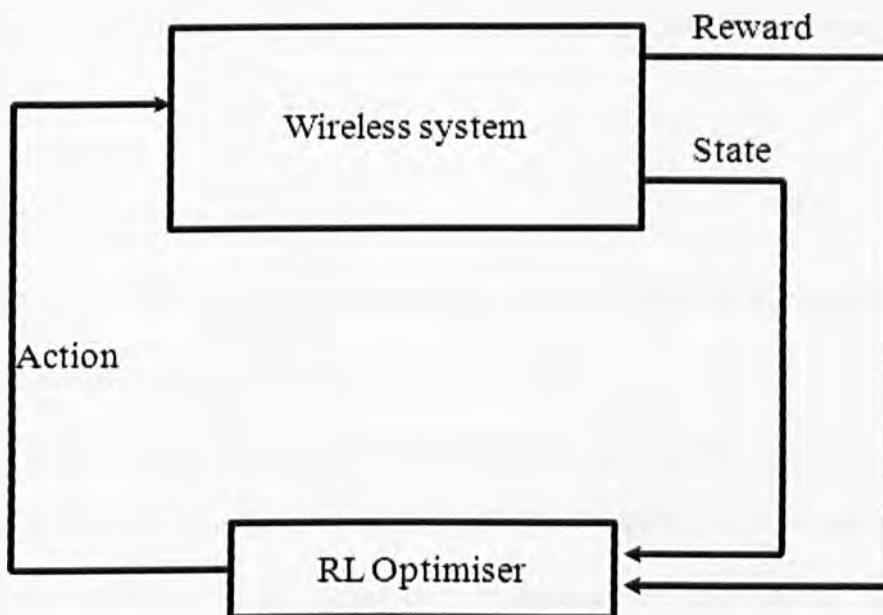


Figure 4.4 The basic RL model [104]

In Q learning approach, there is a table called Q that maps learning knowledge to set of possible states and actions. Usually the rows of the table represent the states and the columns represent the actions. In other words $Q[s,a]$ means the Q value of state 's' and action 'a' of Q-table. Figure 4.4 illustrates the basic structure of RL model. The RL algorithm can be summarised in the following tasks [105]:

Task 1: Recognizing the system state at time step k

Task 2: The optimiser will determine an *action* (A_k) based on the system state S_k .

The action A_k in the wireless network case includes a combination of modulation type, coding rate, PSNR, and frame rate.

Task 3: The state-action pair (S, A) will be determined then an immediate cost or reward $c(S, A)$ is defined.

Task 4: The objective of the agent is to discover an optimal action (A) corresponding to the state (s), which satisfies some cumulative measure of the cost/reward function $c_k = c(S_k, A_k)$ received over time. An evaluation function, denoted by $Q(S, A)$, which is referred as the total expected reward (or cost) from the initial state-action pair (S, A) over an infinite time/action, is given by

$$Q(S, A) = E \left\{ \sum_{k=0}^{\infty} \gamma^k c(S_k, A_k) \right\} \quad (4.4)$$

Where E is the expectation function and $0 \leq \gamma < 1$ is called the discount factor that is experimentally selected as $\gamma = 0.8$.

Then an algorithm is designed to determine an optimal action in state S which maximizes the Q -function represented in Eq. (4.4) above. In this work, the scenario of the maximization of the Q -function represents the achievement of the m-QoS requirements defined in chapters 2 and 3. Based on the Bellman's theory in Dynamic Programming [103], there is at least one optimal policy that satisfies the maximization of the Q -function represented in (4.4), which is $Q^*(S, A)$.

Hence, Eq. (4.4) can be re-written as:

$$Q^*(S, A) = C(S, A) + \gamma \sum_y P_{sy}(A) \max_B (Q^*(y, B)) \quad (4.5)$$

Where $C(S, A) = E\{c(S, A)\}$.

Eq. (4.5) indicates that the Q -function of the current state-action pair can be represented in terms of the expected immediate cost of the current state-action pair

$(C(S,A))$ and the maximum Q-function of the next state y and action B . $P_{sy}(A)$ is the state transition probability from state s with action A to the next state y .

Since it is difficult to find the state transition probability $P_{sy}(A)$ to solve equation (4.5). The Q-learning approach, allows the optimal rate control to be achieved without a priori knowledge of $P_{sy}(A)$ [103]. And it does not require a priori knowledge of the state transition probabilities. To find the optimal $Q^*(S,A)$, the Q-learning algorithm computes the values of (Q) using available information $(S, A, c(S,A))$, where S is the current states. A and $c(S,A)$ are the action for current state and its immediate cost of the state-action pair respectively. The Q-learning rule is defined as:

$$Q(S,A) = Q(S,A) + \alpha \Delta Q(S,A) \quad (4.6)$$

where α is the learning rate $0 \leq \alpha \leq 1$ (α in this work is chosen to be 0.5).

And

$$\Delta Q(S,A) = c(S,A) + \gamma \max_B Q(y,B) - Q(S,A) \quad (4.7)$$

Since only one state-action pair is chosen for evaluation in each learning period, for the Q-learning rule, only the Q value of the chosen action pair is updated, while others are kept unchanged. The main advantage of Q-learning method is that it allows dynamic adaptation. In (4.7) the operation of $\max_B Q[(y,B)]$ is executed by comparing the Q values of all the possible action candidates for state (y) and then choosing the desired action (B) with maximal (Q) value.

In this work, we use Eq. 4.8 to modify the Q table as an immediate consequence of a decision.

$$Q(S,A) = Q(S,A) + \alpha [c(S,A) + \gamma \max_B Q(y,B) - Q(S,A)] \quad (4.8)$$

4.2.1.2 Data abstraction

The other relevant issue within the cross layer design that needs clarification is the data abstraction. In the cross layer architecture the layer parameters are categorised to four groups [35, 44, 46]:

- (i) Directly Tuneable (DT) e.g. Time slot assignment in a TDMA
- (ii) Indirectly Tuneable (IT) e.g. Bit-error rate depends on coding
- (iii) Descriptive (D) e.g. SNR
- (iv) Abstract (A) e.g. Frame-loss probabilities derived from channel state transition probabilities of Gilbert-Elliot model

The parameters which are used in the cross layer optimizer are chosen from application, data link and physical layers as shown in table 4.1. The optimiser makes an optimum solution for the requested quality of service which can be affect different layers configuration [40].

Layer	Parameters
Application	PSNR, Coding
Data link	FEC, ARQ, CQI, SNR, BER
Physical	Modulation, Coding

Table 4.1 Cross layer QoS parameters

In this work, the video quality is abstracted from application layer in terms of frames per second, PSNR, and frame size which considers 5, 10 and 20 fps (frames per second) with 3 different frame sizes as follows:

- (i) QCIF (Quarter Common Intermediate Format)
- (ii) CIF (Common Intermediate Format)
- (iii) 4CIF ($4 \times$ CIF).

Figure 4.5 illustrates the general architecture of the data abstraction process representing the input for cost/reward function used in this work. This function returns a numerical index that can be used in the cross layer optimiser architecture.

The quality index is estimated at the sender's end by comparing the compressed image frame with the original image frame. The quality index used here is the PSNR indicator. If one assumes that there is some sort of error concealment technique applied at the receiver's end that can detect and correct the error caused by the wireless transmission on the erroneous/ corrupted received images. However, the SSIM index can be used as well, the technique and software used to calculate the SSIM is as in [106].

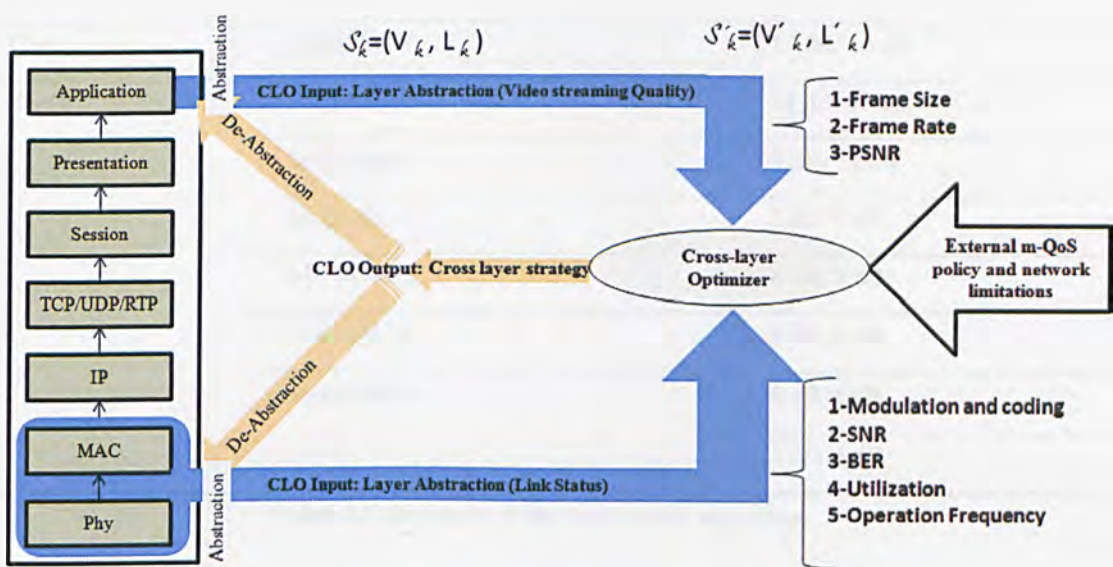


Figure 4.5 Schematic diagram of implemented cross layer approach

A similar technique used by [107] is another option that can be used to measure the received image quality based on non-reference techniques where there is no need for the image before transmission to be available for quality measurement and comparison. This value of the received image quality can be fed back to the sender and by using some sort of modeling, the current image quality can be predicted based on the quality

measures of the previous images and hence the rate control algorithm can be modified accordingly. However, such option can be pursued in future work.

Tables 4.2 and 4.3 show both state and action parameters respectively that are used in the RL optimisation approach.

In this work, 216 states, and 8 actions for each state were used. These were determined experimentally. The formulation of the initialization of the reward matrix is considered a critical part of the reinforcement algorithmic approach and it affects the performance of the learning process.

PSNR (2bits)	Modulation and coding (3bits)	SNR groups (4bits)
35 dB	QPSK1/2	15 dB : 18 dB
37 dB	QPSK3/4	13 dB: 15 dB
40 dB	16-QAM1/2	11 dB: 13 dB
	16-QAM3/4	9 dB: 11 dB
	64-QAM1/2	7 dB: 9 dB
	64-QAM2/3	6 dB: 7 dB
	64-QAM3/4	5 dB: 6 dB
	64-QAM5/6	4 dB: 5 dB
		3 dB: 4 dB

Table 4.2 Segments of the State in RL algorithm

Modulation & coding	Video quality (PSNR, frame rate, frame size)
Increasing	Increasing
Decreasing	Decreasing
No-change	No-change

Table 4.3 Segments of the Action in RL algorithm

4.3 Implementation of proposed cross layer

As explained in the earlier section, we adopted the Q-learning as a Reinforcement Learning (RL) method to find the best action for different cross layer parametric variations. In this approach, RL agents learn how to act so as to maximise a numerical reward signal. The process of optimising in the cross layer is based on a discrete-time Markov Decision Process (MDP), which is a stochastic process modelled by a finite number of states S . For each state S , a finite set of actions A is possible. By selecting the action $\alpha_k \in A$ at the time step k , we incur a cost/reward $c(S_k, \alpha_k)$; The schematisation of this method is shown in Figure 4.6. A policy in the agent (π) is in charge of the assignment of an action α_k in correspondence with the state S_k at each time step k . The cross layer optimiser acts as the decision maker, known as the agent that monitors the environment state and assigns actions accordingly. When the agent releases this action, the environment's state changes; the agent receives the new environment's state and immediate reward or cost as a consequence of the previous action. Based on this information, the agent updates its knowledge database.

The process is repeated until the agent reaches an optimal policy π that assigns optimal actions leading the environment to a state that satisfies the system requirements. The objective of the agent is to find an optimal policy resulting in the action α_k for each S_k , which satisfies the cost function [31, 32, 97].

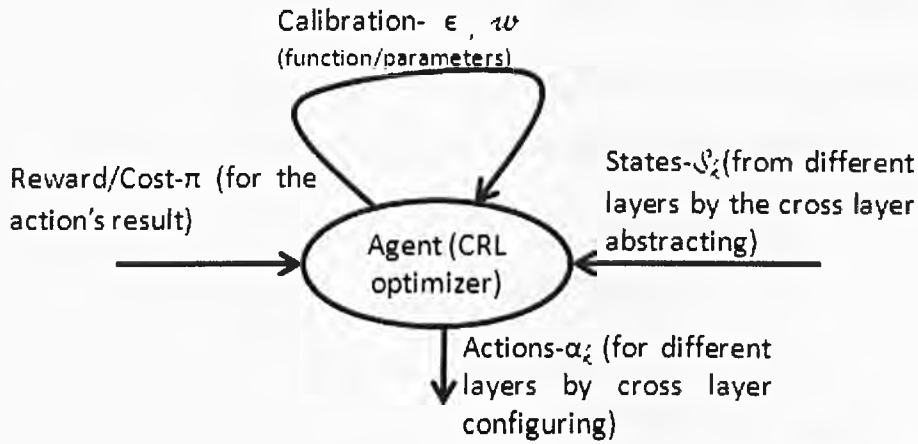


Figure 4.6 Schematisation of the CRL algorithmic approach

The principle of the Q-learning approach is based on a trial and repeat process. The agent tries an action at a particular state and evaluates its consequences in terms of the immediate rewards or cost it receives then estimates the value of the state to which it is taken. By trying all actions in all states repeatedly, the Q matrix will be created to be referred for finding the best action in a specific situation. The Q matrix and Reward matrix are monitored to be updated if required [31, 32, 97].

After indicating the legal actions and states for every possible state and action, we will calculate its cost by a cost function which is defined in equation (4). If the state-action pair (S_k, α_k) has been determined, an immediate cost is defined by the cost function [47]. S_k includes video stream quality and link quality (V_k, L_k) and S'_k is created after abstracting the state. In total, we use 216 states, and 27 actions for each state, it means cost function needs about 216×27 actions to be ready. This process needs to be carried out at the initialization stage only. Then during the online process, the Q matrix will be scanned and an action will be selected based on the state condition of the system. The Q-relearning process will be carried out as a background process.

Cost function is based on a min-max theory to trade off between different consequences of the operations as shown in equation 4.4. This function represents a multiobjective optimisation design problem with four objective functions.

$$Cost_Function(\mathcal{F}) = Function\ of \begin{cases} Framerate_{Cost} = Max\left\{\frac{Framerate - \epsilon_1}{w_1}, 0\right\} \\ Delay_{Cost} = Max\left\{\frac{\epsilon_2 - Delay}{w_2}, 0\right\} \\ PSNR_{Cost} = Max\left\{\frac{PSNR - \epsilon_3}{w_3}, 0\right\} \\ Imagesize_{Cost} = Max\left\{\frac{Imagesize - \epsilon_4}{w_4}, 0\right\} \end{cases} \quad (4.9)$$

The parameters $\epsilon_1=10$ frame/s, $\epsilon_2= 0.09$ s, $\epsilon_3= 35$ dB, $\epsilon_4= CIF$ are the bounds set for this research work. w_1 , w_2 , w_3 and w_4 are the effect-weight for frame rate, delay, PSNR and image size respectively, and we experimentally identified these values as 2.0, 1.5E-3, 0.1 and 2.0 respectively. The values are derived from comparing the simulation results with different cost-function parameters to find the proper value to satisfy the reinforcement algorithm.

The cross layer optimiser (CLO) uses system feedback approach to recalibrate the CRL algorithm. There is an inherent policy in the RL algorithm to prevent deadlock while finding a convergence in optimal solution. And also the algorithm deploys a statistical strategy to acquire the steady network status [97].

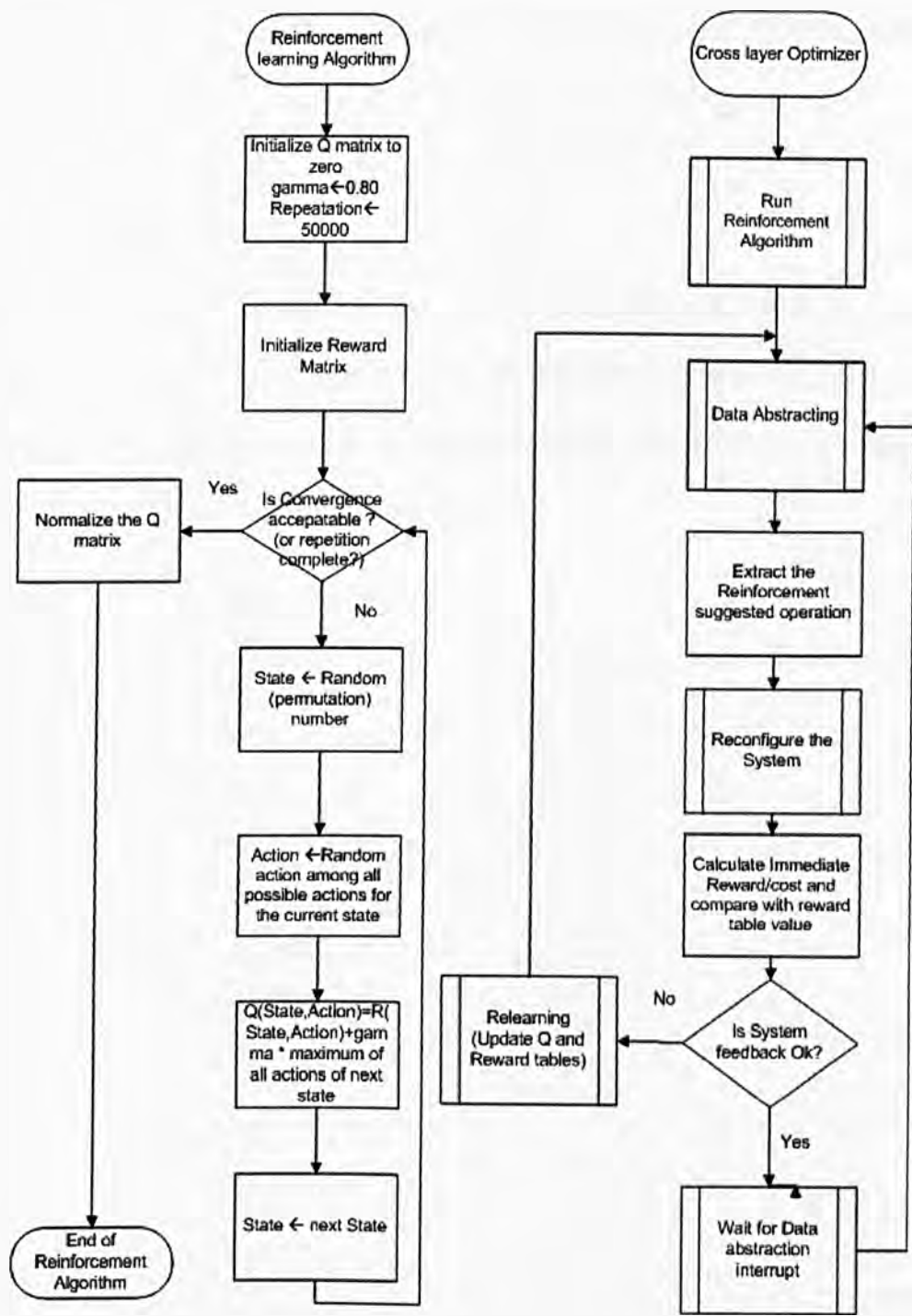


Figure 4.7 (a) Reinforcement algorithm (b) Cross layer optimizer using the reinforcement algorithm

Figure 4.7 (a) illustrates the algorithmic approach of the reinforcement algorithm and Figure 4.7 (b) shows the cross layer optimisation system that uses feedback approach to recalibrate the algorithm.

In the following sub-sections, we present a brief introduction to OPNET Modeler[®] and implementation of the proposed cross layer using this modeller.

4.3.1 OPNET implementation

The project editor in OPNET Modeler[®] has the proper tools to create the required network models as shown in Figure 4.8. The main functions of project cycle includes creating a project, creating baseline scenario, running the simulation, duplicating the scenario, rerunning, and comparing the results.

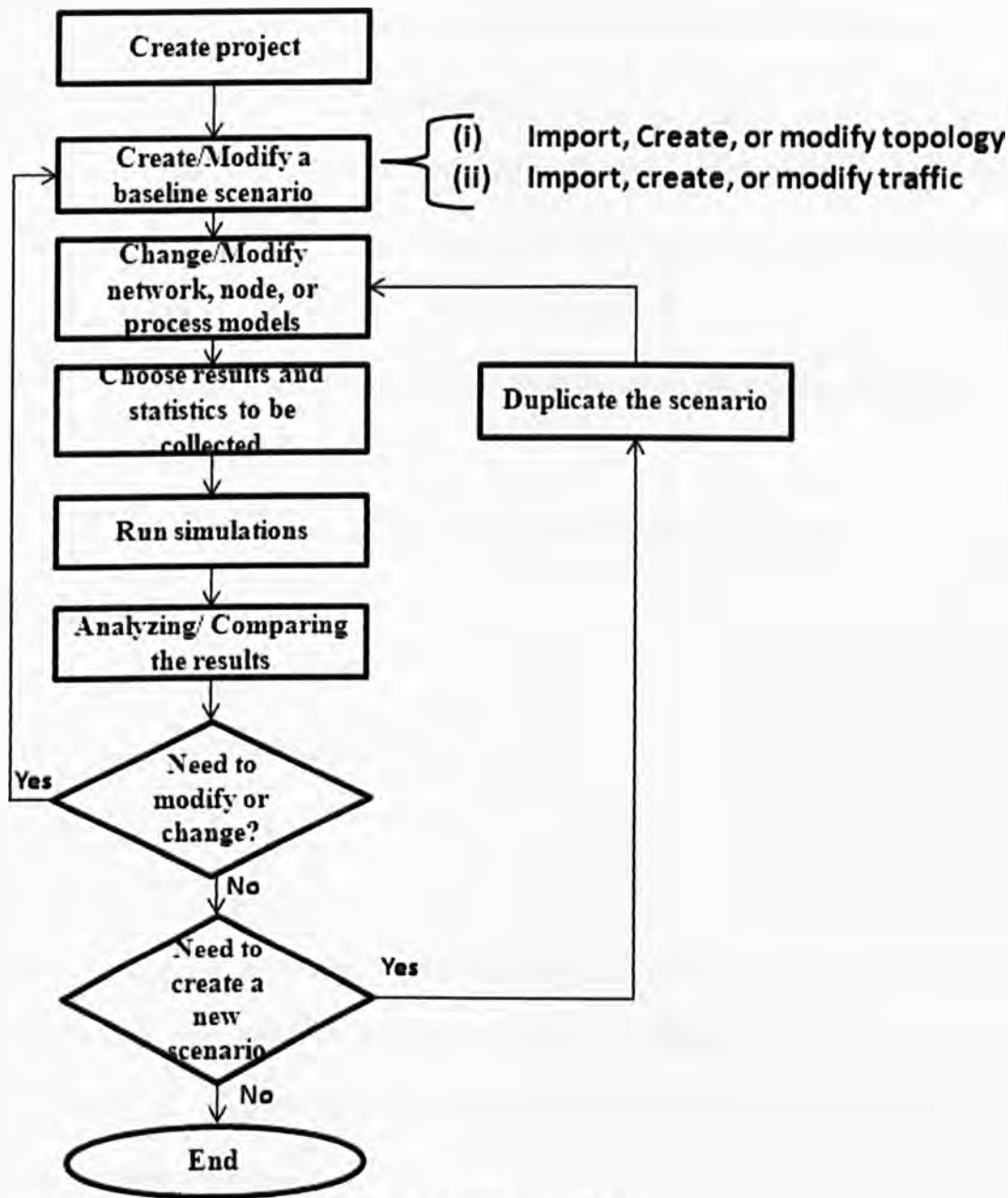


Figure 4.8 OPNET workflow

Figure 4.9 illustrates the OPNET hierarchy that includes network, node, and process models. Network model describes the scenarios, topologies and connections between different nodes. Node models can be categorized as follows:

- (i) Basic building blocks includes
 - a. Processors: These modules are programmable via the process model
 - b. Queues: These blocks manage data packets and buffering issues

- c. Transceivers: These block are interface between different nodes
- (ii) Interfaces between modules includes:
- a. Packet streams: carry data packets from a source to a destination module
 - b. Statistic wires: carry a single data value from a source to a destination module
 - c. Logical associations: tier individual transmitter and receivers together to make transceiver pair

The process domain is a state diagram that includes following elements:

- (i) State transition diagrams
- (ii) Blocks of C/C++ code
- (iii) OPNET Kernel Procedures (KPs)
- (iv) State variables
- (v) Temporary variables

There are two kinds of states in OPNET: Forced and Unforced state. The forced state is illustrated as a green state and uses as a transition but unforced state that is red state can be used as an idle state and the network designer can choose one of these states based on the requirements.

In the next sections, the implementation steps are described in the hierarchy based design.

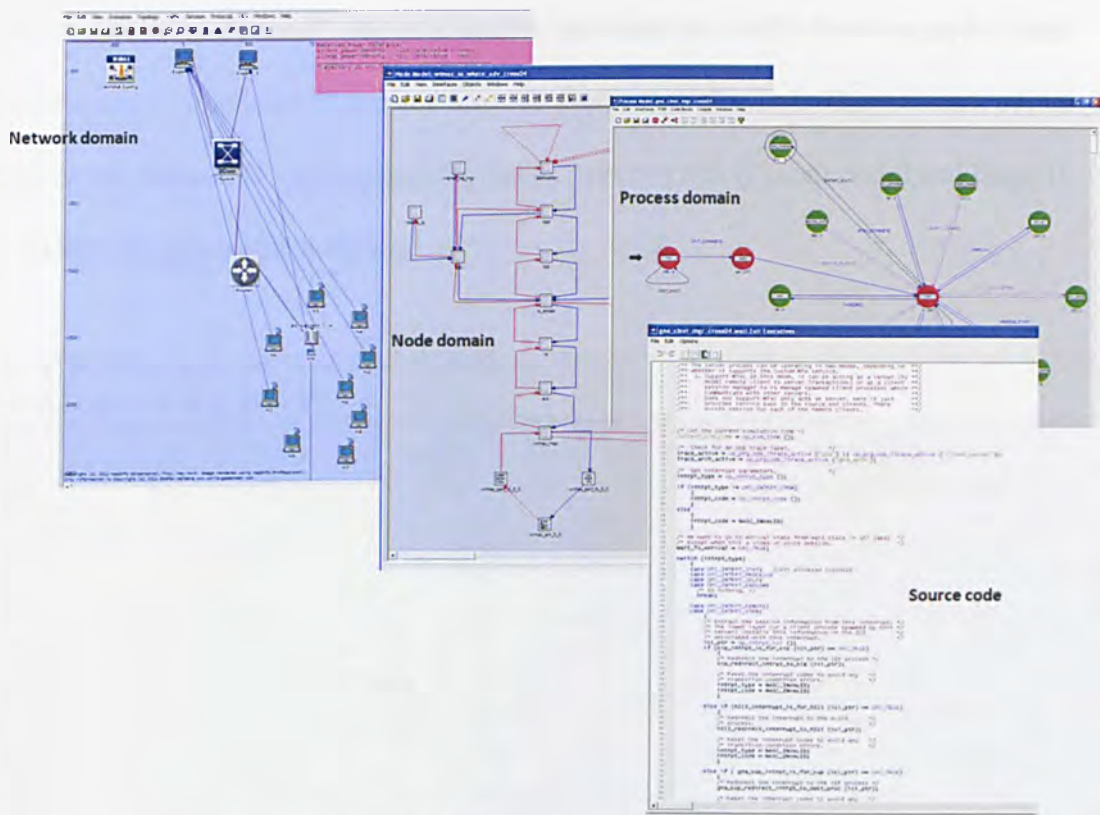


Figure 4.9 OPNET Modeler® hierarchy

4.3.1.1 Network domain scenarios and parameter settings

In order to validate the algorithmic concept introduced earlier, a simulated medical ultrasound model over mobile WiMAX in OPNET Modeler® is developed that is shown in Figure 4.10; the scenario includes 1 BS and 10 MSs, where one of MSs is connected to the ultrasound scanning machine and the rest of the MSs are generating different range of cross traffic. The medical expert’s station is connected to the BS through a LAN.

Table 4.4 shows the relevant WiMAX-system parameters that have been used in the simulation process. The gap between the downlink and uplink subframe is selected 100.8ms and the gap between the uplink subframe of one frame and the downlink subframe of the following frames is 302.4ms.

The “application-demand” object is used to simulate the traffic between nodes. And the traffic can be imported or scripted into the application demand. This network object simulates the ultrasound video streaming traffic between MS (Patient node) and Expert1 (Specialist) through traffic scripting.

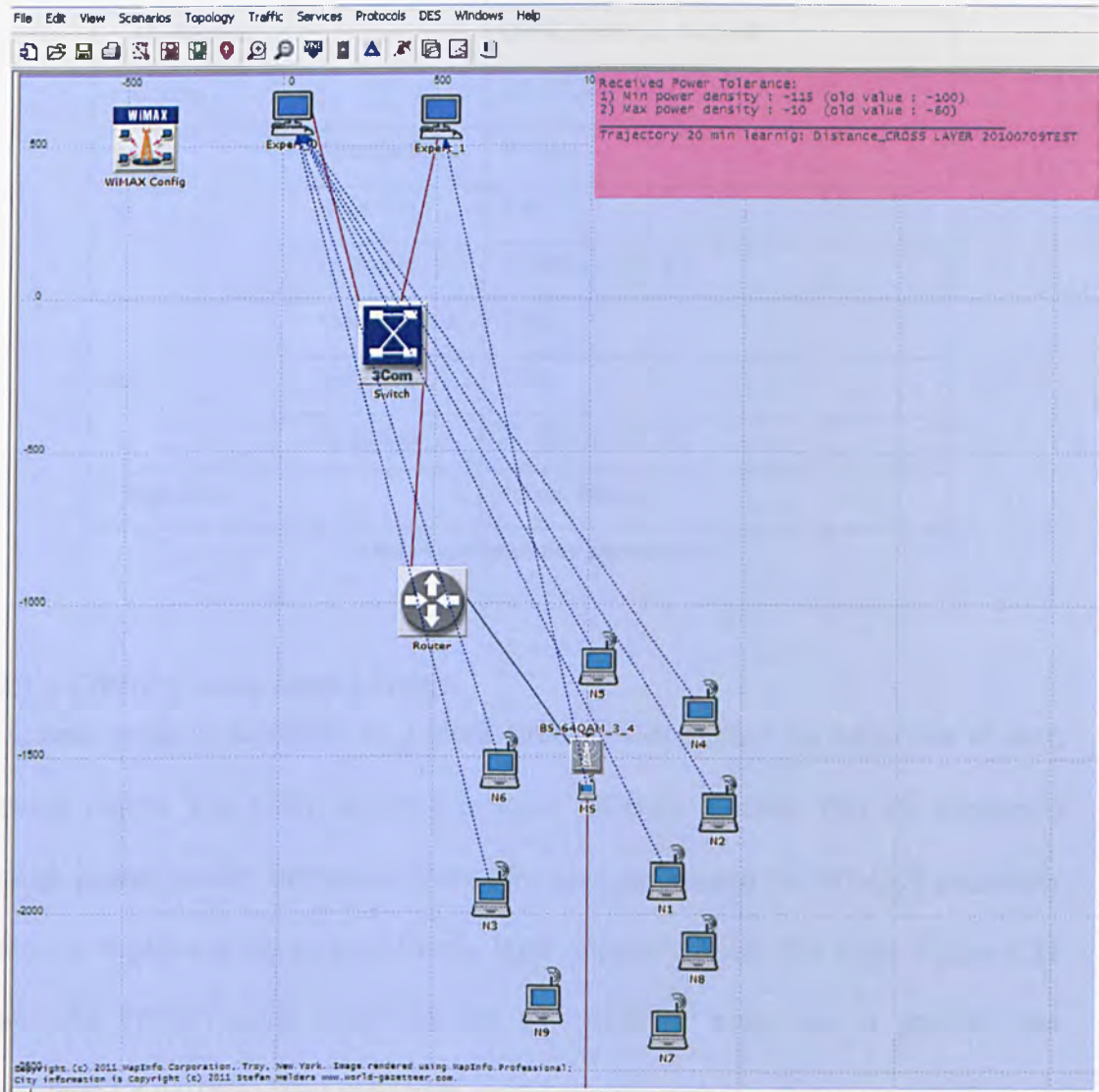


Figure 4.10 OPNET network model of the implementation

As explained earlier in section 3.4.1, the MAC service class for ultrasound video streaming will be set as rtPS class. In this scenario, we use “Trajectory” to move MS node. Therefore SNR will be changed and different wireless situation will be simulated.

Parameters		Value
Duplex Mode		TDD
Carrier frequency		5.8 GHz
Bandwidth		5 MHz
Frame length		5 ms
Modulation		QPSK, 16QAM, 64QAM
Coding		1/2,2/3,3/4, 5/6
BS	Antenna Gain	16 dBi
	Noise Fig.	5 dB
	Tx Power	35 dBm (3.162 W)
MS	Antenna Gain	0 dBi
	Noise Fig.	7 dB
	Tx Power	27 dBm (0.501 W)
Path loss		Free Space

Table 4.4 Simulation parameters

4.3.1.2 OPNET node model design

A node model is described by a block structure that defines the behaviour of each network object. The block structure includes different modules that are connected through packet streams or statistic wires. We have customised the WiMAX subscriber station to implement the proposed cross layer approach inside this node. Figure 4.11 shows the OPNET node model of MS that statistics wires use to provide data abstraction for the cross layer optimizer.

The cross layer optimizer uses several statistics to abstract the certain information; some of the statistics are inside the application module that will be explained in the process model design. Uplink SNR, Uplink BER, and Response time are captured through statistic wires from different layers to be used in optimiser module. Uplink

SNR records the Uplink SNR value in dB for packet transmissions through the WiMAX physical layer. Uplink BER records the Uplink BLER values obtained from the WiMAX MAC statistics feedback; and Response Time records the time elapsed between the sending of the request from the source and the reception of the response at the source. These statistic wires are listed in table 4.5.

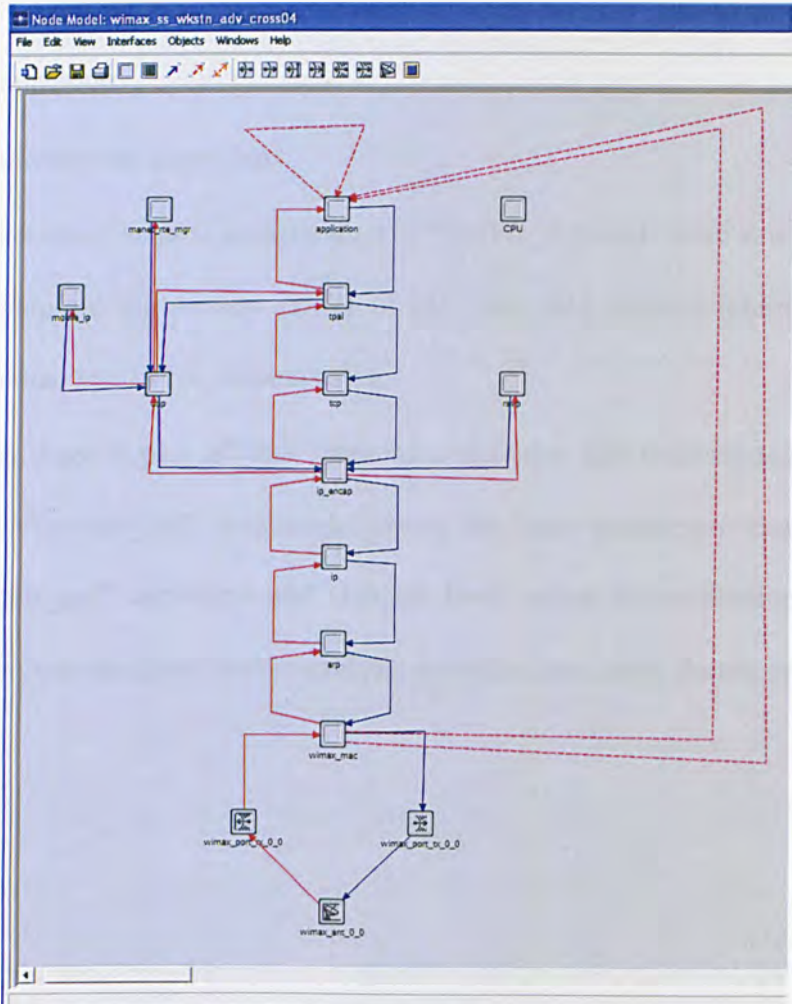


Figure 4.11 Node model of the implementation

Source statistic	Destination statistic
WiMAX PHY.Uplink SNR (dB)	Instat[0]
WiMAX PHY.Uplink BER	Instat[1]
Application Demand.Response Time (seconds)	Instat[2]

Table 4.5 The WiMAX statistics wires in node model design

4.3.1.3 OPNET process model implementation

The process models implement the underlying functionality of the node models which are represented by finite state machines (FSM). We use the process model to implement the proposed cross layer functionality inside the MS. The cross layer implementation in process model includes three major components as follows:

- (i) Data abstract
- (ii) Initialization
- (iii) Reinforcement algorithm

Data Abstract component is implemented in “DATA_Abstract” state as a green state. Figure 4.12 represent the process model of MS. The data abstract interrupt in node model will handled by DATA_Abstract state.

Initialization stage is part of “Init” state as a red state that includes registration of parameters by “op_stat_reg” command, getting the node parameters and setting by “op_ima_obj_attr_get” command and also we have added the simulation probes to evaluate and record the performance analysis statistics and states during simulation in text files.

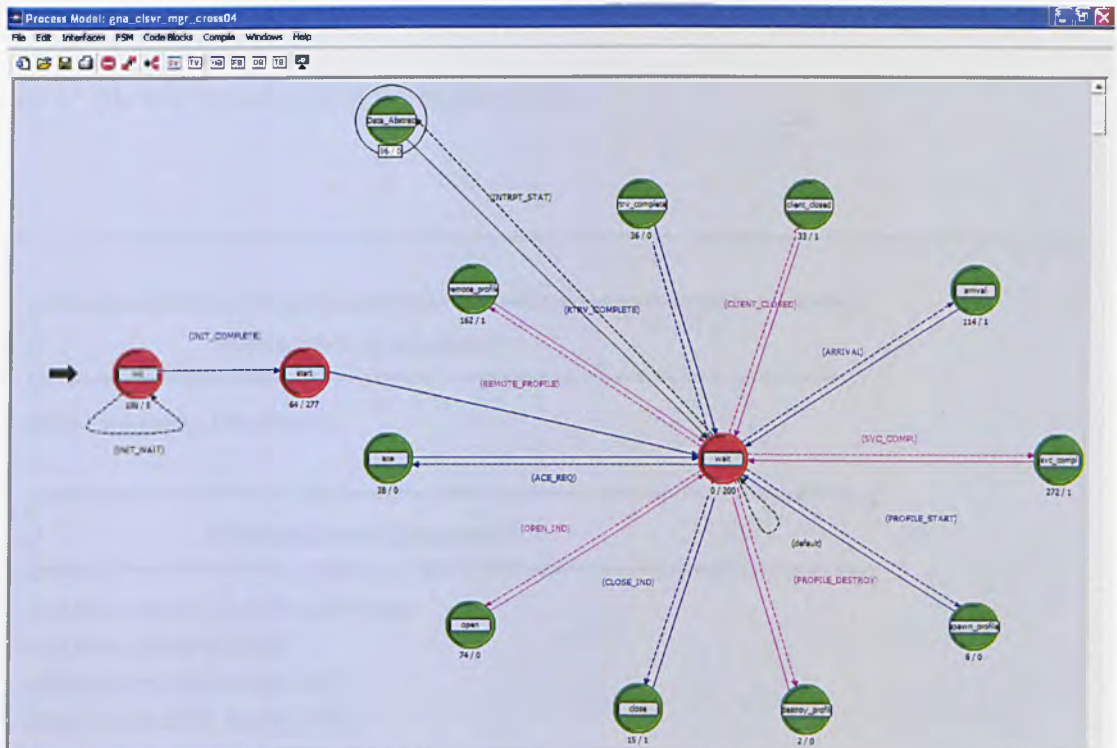


Figure 4.12 OPNET process model of the implementation

Reinforcement algorithm and the required functions have been implemented in “Function block” of process model. Figure 4.13 provides a definition list of these components.

The OPNET process models are developed by “Proto-C” that includes state-transmission-diagram, C/C++ codes, and a library of high level commands known as kernel procedures that provide a vast range of pre-coded functions for information processing, data analysis, data storing, and data retrieving.

Proto-C processes use three distinct categories of variables called state variables (SV), temporary variables (TV), and global variables. Temporary variables are accessible in states execution. But state variables are accessible in state execution and function block. The state variables can be modified by kernel processes. Figure 4.14 shows the state variables and their types. And finally the global variables are accessible in state execution, function block, and external files (*.ex.c files). These variables are

declared in header block (HB). The cross layer's global variables are defined in "cross.h" file that is included in the header block.

```

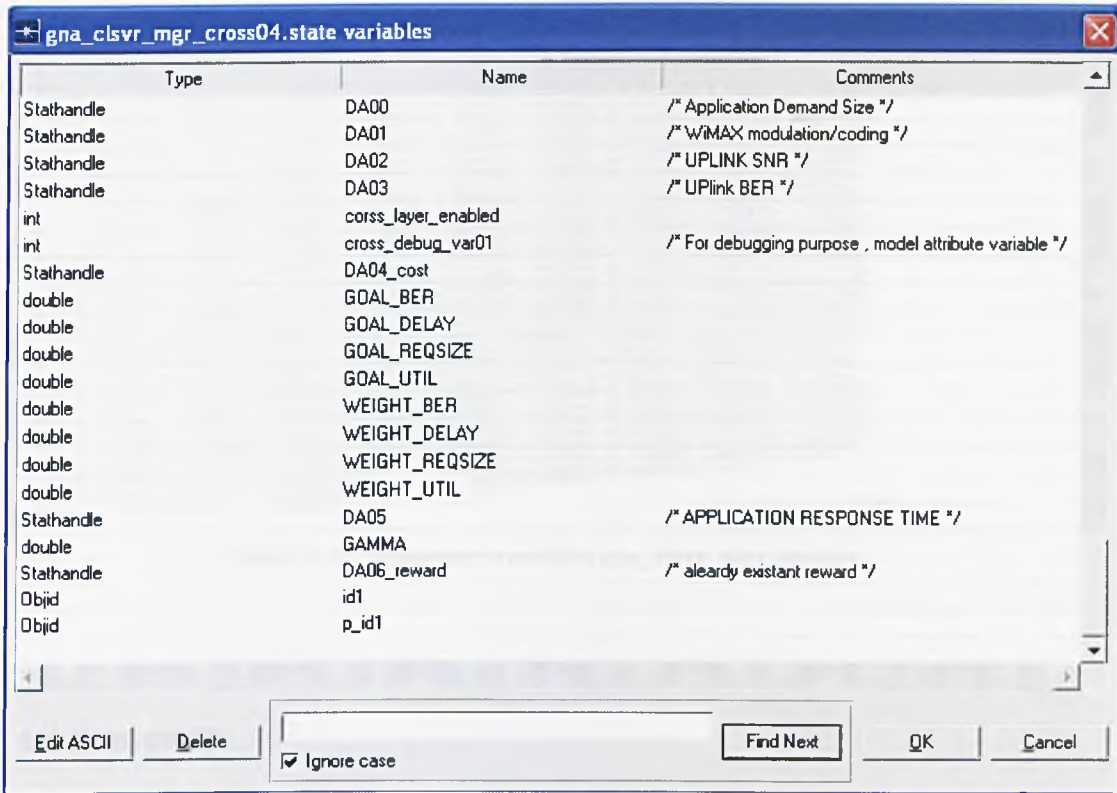
//*****
//          CONFIG_CROSS() 20100510          //
//*****
static void config_cross(void );

//*****
//          REINFORCEMENT() 20100510          //
//*****
void Find_maximum_action(int state);
void force_decision(void);
static void reinforcement(void );
static double COST_function(void );
static void Remove_perm (int o );
static void Generate_Permutation_Random(void );
static void DECODE_State(int st); //Extract: Current_BER and Current_Delay
static void ReinforcementLearnng(void);

//*****
//          LEARNNG PROCESS 2010/06/21          //
//*****
static int lp_state_detect(void );
static void learning_process(void);

```

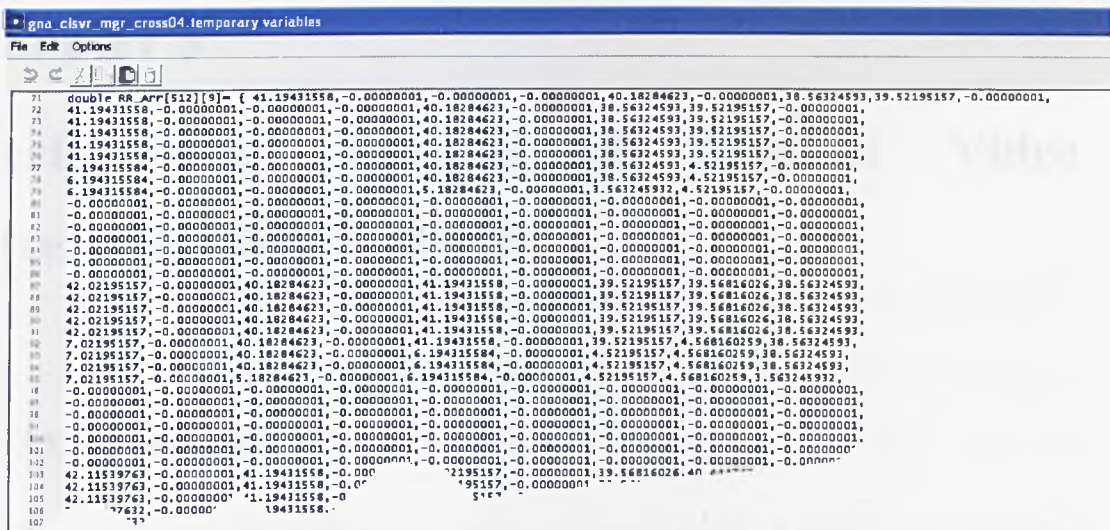
Figure 4.13 Definition list of function block



Type	Name	Comments
Stathandle	DA00	/* Application Demand Size */
Stathandle	DA01	/* WIMAX modulation/coding */
Stathandle	DA02	/* UPLINK SNR */
Stathandle	DA03	/* Uplink BER */
int	corss_layer_enabled	
int	cross_debug_var01	/* For debugging purpose , model attribute variable */
Stathandle	DA04_cost	
double	GOAL_BER	
double	GOAL_DELAY	
double	GOAL_REQSIZE	
double	GOAL_UTIL	
double	WEIGHT_BER	
double	WEIGHT_DELAY	
double	WEIGHT_REQSIZE	
double	WEIGHT_UTIL	
Stathandle	DA05	/* APPLICATION RESPONSE TIME */
double	GAMMA	
Stathandle	DA06_reward	/* already existant reward */
Objid	id1	
Objid	p_id1	

Figure 4.14 State variables of gna_clsvr_mgr process

In the reinforcement algorithm, it is necessary to assign a proper set of initial values. An appropriate initialization can provide a fast convergence in Q table, and the learning process will be fast and effective. Figure 4.15 shows a sample of temporary variables that include the initial learning table. This table has been produced by a C#.NET program as offline and imported to the OPNET. More details of this program will be presented in Appendix A. The reinforcement learning knowledge table can be improved by OPNET simulation model and is exported to an external file to be used in other scenarios.



4.4 Summary

In this chapter, we introduced different cross layer approaches and the details of the cross layer optimiser approach using the reinforcement method. The process of optimising in the cross layer is based on a discrete-time Markov Decision Process (MDP). As a result, the principle of the Reinforcement learning and Q-learning approaches were discussed. In addition, the algorithmic approach of the reinforcement learning and the cross layer optimisation system were illustrated. The OPNET Modeler[®] implementation with the simulation process and the procedure of the approach were also presented. The implementation steps were described in the hierarchy based design including network domain, OPNET node model design, and OPNET process model implementation. Also three major components of process model implementation were described as follows: data abstract, initialization, and Reinforcement algorithm.

Chapter 5

Performance Analysis of Medical Video Streaming Over WiMAX

5.1 Introduction

This chapter includes a discussion summary of the proposed cross layer simulation results. Then we present simulation scenario of medical QoS mapping to typical WiMAX QoS parameters. Preliminary performance analysis of the proposed multiparametric scenarios are shown and evaluated. Furthermore, objective and subjective analysis for tested ultrasound video streaming and the effect of packet loss on medical images are also presented.

5.2 Cross Layer medical video streaming over WiMAX networks

In the previous chapters, we explained the m-QoS requirements of mobile healthcare applications and in particular m-QoS metrics for ultrasound video streaming. The bounds on the video quality were reported in terms of the PSNR, MSE, and SSIM indices. In this section, the proposed cross layer scenario will be evaluated and the results will be discussed.

The proposed cross layer is based on the integrated cross layer architecture model architecture and RL algorithmic discussed in chapter 4.

5.2.1 Simulation set-up

In order to validate the proposed cross layer model, a simulated medical ultrasound model over mobile WiMAX in OPNET is developed. The OPNET implementation stages have been explained in the previous chapter.

This set-up is shown in Figure 5.1. This Figure illustrates both the ultrasound traffic and cross traffic paths. JM Reference Software¹ Ver. 16.0 is used to extract the traffic specification of different ultrasound video data. The ultrasound video data is analysed in terms of frame rate and quantisation indices, Figure 5.2 shows the block diagram of traffic specification analysis. The main traffic is used to simulate ultrasound video streaming between the patient side (node MS) and the expert side (hospital); and the cross traffic is deployed to emulate the real environmental traffic between the nodes.

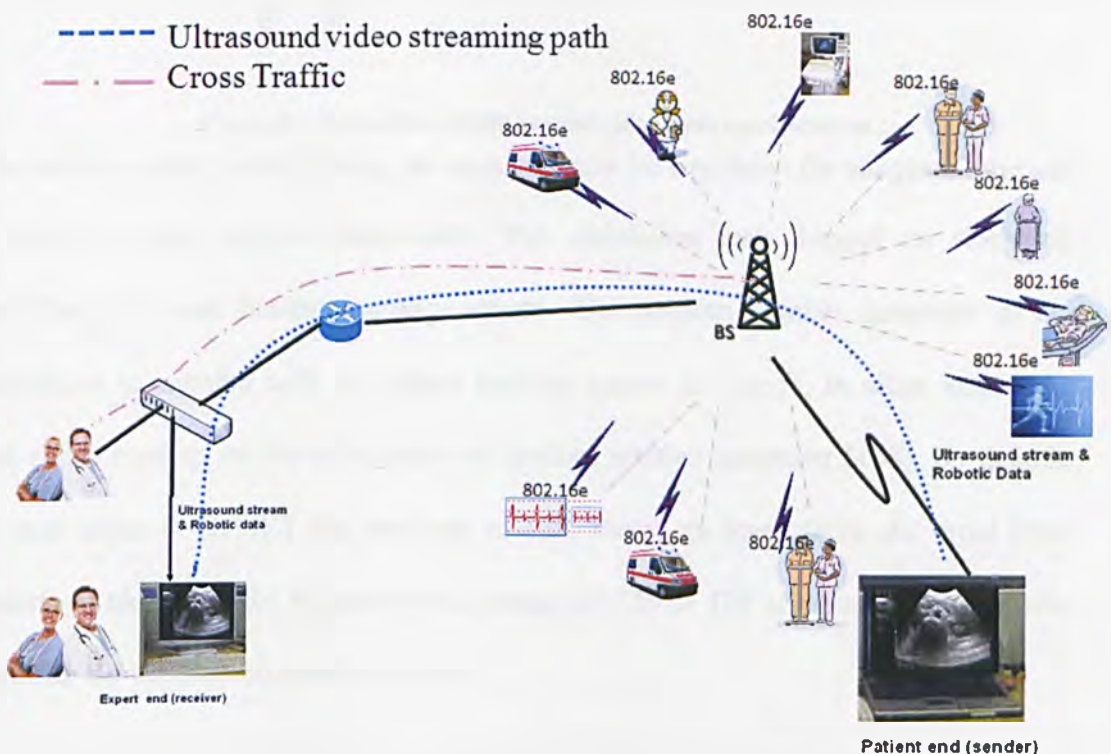


Figure 5.1 Typical remote ultrasound video streaming scenario

¹ The latest version of JM Reference Software is available at <http://iphone.hhi.de/suehring/tml> [accessed on Feb 2012]

The different traffic specifications have been listed in table 5.1. The ultrasound video streaming is used with three different and clinically acceptable PSNR values namely: 35, 37, and 40 dB respectively. The optimiser chooses the video streaming type based on the system status. As explained in chapter 3, the proper WiMAX service class of ultrasound video streaming is rtPS service class. However, the other service classes can also be used by the cross traffic nodes.

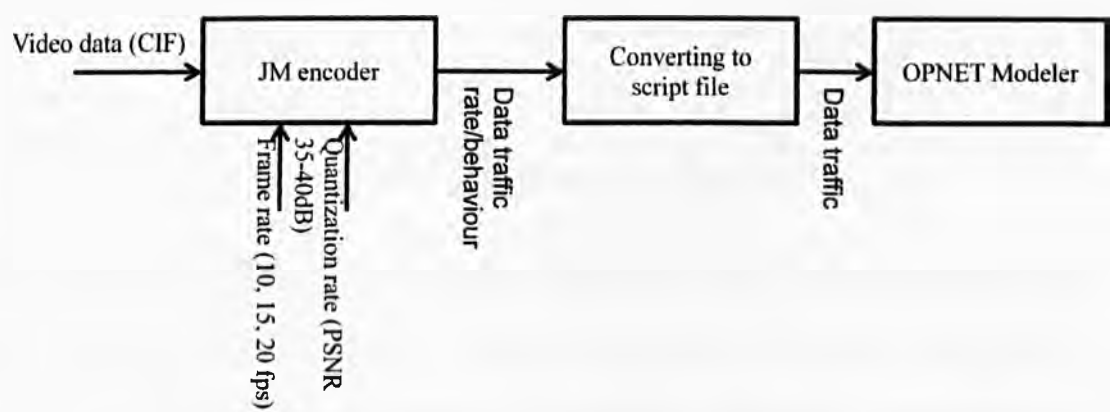


Figure 5.2 Extraction of ultrasound video data specifications

In order to collect valid results, the scenario must be simulated for adequate time and be able to create variable behaviours. The simulation tests depend on stochastic modelling that uses random number stream. The random number generator in the simulations is initiated with an integer number knows as “seed”; In other words, the seed is deployed to set the initial state of random number generator [108]. By default, the seed value in OPNET has been set to 128. Based on these facts, the cross layer scenario is simulated for 4 hours with a range of 126 to 129 seed numbers to ensure acquiring the accurate simulation results.

Traffic type	Traffic parameters		Value
Main traffic	Average uplink traffic size (QCIF video)	PSNR: 35dB	800 Bytes/Frame
		PSNR: 37dB	1200 Bytes/Frame
		PSNR: 40dB	2800 Bytes/Frame

	Traffic rate	36000 per hour
	Type of service	Streaming multimedia
	Transport protocol	UDP
	MAC service class	rtPS
Cross traffic	Average uplink/downlink traffic size	UL:1024/DL:1024 Bytes
	Traffic rate	36000 per hour
	Type of service	Streaming multimedia, background
	Transport protocol	UDP, TCP
	MAC service class	rtPS, ertPS, UGS

Table 5.1 Traffic specification of cross layer scenario

As explained in chapter 4, the optimiser required an initial Q-learning knowledge known as Q table and Reward table. These are produced by an external Visual studio C#.Net program (described in Appendix A) considering all possible state-transitions. During the simulation process, the reward table will be optimised by RL algorithmic approach during the cross layer optimisation process.

5.2.2 Optimisation results

The preliminary results achieved in terms of the PSNR, BER, and end-to-end delay show the successful correlation of the proposed cross layer algorithmic approach with the m-QoS bounds presented earlier. Figure 5.3 shows the simulation results, this figure shows the video quality and end-to-end delay results in both cross layer enabled scenario and AMC enabled scenario with three different ultrasound video streaming data. Figure 5.3 (a) compares the average PSNR of cross layer enabled scenario with AMC scenarios. The cross layer scenario has different optimised PSNR depending on wireless SNR. In other words, the cross layer scenario sometimes reduces the PSNR value to have an acceptable overall m-QoS. But fixed PSNR cannot guarantee other m-

QoS indices. Figure 5.3 (b) shows end-to-end delay results for these scenarios. The optimization are changing against the SNR to have optimal m-QoS with consideration of the quality of service goal which is considered in cross layer optimiser algorithm ($\text{PSNR} \geq 37$, $\text{delay} \leq 90\text{ms}$ and $\text{BER} \leq 1.0\text{E-}7$). The overall performance result shows improved m-QoS gain in terms of delay and video quality. Figure 5.3 (c) shows SNR variation during the simulation. The MS trajectory is used to generate different SNR values during the simulation.

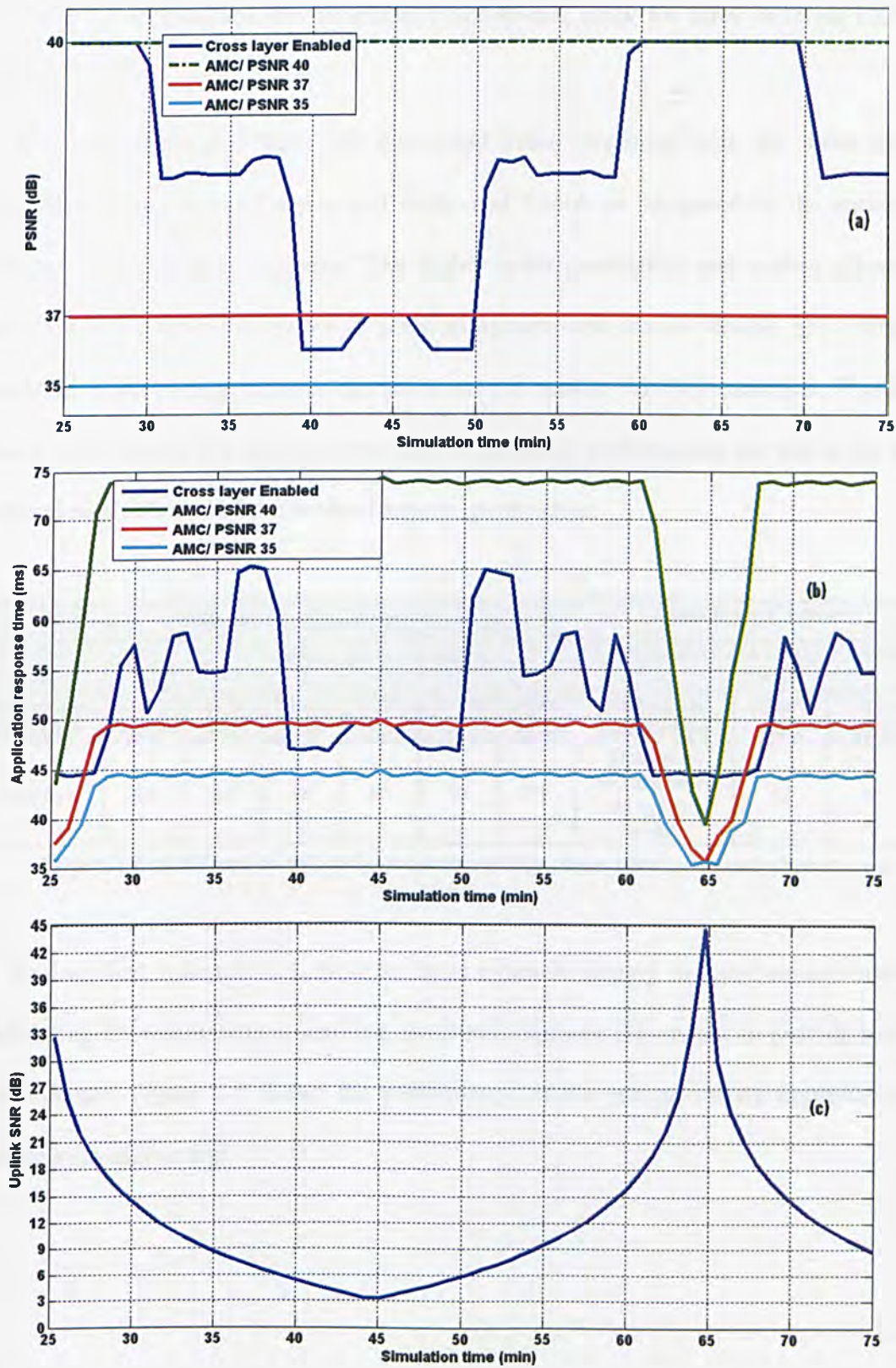


Figure 5.3 Cross layer simulation results. (a) PSNR vs. simulation time (b) Application response time vs. simulation time (c) Uplink SNR vs. simulation time

Table 5.2 summarises the comparative end-to-end delay for three different PSNR values.

It is clear from this table that ultrasound video streaming with the cross layer optimiser attains optimal end-to-end delay and PSNR as compared to the scenario without the cross layer optimiser. The higher order modulation and coding schemes have lower end-to-end delay but in practical systems and due to variable SNR, single modulation and coding schemes cannot be used in mobile WiMAX networks. Also the lower video quality (35 dB) has better end-to-end delay performance, but this is not the optimal result obtained from medical experts' perspective.

Without cross layer							Cross layer Enabled		
Video quality	PSNR: 35		PSNR: 37		PSNR: 40		Video quality	Average PSNR: 39 dB	
Modulation and Coding	Mean (ms)	Max (ms)	Mean (ms)	Max (ms)	Mean (ms)	Max (ms)	Modulation and Coding	Mean (ms)	Max (ms)
Adaptive	43	45	48	50	70	74	Optimiser decides based on system variables	52	65

Table 5.2 WiMAX end-to-end delay simulation results comparison (with and without cross layer)

As described in section 4.3, the cross layer optimiser deploy an initial reward matrix and during the reinforcement learning algorithm improves this matrix to provide better performance. Figure 5.4 shows the performance of the reward matrix improvement during a simulation test.

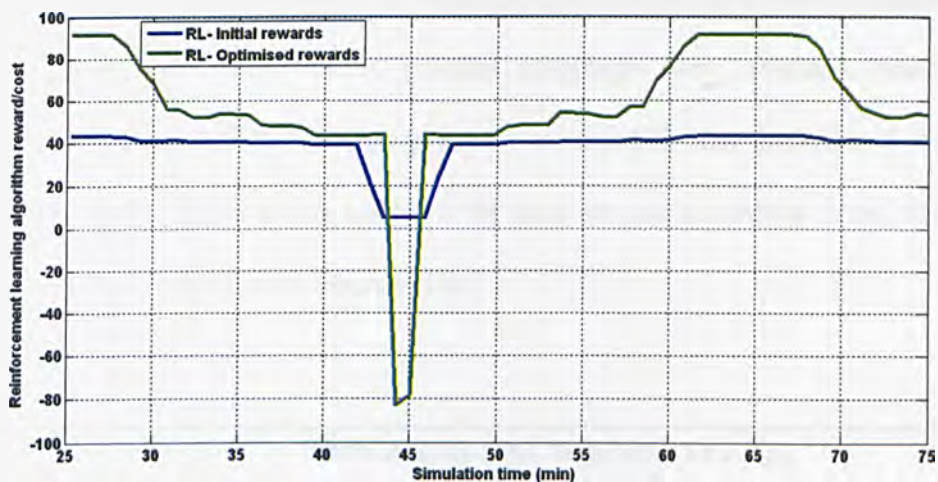


Figure 5.4 Reward matrix optimization

5.3 Multiple Parameter m-health Scenarios

Multiparametric evaluation of different m-health scenarios using cellular networks (3G, GPRS, and HSPA) has been reported in [2]. However, to-date there is no such study addressing the performance of such multiparametric m-health scenarios in WiMAX networks. In this section, we map the relevant m-QoS to typical WiMAX QoS network parameters to optimise the performance of these multiparametric m-health scenarios in different wireless conditions.

In particular, we address the mapping of medical QoS to typical WiMAX QoS parameters and the need to consider these boundaries in future m-health applications. Three medical scenarios (accident, clinical, and homecare scenarios) were defined over mobile WiMAX using OPNET[®] modeler to investigate the network performance and the functionality of the QoS mappings.

5.3.1 Simulation set-up

Table 5.3 shows some of the relevant m-health services and their allocations for each corresponding m-health scenario together with their traffic allocation priorities and

WiMAX QoS classes. Further details of WiMAX QoS classes have been discussed in chapter 3 (Table 3.8). These traffic priority mappings were obtained based on recommendation of our NHS clinical partners in the UK that includes 4 expert specialists. The traffic priority was assigned for each service according to the clinical importance and the critical level of the service.

m-health service	Traffic Priority (0 for No-priority 7 for high priority)			WiMAX QoS class
	Accident case	Clinical care case	Homecare case	
Electrocardiography (ECG) monitoring	NA	3	5	UGS
Blood pressure monitoring (Sphygmomanometer)	1	2	5	UGS
Digital audio stethoscope (heart sound)	1	2	5	UGS
Region of Interest JPEG Image	5	6	5	nrtPS
Radiology	NA	6	NA	nrtPS
Magnetic resonance imaging (MRI)	NA	6	NA	nrtPS
Ultrasound video streaming	7	7	5	rtPS
Videoconferencing (Teleconsultation)	2	5	3	rtPS
Voice conferencing (Teleconsultation)	4	5	3	rtPS

Table 5.3 Mobile broadband m-health service QoS mapping [112]

In order to validate the medical scenarios and QoS mapping issues explained earlier, a simulated medical traffic model over mobile WiMAX using OPNET[®] is implemented.

The simulation scenario includes 3 BSs and 30 MSs, where the 3 BSs generates different types of m-health data traffic presented earlier. And the rest of MSs are used to generate cross traffic. The medical expert's station is connected to the BS through a LAN as shown in the simulation set-up (Figure 5.5).

The WiMAX system parameters used in the simulation process are similar to the pervious simulation project described in sections 4.3.1.1 and 5.2.

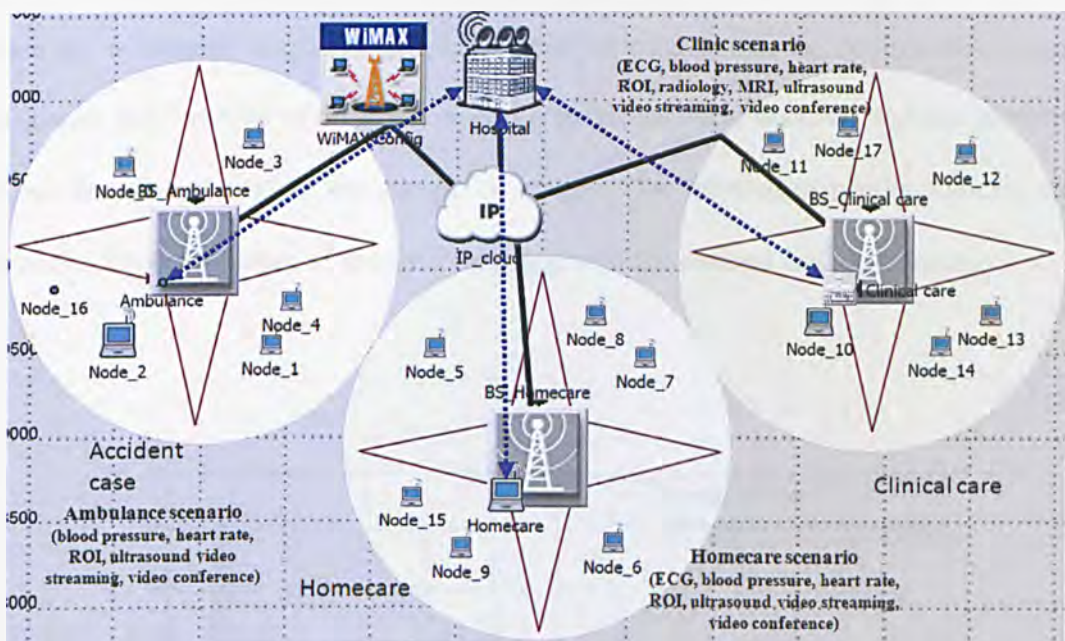


Figure 5.5 OPNET simulation set-up of the multiparametric m-health WiMAX network [112]

5.3.2 Optimisation results

Figure 5.6 shows a sample of the simulation results. This figure shows the probability density function of ultrasound video streaming and blood pressure delay based on QoS mapping, ultrasound video streaming service achieves better latency time in comparison to blood pressure data transmission. The preliminary results obtained in terms of the application end-to-end delay and jitter shows the successful correlation of the proposed multiparametric QoS mapping with the acceptable (m-QoS) bounds defined earlier [32].

The maximum delay is 160 ms; this represents an acceptable delay for ultrasound video streaming [32].

Figure 5.7 shows the delay jitter of the ultrasound video streaming in the three described scenarios (accident, clinical care and homecare). The Delay jitter needs to be guaranteed by the delivering network in order to provide a satisfactory video streaming service. These results indicate that the clinic and home care scenarios have higher jitter because of the higher medical applications load in these scenarios. However all jitter values are within the acceptable range (70ms) [32]. Table 5.4 summarises the comparative mean¹ end-to-end delay results of different m-health services. These indicate that the obtained m-QoS bounds are within the acceptable range. The simulation results indicate the successful implementation of the QoS mapping with the defined m-QoS bounds.

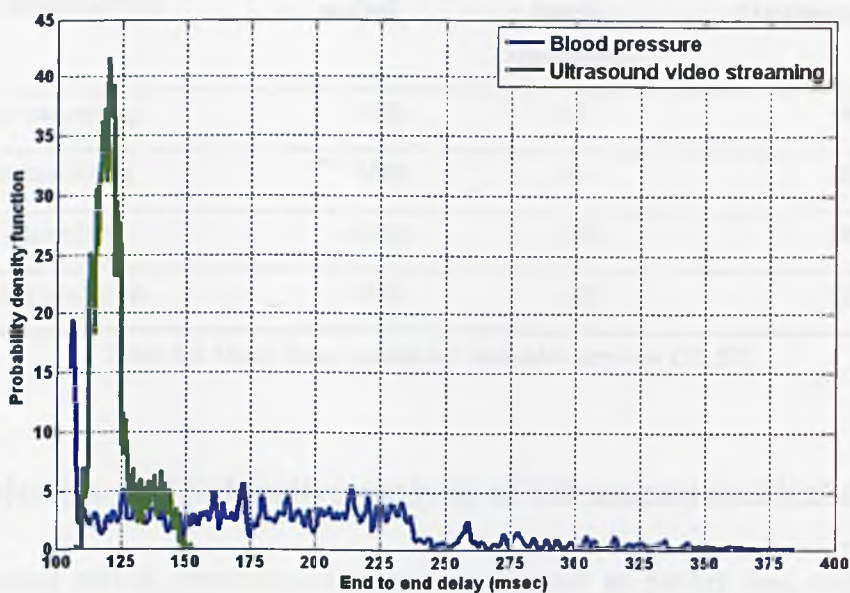


Figure 5.6 Probability density function of ultrasound video streaming and blood pressure latency

¹ Arithmetic mean: calculated as the sum of the delay values divided by number of samples.

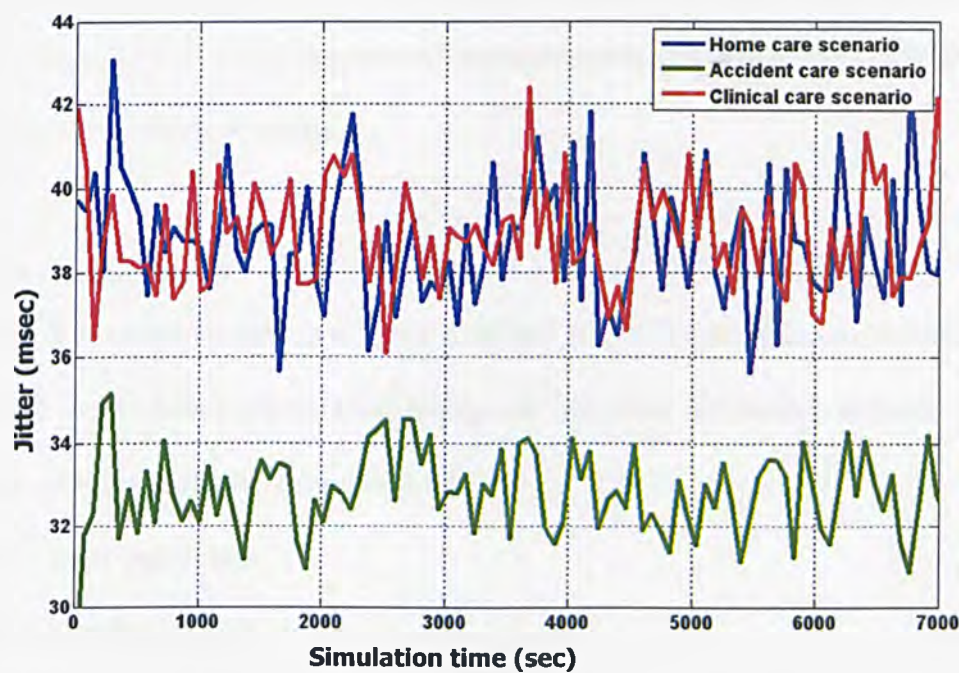


Figure 5.7 Jitter of ultrasound video streaming in clinic, homecare, and ambulance scenarios

m-health service	Mean delay (msec)		
	m-QoS	Single application	Multiparametric
ECG monitoring	<300	167	189
Blood pressure monitoring	<1000	160	185
Heart Rate	<1000	297	300
Ultrasound video streaming	<300	122	125

Table 5.4 Mean delay results for m-health services [32, 57]

5.4 Objective and Subjective analysis of ultrasound medical data

As explained earlier, transmission impairments, such as packet loss, will impact differently on the medical expert’s perception depending on where the loss occurs within the video clip. In this section, the effects of packet loss on the medical image quality in terms of objective and subjective indices are studied. Objective index

includes PSNR, SSIM, and MSE. In the Cloud™ emulator we have varied the packet loss in the range of 0.01 to 0.2 percent and accordingly measured the PSNR, SSIM and MSE values of the received images.

5.4.1 Simulation set-up

A WiMAX connectivity link and experimental setup were used to measure the end-to-end system performance when transmitting the relevant ultrasound streams. The following performance metrics are measured:

- PSNR versus Packet loss
- SSIM versus Packet loss
- MSE versus Packet loss

Figure 5.8 shows the end-to-end system connectivity. The network behaviour has been simulated. The expert and patient stations were connected through an Emulator running WAN Network (Shunra/Cloud™, Licensed software, headquarters: USA) to emulate the operation of the system on WiMAX network. The WiMAX channel information in terms of channel bandwidth, latency and packet loss are extracted via implementing and monitoring a medical ultrasound streaming scenario over WiMAX in OPNET® Modeler ver. 15.0 (headquarters Bethesda, USA). The OPNET simulation is carried out for different possible supported modulation and coding, and signal to noise ratios.

The selected uplink throughput was 1.54 Mbps which is the most likely to be offered by used commercial testbed (Rinicom). Ultrasound scans video was streamed by using a commercial video streaming program (VLC™ software¹). The video codec used in this experiment is WMV1 and the image size considered in this work is CIF (Common

¹ VLC is open-source software that is backed up by volunteer non-profit organisation (in Paris, France).

Intermediate Format), the video streaming with two different qualities, PSNR 41dB and PSNR 38.5dB are used in the emulator, they were selected based on earlier experimental studies [21, 91].

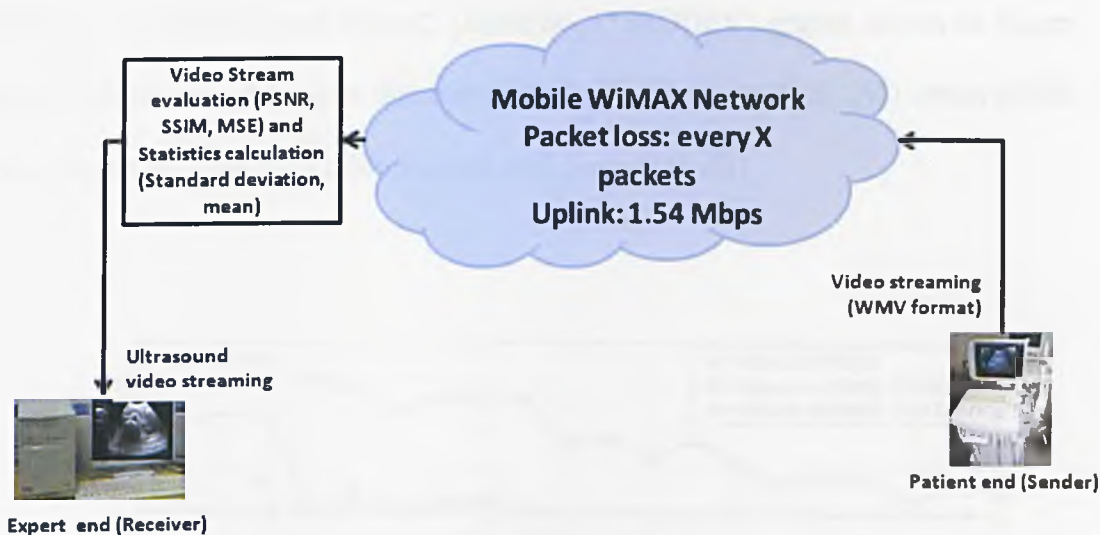


Figure 5.8 WiMAX ultrasound streaming system and emulation model [21, 91]

5.4.2 Performance results

Figures 5.9 and 5.10 show the results of the MPSNR (Mean PSNR), MPSNR-1*stddev (standard deviation) and MPSNR-2*stddev for different packet loss values of the tested *video1* and *video2* samples. In these figures, the PSNR value is gradually reduced as the packet loss increases to a max reduction of 3.6 dB and 6.2 dB at 0.2% packet loss for *video1* and *video 2* samples respectively. However the results of the MPSNR-1*stddev and MPSNR-2*stddev show a more accurate picture. These results show the standard deviation for the target PSNR in this experiment. It shows that in some cases the PSNR is as low as 27 dB with 0.10 packet losses and 23dB with packet loss of 0.18. However, these are not clinically acceptable values as examined by the medical experts.

Video quality can be interpreted as the quality of the majority of the frames. In the tested data streams, the majority of frames (68.2% and 95.4%) are within the one time

standard deviations ($\mu \pm \sigma$) and two- times standard deviations ($\mu \pm 2\sigma$) respectively, where μ is average and σ is standard deviation. The visual evaluation shows if packet loss is less than 0.10%, the effected medical video stream is acceptable. The Video1: (MPSNR- 1*STDDEV) and Video2: (MPSNR- 1*STDDEV) graphs shown in Figure 5.9 and 5.10 indicate the region that more than half of the frames (68.2%) obtain PSNR values greater than the acceptable medical QoS bound (35 dB).

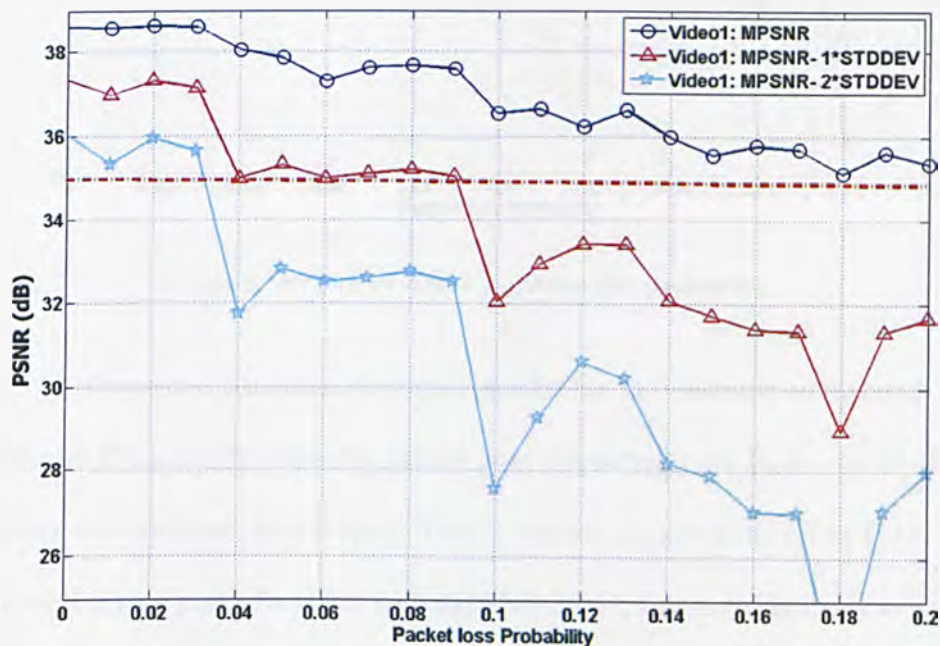


Figure 5.9 PSNR of video1 vs. packet loss probability

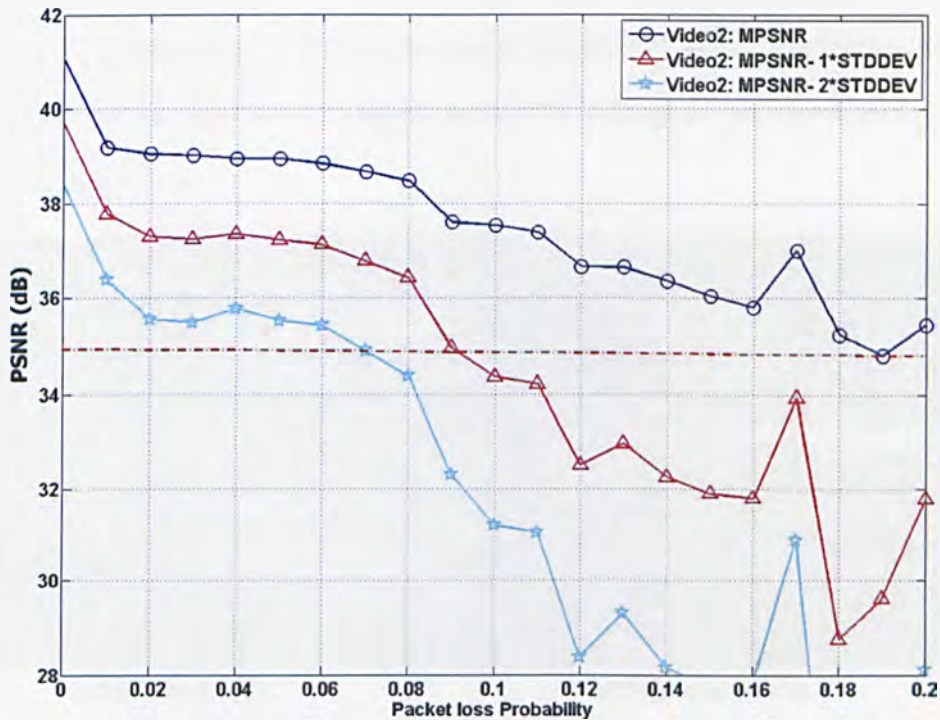


Figure 5.10 PSNR of video2 vs. packet loss probability

Figure 5.11 shows the comparative visual results for the obstetric ultrasound video frames. Images (b) and (d) show the packet loss impairment on I-, P-, or B- frames which affects several macro-block rows. This is known as slice error effect [115, 116]. Images (a) and (c) are part of a video with MPSNR 38.61, Image (b) belongs to a video with MPSNR 35.37 and Image (d) is part of a video with MPSNR 34.97, however the PSNR of images (b) and (d) [22.94 dB and 22.34 dB respectively] are less than acceptable range. In other words the mean PSNR is not sufficient for evaluating the packet loss.

We also measured the SSIM and MSE metrics in this study. Figure 5.12 and 5.13 show the mean SSIM and mean MSE analysis results. These two parameters together can be used for investigating the effect of packet loss on medical video streaming. According to the visual evaluation, the video streaming with SSIM that is less than

0.959 and MSE greater than 14.07 is not acceptable clinically. Table 5.5 summarizes the video1 performance and relevant analysis results; the highlighted part represents the acceptable range.

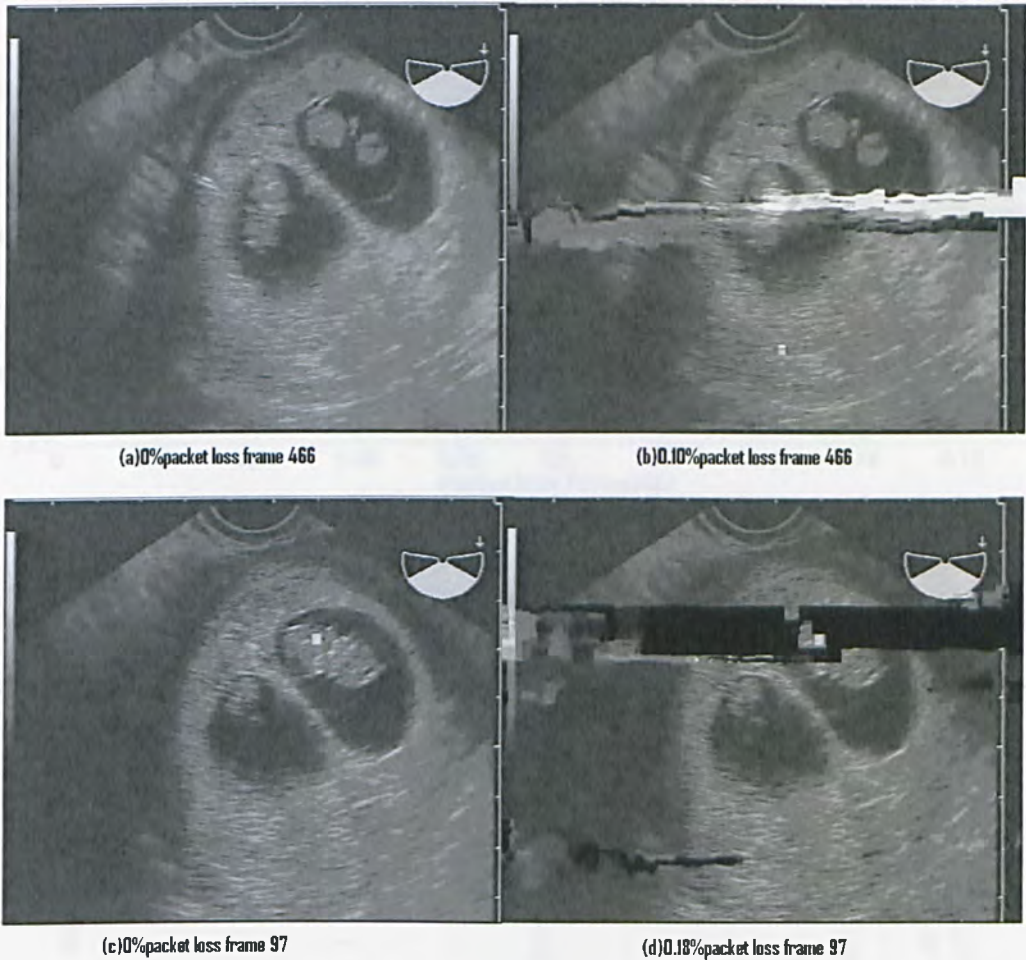


Figure 5.11 Experimental test ultrasound images (a), (c) Packet loss =0.00% Average PSNR=38.61dB Average SSIM=0.966 Average MSE =9.43 (b) Packet loss =0.10% Average PSNR=35.37dB Average SSIM = 0.944 Average MSE =20.00 (d) Packet loss =0.18% Average PSNR=34.97dB Average SSIM = 0.941.

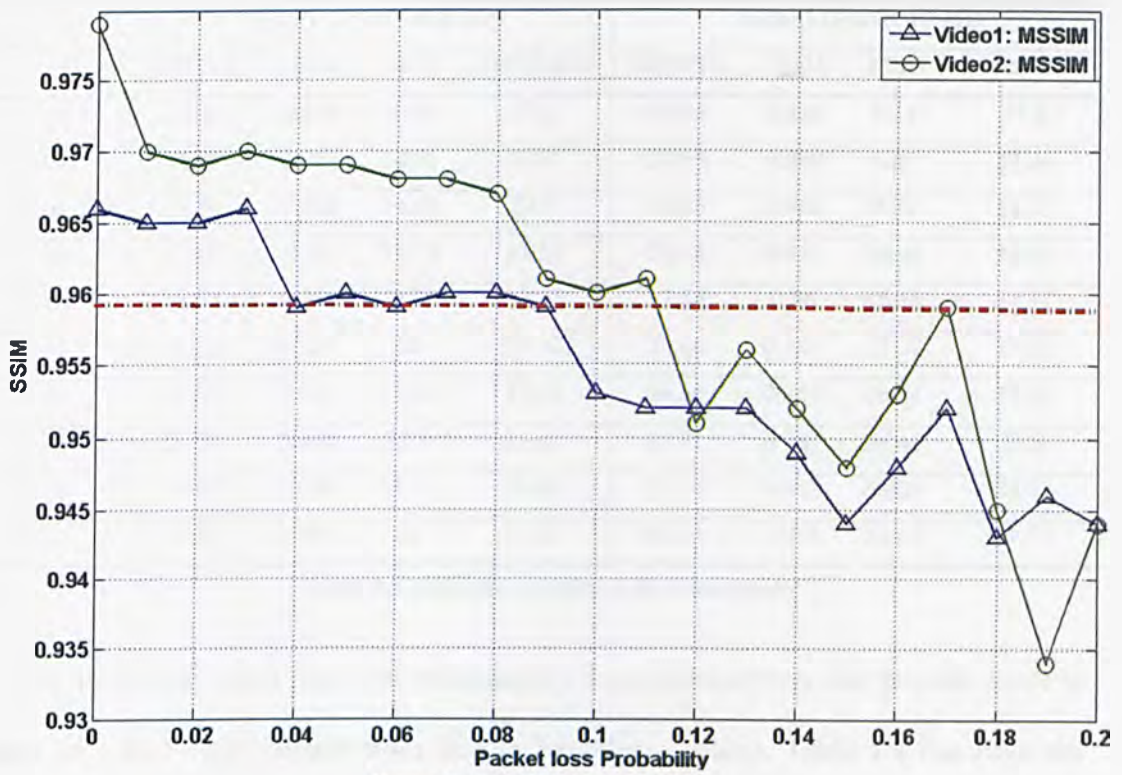


Figure 5.12 SSIM vs. packet loss

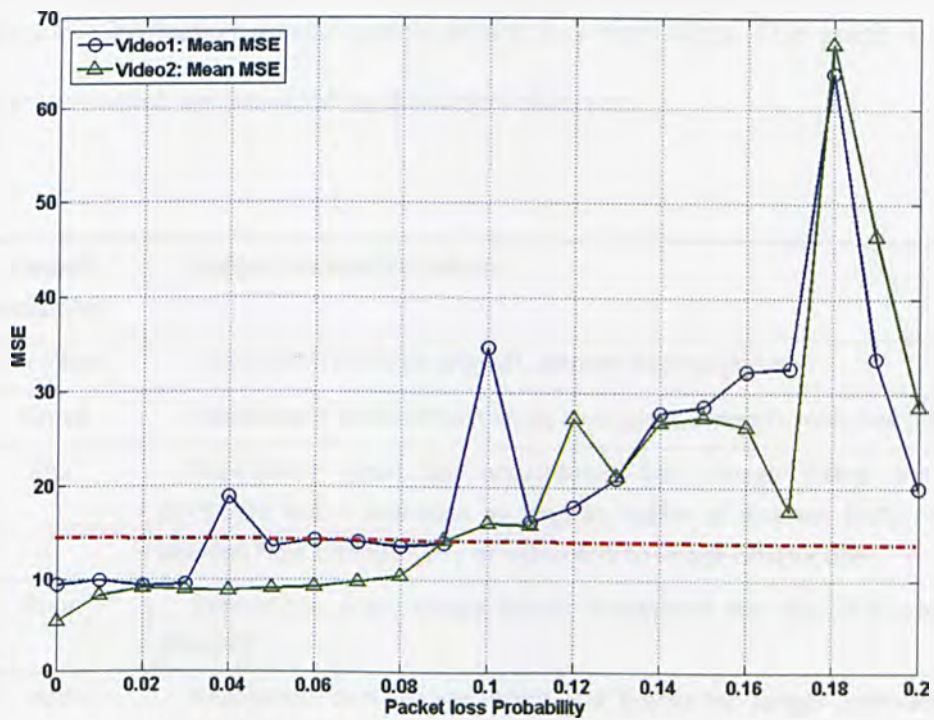


Figure 5.13 MSE vs. packet loss

Packet loss	Video1 (PSNR 38.5 dB)				Video1 (PSNR 40 dB)			
	MPSNR	SSIM	MSE	MPSNR- δ	MPSNR	SSIM	MSE	MPSNR- δ
0.02	38.5	0.965	9.33	37.3	39.05	0.969	9.11	37.3
0.04	38.05	0.959	18.91	34.9	38.95	0.969	8.85	37.36
0.06	37.29	0.959	14.38	34.9	38.85	0.968	9.25	37.13
0.08	37.67	0.96	13.71	35.21	38.48	0.967	10.48	36.43
0.10	36.53	0.953	34.73	32.05	37.54	0.96	16.18	34.37
0.12	36.22	0.952	18	33.42	36.66	0.951	27.27	32.52
0.14	35.99	0.949	27.85	32.08	36.36	0.952	26.81	32.26
0.16	35.79	0.948	32.3	31.41	35.81	0.953	26.41	31.8
0.18	34.97	0.941	63.31	28.96	35.24	0.945	67.05	28.77
0.20	35.37	0.944	20	31.67	35.44	0.944	28.56	31.77

Table 5.5 Objective quality indices summary

The ultrasound video has been evaluated by 4 expert observers that provide score in range of 1 to 5 (equivalence from Bad to Excellent quality). Table 5.6 describes the observation criteria and the scores. Figure 5.14 shows the mean opinion score (MOS) based subjective evaluation results against packet loss probability. This graph is mean of all the scores which are provided by the expert observers.

MOS	Overall conception	Subjective Quality indices
5	Excellent	Resolution: same as original, Smooth and no jitters
4	Good	Resolution: good, almost same as original, smooth. Very few jitters
3	Fair	Resolution: good but occasionally bad, Image jitters and breaks at periphery but is tolerable as long as region of interest (ROI) not affected, obvious flow discontinuity of video due to image obstruction
2	Poor	Resolution: poor, Image jitters throughout the clip. ROI was minimally affected
1	Bad	Resolution: bad, Image jitters and breaks for longer intervals in various areas affecting ROI: Not acceptable

5.6 Mean opinion score evaluation indices



5.14 MOS vs. packet loss probability for the tested ultrasound video data

The result shows that the proper combination of objective quality metrics can provide clinically acceptable evaluation of the medical video streaming data. However, it can be concluded that the overall packet loss greater than 0.09% is not acceptable clinically for the wireless ultrasound video streaming application.

5.5 Summary

In this chapter, we evaluated the new cross layer controller algorithm (CRL) using the OPNET[®] modeler simulation platform. The preliminary simulation results indicate the successful implementation of the proposed algorithm with the relevant (m-QoS) bounds. The results show average PSNR and end-to-end delay of the cross layer enabled scenario and AMC scenarios. The cross layer scenario has different optimised

video quality (PSNR value) depending on wireless status (SNR). In other words, the cross layer scenario sometimes reduces the video quality (PSNR value) to have an acceptable overall m-QoS. Because fixed PSNR cannot guarantee other m-QoS indices.

The mapping of multiple parameter m-health scenarios over mobile WiMAX network is also presented. Three m-health scenarios (accident, clinical, and homecare scenarios) defined over mobile WiMAX using OPNET[®] modeler with relevant m-QoS are also studied. The simulation results indicate the successful mapping approach.

The chapter also investigated the effect of the packet loss on the quality of ultrasound video streaming over WiMAX wireless network environment including the subjective and objective analysis. The following performance metrics were measured: PSNR versus Packet loss, SSIM versus Packet loss, and MSE versus Packet loss. The result shows that the proper combination of the objective quality metrics can provide precise evaluation of clinically acceptable medical video streaming over mobile WiMAX networks. It is also concluded that the overall packet loss probability greater than 0.09% is not acceptable clinically for the wireless ultrasound video streaming application.

To analyse the performance of the ultrasound video streaming over WiMAX and HSUPA networks as shown in Figure 6.1, we developed two experimental real-time testbeds for this application. The following evaluation metrics are used as performance outcomes:

- 1) Video quality including PSNR, frames per second, and frame size versus throughput.
- 2) Round trip time (RTT) versus packet size.

Figure 6.2 shows the experimental end-to-end system connectivity over both WiMAX and HSUPA networks. Real medical video streaming samples are used in the patient end to emulate the portable ultrasound scanning device (shown in figure 6.1).

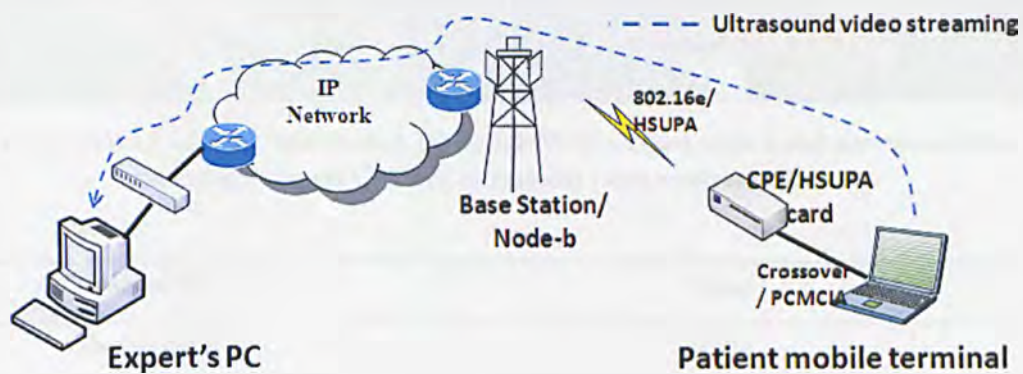


Figure 6.2 Testbed setup of the WiMAX and HSUPA networks

The ultrasound scan video data are streamed using the commercial video streaming program (VLC™ software). The video codec used in this experiment is Windows Media Video2 and the image sizes considered in this work are QCIF, CIF, and 4CIF with the video streaming of different PSNR and frames per second in the patient end. The experimental tests were carried out at different network loading conditions, especially at peak working hours with repeated tests.

6.2.1 Experimental WiMAX system set-up

The experimental test mobile WiMAX system used in this study was developed by Rinicom Ltd, Lancaster, UK. The system specifications are presented in appendix B. The laboratory experimental testbed is shown in Figure 6.3. Figure 6.3(a) shows the base station, which is connected to the expert end node through an IP network, and Figure 6.3(b) shows the customer premises equipment (CPE) linking the ultrasound video streaming node.



Figure 6.3 WiMAX experimental testbed. (a) Mobile WiMAX base station and ultrasound video streaming node; (b) CPE and ultrasound video receiver node

Parameter	Value
Duplex mode	TDD
Carrier frequency	2.58 GHz
Channel bandwidth	10 MHz
Tx Power	20 dBm
Noise Fig.	5 dB
Modulation/coding	Adaptive
ARQ	Disabled
Service class	rtPS

Table 6.1 WiMAX settings

Table 6.1 shows the relevant WiMAX configuration parameters that have been used in the testbed. The WiMAX devices are used in line of sight (LOS) propagation with almost strong signal coverage. We configured WiMAX QoS class to rtPS, and the Automatic Repeat reQuest (ARQ) has been disabled.

6.2.2 HSUPA system set-up

In the HSUPA experimental testbed, the Vodafone (HSUPA) ExpressCard connectivity is used for the patient’s end. The ExpressCard was provided by Vodafone, Berkshire, U.K.; and the expert’s end receives the video stream through an IP network connected to Node-B. The system is shown in Figure 6.4(a) and (b).



Figure 6.4 HSUPA experimental testbed. (a) HSUPA card and ultrasound video streaming node; (b) Ultrasound video receiver node

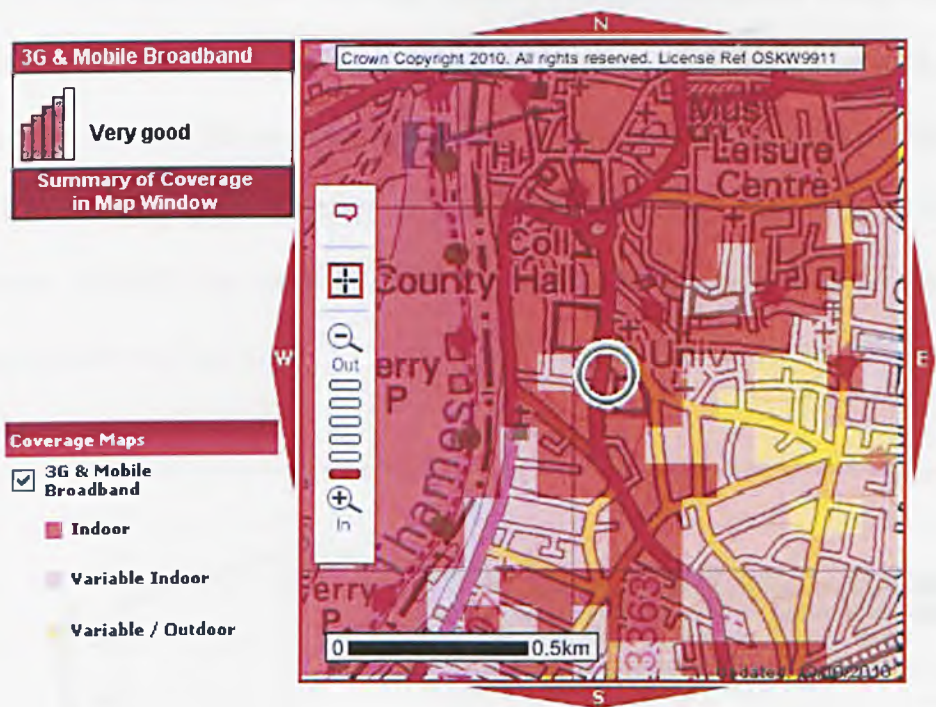


Figure 6.5 Coverage of the testbed Vodafone HSUPA cellular link [109]

Figure 6.5 shows the typical coverage area of HSUPA link and the tested area of South West London region. The figure shows a good and acceptable coverage area with good signal strengths within the geographical test area.

6.3 Performance analysis and results

The experimental performance results were captured by the *Ethereal*[®] network analyzer¹; and the *MATLAB*[®] software² was used to generate the plots. Figure 6.6 shows sample of the arithmetic mean throughput of the ultrasound data stream captured by the expert using the WiMAX and HSUPA testbed platforms. The mean throughput was calculated by repeating the experimental test 20 times for each frame size value.

¹ *Ethereal* (version 0.10.11) is open-source network analyzer (available at <http://www.ethereal.com>)
² *MATLAB* (matrix laboratory version 7.8.0.347) was developed by MathWorks, Inc (Headquarters: Massachusetts, USA) which is used for mathematical computation, data analysis, visualization, and algorithm implementation.

Both WiMAX and HSUPA networks support different ultrasound video qualities of QCIF and CIF. The WiMAX network can also support 4CIF frame size with different frames per second. The experimental results show that practically both WiMAX and HSUPA networks support uplink medical video streaming with average 0.6 Mb/s. However, WiMAX can support uplink medical video streaming with an average 1.2 Mb/s, as shown in Figure 6.6.

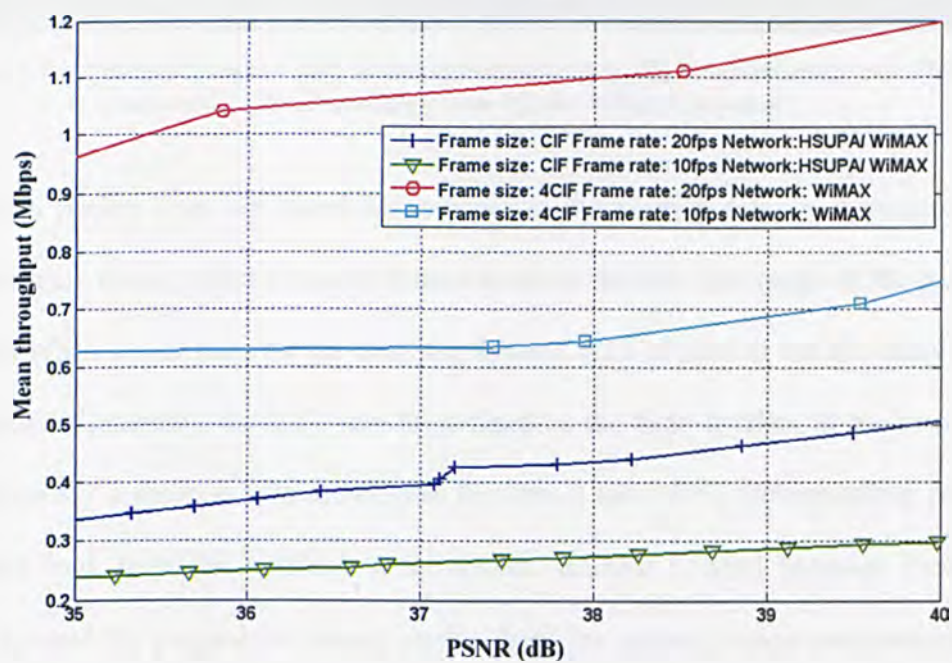


Figure 6.6 Mean throughput vs PSNR

Figure 6.7 shows the comparative visual results for the tested ultrasound video sequences. Figure 6.7(a) is a part of a CIF video with an average PSNR of 38.86 dB transmitted to the expert end over HSUPA and mobile WiMAX networks. Figure 6.7(b) shows the received video over the HSUPA network and figure 6.7(c) shows the received video over the mobile WiMAX network. The received images are clinically acceptable according to our 4 medical expert observers (as discussed in section 5.4). From these results, it can be seen that figure 6.7(c) has a higher PSNR resolution

compared to Figure 6.7(b). The results have been evaluated and confirmed by our clinical advisors.



Figure 6.7 Ultrasound images PSNR 38.86. (a) Original image. (b) Received image over HSUPA network. (c) Received image over Mobile WiMAX network

Different packet sizes are tested to characterize the various delay performances of both networks. These packet sizes are chosen to cover the best size range of the packet-generated WMV codec used by the encoding system. RTT is used to test the delay time performance. Generally, the RTT can be defined as the time it takes to transmit one packet from say a server to a terminal, plus the time it takes for a corresponding packet to be sent back from the terminal to the server. Internet Control Message Protocol (ICMP) is used for pinging the expert station from the patient station continuously to find the average RTT. The small size ICMP packet measures the network processing element and interface delays. Figures 6.8 and 6.9 show the comparative results of the RTT values for different packet sizes over HSUPA and different WiMAX modulation and coding schemes. The results show that the WiMAX provides better RTT performance compared to HSUPA network; this is due to the higher available downlink and uplink bandwidth in the WiMAX network compared to HSUPA network. However, according to the results shown in Figures 6.8 and 6.9, the application response times in both networks are within the acceptable range of clinical diagnosis, and acceptable range of ultrasound video streaming has been defined in [32].

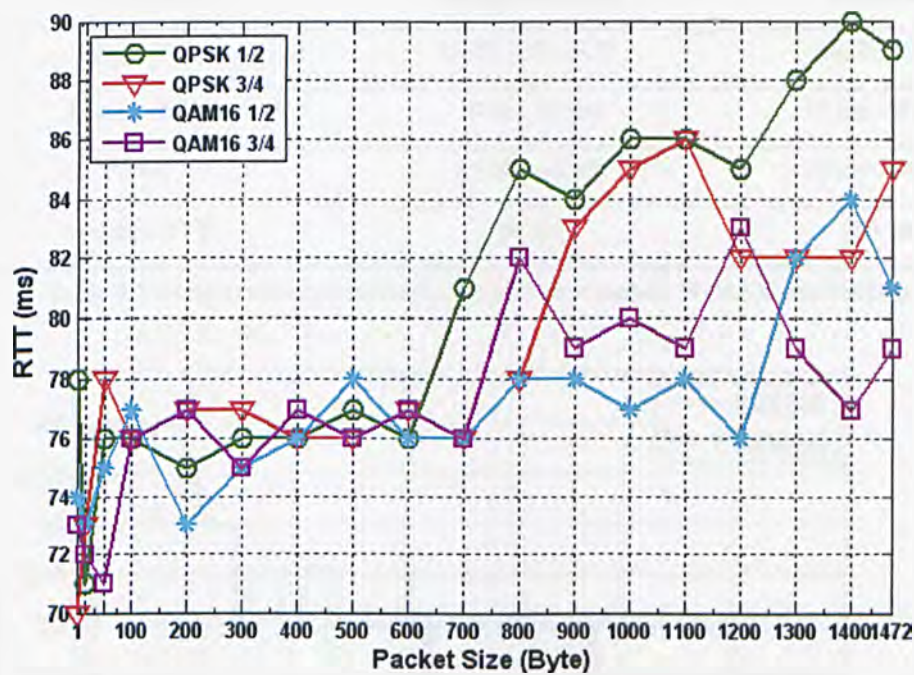


Figure 6.8 RTT results of different ultrasound video stream packet sizes over WiMAX

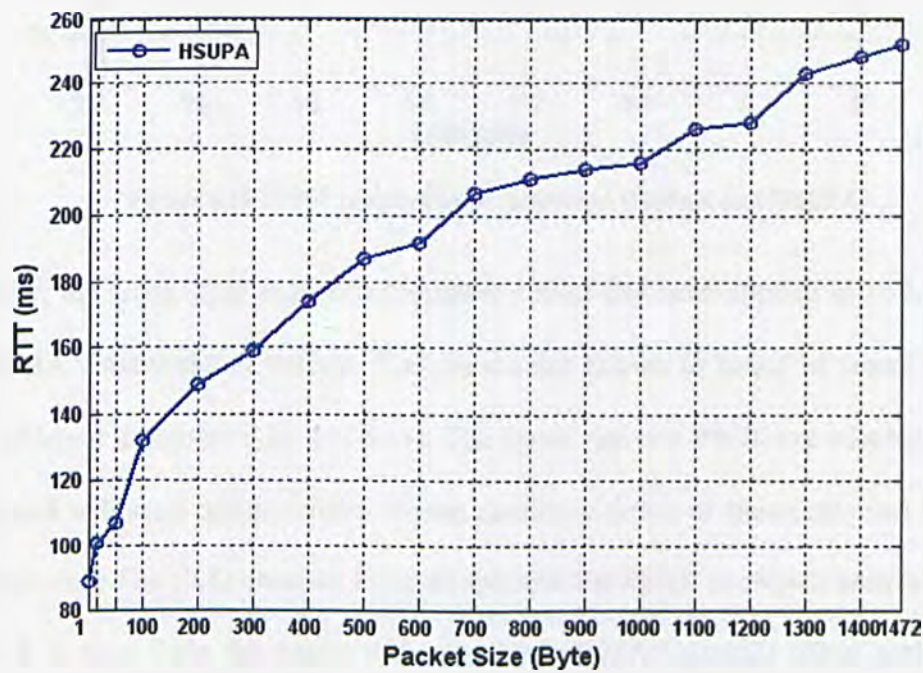


Figure 6.9 RTT results of different ultrasound video stream packet sizes over HSUPA

Table 6.2 summarizes the ultrasound video streaming results over WiMAX and HSUPA networks.

QoS index	Mobile WiMAX	HSUPA
Image Size	QCIF, CIF, 4CIF	QCIF, CIF
Frame Rate	10 fps, 20 fps	10 fps, 20 fps
PSNR	35 dB~ 40 dB	35 dB~ 40dB
Average RTT	80 ms	150 ms

Table 6.2 Comparative performance results over mobile WiMAX and HSUPA

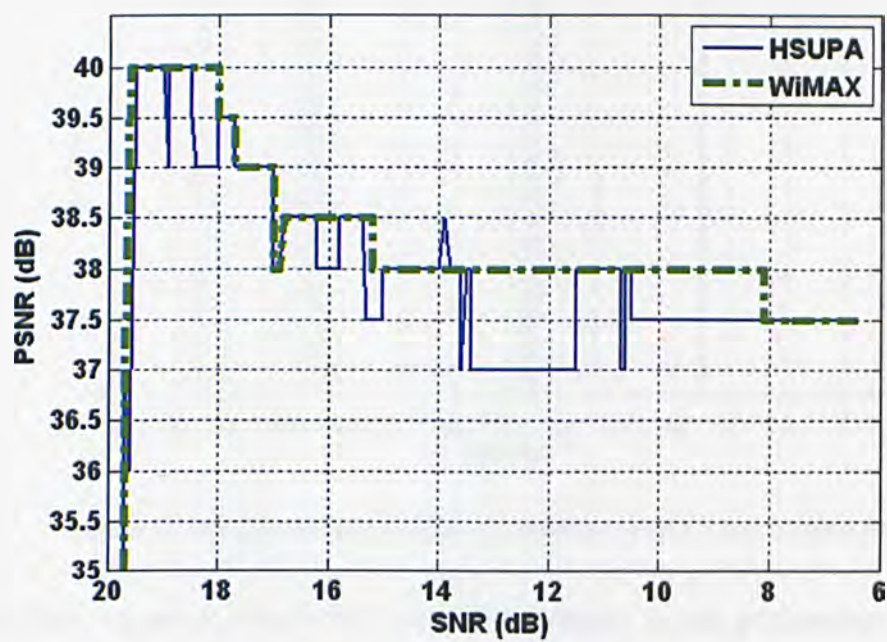


Figure 6.10 PSNR comparison of optimised WiMAX and HSUPA

Finally, the cross layer approach presented earlier has been applied to both HSUPA and WiMAX networks as offline. The results are shown in terms of frame rate and PSNR (Shown in figures 6.10 and 6.11). The frame rate and PSNR are adapted, and the patient end will send optimal video stream quality in terms of frame rate and PSNR to the expert end; The CLO chooses 10 or 20 fps, and the PSNR is chosen between 35 and 40 dB. It is clear from the results that optimized WiMAX provide better performance than HSUPA. The frame sizes used in the tests are QCIF and CIF. However, The WiMAX tests show that it can also have acceptable m-QoS support for 4CIF frame size. These experimental test results shown in Figures 6.10 and 6.11 clearly show that the

optimization approach performs successfully within the selected frame rate and image quality adaption, depending on the link layer condition.

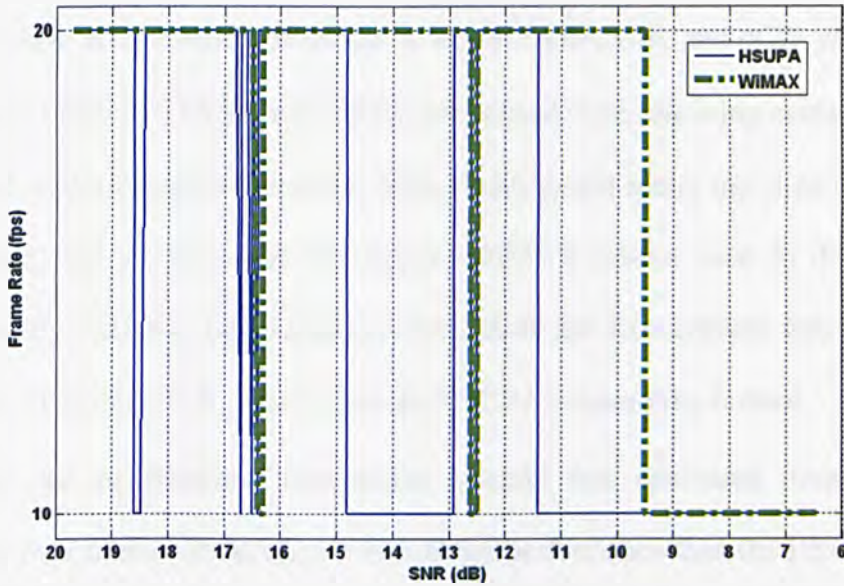


Figure 6.11 Frame rate comparison of optimised WiMAX and HSUPA networks

Another important observation from these results is the performance in terms of average frame rate, and PSNR increases in both cases; this is due to the effective use of wireless resources by deploying the cross layer approach. In other words, the WiMAX system has an acceptable dynamic QoS mechanism for such application.

6.4 Summary

In this chapter, we presented the experimental comparative analysis study of optimized cross layer video streaming over mobile WiMAX and HSUPA networks. The experimental performance of the proposed method was validated in terms of m-QoS parameters and network constraints. The optimized video streaming approach is based on an integrated cross layer approach (based on the RL method) to provide the real-time

adaptability of the rate and quality control in the ultrasound video streaming. The approach was applied to both mobile WiMAX and HSUPA networks to illustrate the practical performance in terms of QoS requirements (m-QoS) and clinically acceptable diagnostic quality. The video codec used in this experiment is Windows Media Video2 and the image sizes considered in this work are QCIF, CIF, and 4CIF with the video streaming of different PSNR and frames per second. The following evaluation metrics were used as performance outcomes: Video quality, and round trip time (RTT) versus packet size. The experimental test mobile WiMAX system used in this study was developed by Rinicom Ltd, Lancaster, UK. And the ExpressCard was provided by Vodafone, Berkshire, U.K. was used as the HSUPA connectivity testbed.

Finally, the experimental test results indicate that optimized ultrasound video streaming over mobile WiMAX provides better performance than the HSUPA in terms of frames per second, PSNR, and frame size, with an average uplink throughput of 1.2 Mb/s that is clinically acceptable for remote diagnostics.

Chapter 7

Conclusions and Future Work

7.1 Introduction

This chapter presents the conclusions and summary of the research work presented in this thesis. Suggestions for future work in this area are also given for further research in this area.

7.2 Conclusions

This thesis has concentrated on the following challenges:

- (i) Providing effective and accurate clinical diagnosis and remote analysis, especially with bandwidth demanding m-health services such as real-time ultrasound video streaming.
- (ii) The Quality of Service provision issues and their guarantee levels to provide robust and clinically approved m-health service.
- (iii) The efficiency and performance of layered model in mobile wireless environment.

This work has reviewed the cross layer design architecture to implement an appropriate cross layer model with considering of m-health requirements. In particular, this thesis addressed the medical QoS issues with the cross layer design approaches for the broadband m-health applications. A complete broadband m-health model has been designed and developed that includes three main multiparametric m-health scenarios:

accident, clinical, and homecare scenarios. This multiparametric m-health model has been evaluated using OPNET[®] modeler.

The proposed cross layer model has been implemented and analysed in OPNET[®] modeler. The cross layer optimiser required an initial Q-learning knowledge known as Q table and Reward table. These were produced by an external Visual studio C#.Net program considering all possible state-transitions. And during the simulation process, the reward table was optimised by RL algorithmic approach. The simulation results show that the cross layer scenario has different optimised video quality (PSNR value) depending on wireless status (SNR). In other words, the cross layer scenario sometimes reduces the video quality (PSNR value) to have an acceptable overall m-QoS. The results (PSNR, BER, and end-to-end delay) show the successful correlation of the proposed cross layer algorithmic approach with the m-QoS bounds presented earlier (average PSNR: 39 dB and end-to-end delay 52 ms).

In addition, there is a comparison performance analysis of mobile ultrasound video streaming over HSUPA and Mobile WiMAX networks.

This thesis has also investigated the effect of the packet impairment on ultrasound video streaming over mobile WiMAX network. To this aim, Ultrasound video streaming has been evaluated in terms of objective and subjective indices. The following performance metrics were measured: PSNR versus Packet loss, SSIM versus Packet loss, and MSE versus Packet loss. The results show that the proper combination of the objective quality metrics can provide precise evaluation of clinically acceptable medical video streaming over mobile WiMAX networks. It is also concluded that the overall packet loss probability greater than 0.09% is not acceptable clinically for the wireless ultrasound video streaming application.

The contributions and achievements of this thesis work can be summarized as follows:

- (1) A comprehensive literature review on mobile broadband m-health systems and relevant cross layer design approach.
- (2) We proposed a new cross layer approach designed for remote ultrasound video streaming. This approach is based on reinforcement learning algorithm that satisfies medical quality of service issues over mobile WiMAX networks.
- (3) The simulation results of the proposed approach using OPNET[®] modeler indicate the successful implementation of the proposed algorithmic approach with the m-QoS bounds defined for this m-health application.
- (4) The mapping of multiple parameter m-health scenarios to mobile WiMAX QoS variables was described. Three m-health scenarios were defined over mobile WiMAX using OPNET[®] modeler to investigate the network performance and the functionality of the relevant QoS mappings. The simulation results indicate the successful implementation of the QoS mapping with the defined m-QoS bounds.
- (5) An experimental comparative analysis study of optimised cross layer video streaming over mobile WiMAX and HSUPA test networks was presented. The experimental performance of the proposed method was validated in terms of different m-QoS. The experimental test results indicate that optimised ultrasound video streaming over mobile WiMAX provides better performance than HSUPA in terms of frames per second, PSNR, and frame size with an average uplink throughput of 1.2 Mbps that is acceptable for remote clinical diagnostics.
- (6) Subjective and objective studies for medical video streaming over WiMAX

network has been carried out. These results show that the proper combination of objective quality metrics can provide precise evaluation of clinically acceptable medical video streaming over WiMAX network. The overall packet loss greater than 0.09% is not acceptable clinically for the wireless ultrasound video streaming application.

7.3 Future Work

Despite the good results obtained in this thesis, there are some aspects that can be improved on to make the wireless ultrasound streaming architecture and methodology presented by this thesis even better.

- (1) Further studies on real time testing of the medical video streaming data over both networks to evaluate the concept on much larger imaging samples.
- (2) More focus on the video coding issues in cross layer optimizer parameters. The effect of coding efficiency and relevant challenges on the presented optimized approach can be further studied in future works.
- (3) Consideration of Non-line of sight (NLOS) communications performance as part of the future work in real-time cross layer performance analysis.
- (4) Further work on IEEE 802.16m. Since IEEE 802.16m supports higher bit rate that can mitigate some of the challenges discussed in this work. The proposed cross layer approach can be easily adapted to the new environment to modify the priorities and parameters in the reinforcement algorithm.
- (5) Further investigation of a new abstraction approach in the radio link layer, suitable for the optimisation approach.
- (6) The application of the concepts presented in real-time robotic remote

ultrasonography system.

Author's publications

Journal papers:

A. Alinejad, N.Y. Philip, R. S. H. Istepanian (2012) '**Cross-Layer Ultrasound Video Streaming Over Mobile WiMAX and HSUPA Networks**' *IEEE Transactions on Information Technology in Biomedicine*, Vol. 16, no. 1, pp. 31-39.

C. Debono, B. Micallef, N.Y. Philip, A. Alinejad, R. S. H. Istepanian '**Cross Layer Design for Optimised Region of Interest of Ultrasound Video Data over Mobile WiMAX**' in *IEEE Transactions on Information Technology in Biomedicine* (2013, To Appear).

Conference papers:

A. Alinejad, N. Philip, R. S. H. Istepanian (2012) **Dynamic Subframe Allocation for Mobile Broadband m-health using IEEE 802.16j Mobile Multihop Relay Networks**, in *34th Annual International Conference of the IEEE Engineering in Medicine and Biology Society (EMBC '12)*, IEEE, Aug 28 – Sep 1, San Diego, USA.

A. Alinejad , N. Philip, R. S. H. Istepanian (2011) **Mapping of Multiple Parameter m-health Scenarios to Mobile WiMAX QoS Variables** in *33rd Annual International Conference of the IEEE Engineering in Medicine and Biology Society (EMBC '11)*, IEEE, Aug 30 - Sep 3, Boston, USA, pp. 1532-1535.

A. Alinejad, N. Philip, R. S. H. Istepanian (2010) **Performance analysis of medical video streaming over mobile WiMAX** in *32nd Annual International Conference of the IEEE Engineering in Medicine and Biology Society*, IEEE, Aug 31 - Sep 4, Buenos Aires, Argentina, pp. 3471-3474.

A. Alinejad, N. Philip, R. S. H. Istepanian (2010) **Reinforcement learning algorithm for optimised cross layer medical video streaming over WiMAX networks** in *7th International Symposium on Communication systems, Networks and Digital signal processing*, IEEE, Jul 21 - 23, Newcastle, U.K., pp. 862-866.

Book chapter:

R. S. H. Istepanian , A. Alinejad, N. Philip, "**Medical Quality of Service (m-QoS) and Quality of Experience (m-QoE) for 4G-health Systems** " in *Multimedia Networking and Coding: From Capture to Display*, (2013, To Appear).

Technical Reports:

A. Alinejad, N. Philip, R. S. H. Istepanian (2009) **Asset Tracking Technologies** in Collaboration with Philips Technologies, UK, August-November.

A. Alinejad, N. Philip, R. S. H. Istepanian (2009) **Potential Needs of Tracking Technology in NHS Environments** in *Collaboration with Philips Technologies, UK*, August-November.

Presentation:

A. Alinejad, N. Philip, R. S. H. Istepanian (2010) **Effectiveness of Wireless Broadband Technologies for Remote Ultrasound Video Imaging and Diagnostics** in *British Society for Gynaecological Imaging (BSGI) Annual Scientific Meeting and Workshops*, April 15-16, London, UK.

References

- [1] Laxminarayan, S. and Istepanian, R.S.H. (2000) 'UNWIRED E-MED: the next generation of wireless and internet telemedicine systems', *IEEE Transactions on Information Technology in Biomedicine*, vol. 4, no. 3, Sep, pp. 189-193.
- [2] Istepanian, R.S.H., Jovanov, E. and Zhang, Y.T. (2004) 'Guest Editorial Introduction to the Special Section on M-Health: Beyond Seamless Mobility and Global Wireless Health-Care Connectivity', *IEEE Transactions on Information Technology in Biomedicine*, vol. 8, no. 4, Dec, pp. 405-414.
- [3] Istepanian, R.S.H. and Woodward, B. (2002) 'Programmable underwater acoustic telemedicine system', *Acoustica*.
- [4] Istepanian, R.S.H. and Petrosian, A.A. (2000) 'Optimal zonal wavelet-based ECG data compression for a mobile telecardiology system', *IEEE Transactions on Information Technology in Biomedicine*, vol. 4, no. 3, Sep, pp. 200-211.
- [5] Istepanian, R.S.H. and Nikagosian, H. (2000) 'Telemedicine in Armenia: A Perception of Telehealth Services in the Former Soviet Republics', *J. Telemedicine and Telecare*, vol. 6, pp. 268-272.
- [6] Istepanian, R.S.H. (1999) 'Telemedicine in the United Kingdom: current status and future prospects', vol. 3, no. 2, pp. 158-159.
- [7] Richards, C., Woodward, B. and Istepanian R.S.H. (1999) 'Exploiting mobile telephone technology for telemedicine applications', *Medical and Biological Engineering & Computing*, vol. 37, pp. 110-111.
- [8] Istepanian, R.S.H., Woodward, B., Balos, P. and Chen, S. (1999) 'The comparative performance of mobile telemedical systems using the IS-54 and GSM cellular telephone standards', *Journal of Telemedicine and Telecare*, vol. 5, no. 2, pp. 97-104.
- [9] Tachikawa, K. (2003) 'A perspective on the evolution of mobile communications', *Communications Magazine, IEEE*, vol. 43, no. 10, Oct, pp. 66-73.
- [10] Al-Jobouri, L., Fleury, M., and Ghanbari, M. (13-14 July 2011). Cross-layer scheme for WiMAX video streaming. *Computer Science and Electronic Engineering Conference (CEECE), 2011 3rd*, pp. 86-91. Colchester, UK: IEEE.
- [11] Panayides, A., Pattichis, M.S., Pattichis, C.S. and Pitsillides, A. (2011) 'A Tutorial for Emerging Wireless Medical Video Transmission Systems [Wireless Corner]', *IEEE Antennas and Propagation Magazine*, vol. 53, no. 2, pp. 202-213.
- [12] Kaur, B. (2010) 'Factors Influencing Implementation of 4G with Mobile Ad-hoc Networks In m-Governance Environment', *International Journal of Computer Applications*, vol. 3, pp. 141-146

-
- [13] Berndt, H. (2008) *Towards 4G Technologies: Services with Initiative*, Wiley.
 - [14] Chao, H.-C., Zeadally, S., Chen, Y.-S., Guest, G. M., and Wang, R.-C. (2010). Editorial: Next Generation Networks (NGNs). *International Journal of Communication Systems*, Vol. 23, no. 6-7, pp. 691–693.
 - [15] ETSI TS 125 308 V5.4.0 (2003-03), 3GPP TS 25.308 version 5.4.0 Release 5.
 - [16] Vaughan-Nichols, S.J. (2004) 'Achieving wireless broadband with WiMAX', *Computer*, vol. 37, no. 6, Jun, pp. 10-13.
 - [17] Cherry, S.M. (2004) 'WiMax and Wi-Fi: separate and unequal', *IEEE Spectrum*, vol. 41, no. 3, Mar, pp. 16-16.
 - [18] Chen, Y., and Darwazeh, I. (2011). End-to-end delay performance analysis in IEEE 802.16j Mobile Multi-hop Relay (MMR) networks. *18th International Conference on Telecommunications (ICT)*, pp. 488-492.
 - [19] Teo, K.H., Tao, Z. and Zhang, J. (2007) 'The Mobile Broadband WiMAX Standard', *Signal Processing Magazine, IEEE*, vol. 24, no. 5, Sep, pp. 144 - 148.
 - [20] Goldsmith, A. (2005) *Wireless Communications*, Cambridge University Press.
 - [21] Andrews, J. G., Ghosh, A., & Muhamed, R. (2007). *Fundamentals of WiMAX: Understanding Broadband Wireless Networking* (1 ed.). Prentice Hall.
 - [22] Craig, J., Patterson, V. (2005) 'Introduction to the practice of telemedicine', *Journal of Telemedicine and Telecare*, vol. 11, no. 1, pp. 3-9.
 - [23] Bachmutsky, A. (2009). *WiMAX Evolution: Emerging Technologies and Applications* (1 ed.). (M. Katz, & F. Fitzek, Eds.) Wiley.
 - [24] Courreges, F., Vieyres P., Istepanian, R.S.H., Arbeille, P. and Bru, C. (2005) 'Clinical trials and Evaluation of a mobile robotic tele-ultrasound System', *Journal of Telemedicine and Telecare*, vol. 11, no. 1, pp. 46-49.
 - [25] Malone, F.D. (1998) 'Effect of ISDN bandwidth on image quality for telemedicine transmission of obstetric ultrasonography', *Telemedicine Journal and e-health*, vol. 4, pp. 161-165.
 - [26] Zvikhachevskaya, A., Markarian, G. and Mihaylova, L. (2009) 'Quality of Service Consideration for the Wireless Telemedicine and E-Health Services', *Wireless Communications and Networking Conference*, Budapest, Hungary, pp. 1-6.
 - [27] Lerouge, C., Garfield, M.J. and Hevener, A.R. (2002), Quality attributes in telemedicine video conferencing, 35th Annual Hawaii International Conference on System Sciences, Washington, DC, USA, pp. 2050-2059.
 - [28] (ViDe), V.D.I. (2005) *The videoconference cookbook*, [Online], Available: <http://www.vide.net/cookbook/cookbook.en/> [2 May 2011].
 - [29] Burgul, R..G.F.J.a.U.P.E. (n.d) 'Methods of Measurement of image quality in teleultrasound', *The British Journal of Radiology*, pp. 1306-1312.

-
- [30] Jamalipour, A. (2003) *The Wireless Mobile Internet: Architectures, Protocols and Services*, 1st edition, Wiley.
- [31] Mehmood, M.A., Sengul, C., Sarrar, N. and Feldmann, A. (2011) 'Understanding Cross-Layer Effects on Quality of Experience for Video over NGMN', *IEEE International Conference on Communications (ICC)*, Kyoto, pp. 1-5.
- [32] Istepanian, R.S.H., Philip, N.Y. and Martini, M.G. (2009) 'Medical QoS Provision Based on Reinforcement Learning in Ultrasound Streaming over 3.5G Wireless Systems', *Selected Areas in Communications, IEEE Journal on*, vol. 27, no. 4, pp. 566-574.
- [33] DeMarca, J.R.B. and Chen, K. (2008) *MobileWiMAX*, New York: Wiley.
- [34] Zhang, Q. and Zhang, Y. (2008) 'Cross-Layer Design for QoS Support in Multihop Wireless Networks', *Proceedings of the IEEE*, vol. 96, no. 1, pp. 64-76.
- [35] Triantafyllopoulou, D., Passas N. and Alexandros K. (2007) 'A Cross-Layer Optimization Mechanism for Multimedia Traffic over IEEE 802.16 Networks', *13th European Wireless 2007*, Paris, France.
- [36] Kawadia, V. and Kumar, P.R. (2005) 'A Cautionary Perspective on Cross-Layer Design', *IEEE Wireless Communications*, vol. 12, no. 1, pp. 3-11.
- [37] Raisinghani, V.T. and Iyer, I. (2004) 'Cross-layer design optimizations in wireless protocol stacks', *Computer Communications*, vol. 27, no. 8, pp. 720-724.
- [38] Kota, S., Giambene, G. and Candio, N.L. (2007) 'Cross-layer approach for an air interface of GEO satellite communication networks', *International Journal of Satellite Communications and Networking*, vol. 25, no. 5, p. 481-499.
- [39] Zhang, Y. and Chen, H.-H. (2007). *Mobile WiMAX: Toward Broadband Wireless Metropolitan Area Networks*. Auerbach Publications.
- [40] Schaar, V.D. and Shankar, N. S. (2005) 'Cross-layer wireless multimedia transmission: challenges, principles, and new paradigms', *Wireless Communications, IEEE*, vol. 12, no. 4, pp. 50-58.
- [41] Akyildiz, I.F. and Xudong, W. (2008) 'Cross-Layer Design in Wireless Mesh Networks', *Vehicular Technology, IEEE Transactions on*, vol. 57, no. 2, pp. 1061-1076.
- [42] Foukalas, F., Gazis, V. and Alonistioti, N. (2008) 'Cross-layer design proposals for wireless mobile networks: a survey and taxonomy', *Communications Surveys & Tutorials, IEEE*, vol. 10, no. 1, pp. 70-85.
- [43] Srivastava, V. and Motani, M. (2005) 'Cross-Layer Design A survey and the road ahead', *Communications Magazine, IEEE*, vol. 43, no. 12, pp. 112-119.
- [44] Choi, L.U., Kellerer, W. and Steinbach, E. (2006) 'On cross-layer design for streaming video delivery in multiuser wireless environments', *EURASIP Journal on Wireless Communications and Networking*, vol. 2006, no. 2, pp 1-10

-
- [45] Jafari, A. and Mohammadi, A. (2009) 'A cross layer approach based on queuing and adaptive modulation for MIMO systems', *Telecommunication Systems*, vol. 42, no. 1-2, pp. 85-96.
- [46] Khan, S., Peng, Y., Steinbach, E., Sgroi, M. and Kellerer, W. (2006) 'Application-Driven Cross-Layer Optimization for Video Streaming over Wireless Networks', *Communications Magazine, IEEE*, vol. 44, no. 1, pp. 122-130.
- [47] Istepanian, R.S.H., Philip, N.Y. and Martini, M.G. (2009) 'Medical QoS Provision Based on Reinforcement Learning in Ultrasound Streaming over 3.5G Wireless Systems', *Selected Areas in Communications, IEEE Journal on*, vol. 27, no. 4, pp. 566-574.
- [48] Martini, M.G., Istepanian, R.S.H., Mazzotti, M. and Philip, N.Y. (2010) 'Robust Multilayer Control for Enhanced Wireless Telemedical Video Streaming', *IEEE Transactions on Mobile Computing*, vol. 9, no. 1, pp. 5-16.
- [49] Winter, R., Schiller, J.H., Nikaein, N. and Bonnet, C. (2006) 'CrossTalk: cross-layer decision support based on global knowledge', *Communications Magazine, IEEE*, vol. 44, no. 1, pp. 93-99.
- [50] Ksentini, A., Naimi, M. and Gueroui, A. (2006) 'Toward an improvement of H.264 video transmission over IEEE 802.11e through a cross-layer architecture', *Communications Magazine, IEEE*, vol. 44, no. 1, pp. 107-114.
- [51] Cross layer design for optimized video streaming over heterogeneous networks, 2010, AA Djamal, E Meddour, T Ahmed
- [52] Song, G. and Li, Y. (2005) 'Cross-layer optimization for OFDM wireless networks-part I: theoretical framework', vol. 4, no. 2, pp. 614-624.
- [53] Milani, S. and Calvagno, G. (2009) 'A Low-Complexity Cross-Layer Optimization Algorithm for Video Communication Over Wireless Networks', *Multimedia, IEEE Transactions on*, vol. 11, no. 5, pp. 810-821.
- [54] Alinejad, A., Philip, N. and Istepanian, R. (2012) 'Cross Layer Ultrasound Video Streaming over Mobile WiMAX and HSUPA Networks', *IEEE Transactions on Information Technology in Biomedicine*, Vol. 16, no. 1, pp. 31-39.
- [55] Lin, C.-F. (2010) 'Mobile Telemedicine A Survey Study', *Journal of Medical Systems*.
- [56] Li, S.H., Cheng, K.A., Lu, W.H. and Lin, T.C. (2011). Developing an Active Emergency Medical Service System Based on WiMAX Technology. *Journal of medical systems* , pp. 1-17.
- [57] Niyato, D., Hossain, E. and Diamond, J. (2007) 'IEEE 802.16/WiMAX-based broadband wireless access and its application for telemedicine/e-health services', *Wireless Communications, IEEE*, vol. 14, no. 1, pp. 72-83.

-
- [58] Pattichis, C.S., Kyriacou, E., Voskarides, S., Pattichis, M.S., Istepanian, R. and Schizas, C.N. (2002) 'Wireless telemedicine systems: an overview', *Antennas and Propagation Magazine, IEEE*, vol. 44, no. 2, Apr, pp. 143-153.
- [59] Komnakos, D., Vouyioukas, D., Maglogiannis, I. and Constantinou, P. (2008) 'Performance Evaluation of an Enhanced Uplink 3.5G System for Mobile Healthcare Applications', *International Journal of Telemedicine and Applications*, Hindawi Publishing Corporation, vol. 2008, Article ID 417870, pp. 1-11.
- [60] Soomro, A. and Cavalcanti, D. (2007) 'Opportunities and challenges in using WPAN and WLAN technologies in medical environments', *Communications Magazine, IEEE*, vol. 45, no. 2, pp. 114-122.
- [61] Prasad, R. and Velez, F.J. (2010) *WiMAX Networks: Techno-Economic Vision and Challenges*, 1st edition, Springer.
- [62] Zhang, Y., Ansari, N. and Tsunoda, H. (2010) 'Wireless telemedicine services over integrated IEEE 802.11/WLAN and IEEE 802.16/WiMAX networks', *IEEE Wireless Communications*, vol. 17, no. 1, pp. 30-36.
- [63] Guainella, E., Borcoci, E., Katz, M., Neves, P., Curado, M., Andreotti, F. and Angori, E. 'WiMAX technology support for applications in environmental monitoring, fire prevention and telemedicine' (2007), *Mobile WiMAX Symposium, 2007. IEEE*, Orlando, FL , pp. 125-131.
- [64] Vouyioukas, D., Maglogiannis, I. and Komnakos, D. (2007) 'Emergency m-Health Services through High-Speed 3G Systems: Simulation and Performance Evaluation', *SIMULATION*, vol. 83, no. 4, pp. 329-345.
- [65] Sublett, J.W., Dempsey, B.J. and Weaver, A.C. (1995) 'Design and Implementation of a Digital Teleultrasound System for Real-Time Remote Diagnosis', *Eighth IEEE Symposium on Computer-Based Medical Systems*, Lubbock, Texas, 292 - 298.
- [66] De Cunha, D., Gravez, P., Leroy, C., Maillard, E., Jouan, J., Varley, P., Jones, M., Halliwell, M., Hawkes, D., Wells, P.N.T. and Angelini, L. (1998) 'The MIDSTEP system for ultrasound guided remote telesurgery', *Engineering in Medicine and Biology Society*, Hong Kong , China , pp. 1266-1269.
- [67] Philip, N.Y. (2008). *Medical Quality of Service for Optimized Ultrasound Streaming in Wireless Robotic Tele-ultrasonography System*. Ph.D. thesis, Kingston University London.
- [68] Oboe, R. (2001) 'Web-interfaced, force-reflecting teleoperation systems', *Industrial Electronics, IEEE Transactions on*, vol. 48, no. 6, pp. 1257-1265.
- [69] Masuda, K., Kimura, E., Tateishi, N. and Ishihara, K. (2001) 'Three dimensional motion mechanism of ultrasound probe and its application for tele-echography system', *Intelligent Robots and Systems*, pp. 1112-1116.
- [70] Jha, S., and Hassan, M. (2002). *Engineering Internet QoS*. Artech House.

- [71] Ahson, S. A., and Ilyas, M. (2007). *WiMAX: Applications*. CRC Press.
- [72] Ergen, M. (2009). *Mobile Broadband: Including WiMAX and LTE* (1 ed.). Springer.
- [73] Zhang, Y. (2009). *WiMAX Network Planning and Optimization*. CRC Press.
- [74] IEEE Standard 802.16-2009 (2009). *802.16-2009 IEEE Standard for Local and metropolitan area networks Part 16: Air Interface for Broadband Wireless Access Systems*. IEEE.
- [75] Peters, S.W., and Heath, R. (2009). The future of WiMAX: Multihop relaying with IEEE 802.16j. *Communications Magazine, IEEE*, Vol. 47, no. 1, pp. 104-111.
- [76] Kwang-Cheng, C., & J.Roberto, B. d. (2008). *Mobile WiMAX*. Wiley.
- [77] Rao, G. R., and Radhamani, G. (2007). *WiMAX: A Wireless Technology Revolution* (1 ed.). Auerbach Publications.
- [78] So-In, C., Jain, R., and Tamimi, A.-K. (2009). Scheduling in IEEE 802.16e mobile WiMAX networks: key issues and a survey. *IEEE Journal on Selected Areas in Communications*, 27 (2), pp. 156-171.
- [79] Holma, H., and Toskala, A. (2006). *HSDPA/HSUPA for UMTS: High Speed Radio Access for Mobile Communications*. Wiley-Blackwell.
- [80] Johnson, C. (2008). *Radio Access Networks for UMTS: Principles and Practice*. Wiley-Blackwell.
- [81] Furht, B., and Ahson, S. A. (2010). *HSDPA/HSUPA Handbook* (1 ed.). CRC Press.
- [82] Ghazal, S., Mokdad, L., and Ben-Othman, J. (2008). Performance Analysis of UGS, rtPS, nrtPS Admission Control in WiMAX Networks. *Proceedings of IEEE International Conference on Communications*, Beijing, China, pp. 2696-2701.
- [83] Etoh, M., and Yoshimura, T. (2005). Advances in Wireless Video Delivery. *Special Issue On Advances In Video Coding And Delivery*, vol. 93, no.1, 111-122.
- [84] Bhargava, A., Khan, M. F., and Ghafoor, A. (2003). QoS Management in Multimedia Networking for Telemedicine Applications. *IEEE Workshop on Software Technologies for Future Embedded Systems*. IEEE, West Lafayette, IN, USA, pp. 39-42.
- [85] Oberoi, V., and Chigan, C. (2005). Providing QoS for sensor enabled emergency applications. *IEEE International Conference on Mobile Adhoc and Sensor Systems Conference*, IEEE, pp. 157-159.
- [86] Wac, K., Halteren, A. V., Bults, R., and Broens, T. (2007). Context-aware QoS provisioning in an m-health service platform. *International Journal of Internet Protocol Technology*, vol. 2, no. 2, pp. 102-108.
- [87] Lage, A., Martins, J., Oliveira, J., and Cunha, W. (2004). A quality of service framework for tele-medicine applications. *WebMedia and LA-Web*, pp. 18-20.

-
- [88] Nishantha, D., Hayashida, Y., and Hayashi, T. (2004). Application level rate adaptive motion-JPEG transmission for medical collaboration systems. *Distributed Computing Systems Workshops*, pp. 64-69.
- [89] Soomro, A., and Cavalcanti, D. (2007). Opportunities and challenges in using WPAN and WLAN technologies in medical environments. *IEEE Communications Magazine* , 45 (2), pp. 114-122.
- [90] Cosman, P., Gray, R., and Olshen, R. (2002). Evaluating quality of compressed medical images: SNR, subjective rating, and diagnostic accuracy. *Proceedings of the IEEE*, vol. 82, no. 6, pp. 919-932.
- [91] Alinejad, A. ,Philip, N.Y., and Istepanian, R.S.H. (2010) Performance analysis of medical video streaming over mobile WiMAX in *32nd Annual International Conference of the IEEE Engineering in Medicine and Biology Society*, IEEE, Aug 31 - Sep 4, Buenos Aires, Argentina, pp. 3471-3474.
- [92] Hands, D., Huynh-Thu, Q., Rix, A., Davis, A., and Voelcker, R. (2004). Objective perceptual quality measurement of 3G video services. *3G Mobile Communication Technologies*, pp. 437-441.
- [93] Istepanian, R.S.H., Philip, N.Y., Martini, M.G., Amso, N., and Shorvon, P. (2008). 'Subjective and objective quality assessment in wireless teleultrasonography imaging' 30th Annual International Conference of the IEEE, *IEEE Engineering in Medicine and Biology Society*, Vancouver, BC, pp. 5346-5349.
- [94] Garawi, S., Courreges, F., Istepanian, R.S.H., Zisimopoulos, H., and Gosset, P. (2004). Performance analysis of a compact robotic tele-echography E-health system over terrestrial and mobile communication links. *3G Mobile Communication Technologies*, pp. 118-122.
- [95] Canero, C., Thomos, N., Triantafyllidis, G., Litos, G., and Strintzis, M. (2005). Mobile tele-echography: user interface design. *Information Technology in Biomedicine, IEEE Transactions on* , 9 (1), pp. 44-49.
- [96] Garawi, S., Istepanian, R.S.H., and Abu-Rgheff, M. (2006). 3G wireless communications for mobile robotic tele-ultrasonography systems. *Communications Magazine, IEEE* , 44 (4), pp. 91-96.
- [97] Alinejad, A., Philip, N. and Istepanian, R.S.H. (2010) 'Reinforcement learning algorithm for optimised cross layer medical video streaming over WiMAX networks', *Communication Systems Networks and Digital Signal Processing (CSNDSP)*, Newcastle upon Tyne, pp. 862-866.
- [98] Jiang, H., Zhuang, W. and Shen, X. (2005) 'Cross-layer design for resource allocation in 3G wireless networks and beyond', *IEEE Communications Magazine*, vol. 43, no. 12, pp. 120-126.

-
- [99] Chermiaki, S., D'Antonio, L., Forti, F., Lalli, R., Petersson, J. and Terzani, A. (2003) 'QoS enhancement for adaptive streaming services over WCDMA', *Selected Areas in Communications, IEEE Journal on*, vol. 21, no. 10, pp. 1575-1584.
 - [100] Alasti, M., Neekzad, B., Hui, J. and Vannithamby, R. (2010) 'Quality of service in WiMAX and LTE networks', *Communications Magazine, IEEE*, vol. 48, no. 5, pp. 104-111.
 - [101] Dayan, P. and Watkins, C.J. (2003) 'Reinforcement Learning', *Encyclopedia of Cognitive Science*, in press.
 - [102] Chen, Y.-S., Chang, C.-J. and Ren, F.-C. (2004) 'Q-learning-based multirate transmission control scheme for RRM in multimedia WCDMA systems', *Vehicular Technology, IEEE Transactions on*, vol. 53, no. 1, pp. 38-48.
 - [103] Dayan, P. (1992) 'Technical Note Q-Learning', *Machine Learning*, vol. 292, no. 3, pp. 279-292.
 - [104] Szepesvari, C. (2010) *Algorithms for Reinforcement Learning*, Morgan and Claypool.
 - [105] Liu, G.P., Yang, J. and Whidborne, J.F. (2002) *Multiobjective Optimisation and Control*, 1st edition, Wiley-Blackwell.
 - [106] Zhou, W., Bovik, A.C., Sheikh, H.R. and Simoncelli, E.P. (2004) 'Image Quality Assessment: From Error Measurement to Structural Similarity', *IEEE Trans. Image Processing*, vol. 13, no. 4, pp. 600-612.
 - [107] Wang, Z., Sheikh, H.R. and Bovik, A.C. (2002) 'No-reference perceptual quality assessment of JPEG compressed images', *International Conference on Image Processing*, pp. 477-480.
 - [108] *OPNET Modeler Documentation Set Version: 15.0*, OPNET Technologies, Inc.
 - [109] <http://www.vodafone.co.uk/personal/price-plans/network-and-coverage/> uk-coverage-map/, [Online] [Accessed Dec 2011].
 - [110] Sheikh, A.A.R.E., Abu-taieh, E.M.O. and El-sheikh, A.A.R. (2009) *Handbook of Research on Discrete Event Simulation Environments: Technologies and Applications*, 1st edition, Information Science Reference.
 - [111] Katzela, I. (1998) *Modeling and Simulating Communications Networks: A Hands-on Approach Using OPNET*, Prentice Hall.
 - [112] Alinejad, A., Philip, N.Y., and Istepanian, R.S.H. (2011) Mapping of Multiple Parameter m-health Scenarios to Mobile WiMAX QoS Variables in *33rd Annual International Conference of the IEEE Engineering in Medicine and Biology Society (EMBC '11)*, IEEE, Aug 30 - Sep 3, Boston, USA, pp. 1532-1535.
 - [113] Hallam-Baker, N. (2006) *Challenges of the Evolving 3G Technology*, Aeroflex.

-
- [114] Maass, M., Kosonen, M., and Korman, M. (2000) 'Transportation savings and medical benefits of a teleneuroradiological network', *Journal of Telemedicine and Telecare* , vol. 6, pp. 142-146.
- [115] Istepanian, R. S., Laxminarayan, S., & Pattichis, C. S. (2005) *M-Health: Emerging Mobile Health Systems*, Springer.
- [116] Greengrass, J., Evans, J., and Begen, A. C. (2009). *Not all packets are equal, part 2, the impact of network packet loss*. CISCO.
- [117] Hua-xia, R., Chong-rong, L., and Sheng-ke, Q. (2006). Evaluation of packet loss impairment on streaming video. *Journal of Zhejiang University - Science A* ,vol. 7, pp. 131-136.

Appendix – A

Visual studio 2008 C#.Net code – Generating initial RL knowledge

A visual studio 2008 C#.Net program has been developed to emulate the cross layer optimizer. This program imports WiMAX behavior form OPNET modeler to provide accurate results. The main purposes of the application can be listed as follows:

- 1) Creating a reward matrix
- 2) Finding the best correlation of max-min parameters

The application also provides a small scale of cross layer emulator and provides the opportunity to debug and optimise the CLO codes. Figure A.1 shows the emulator’s user interface.

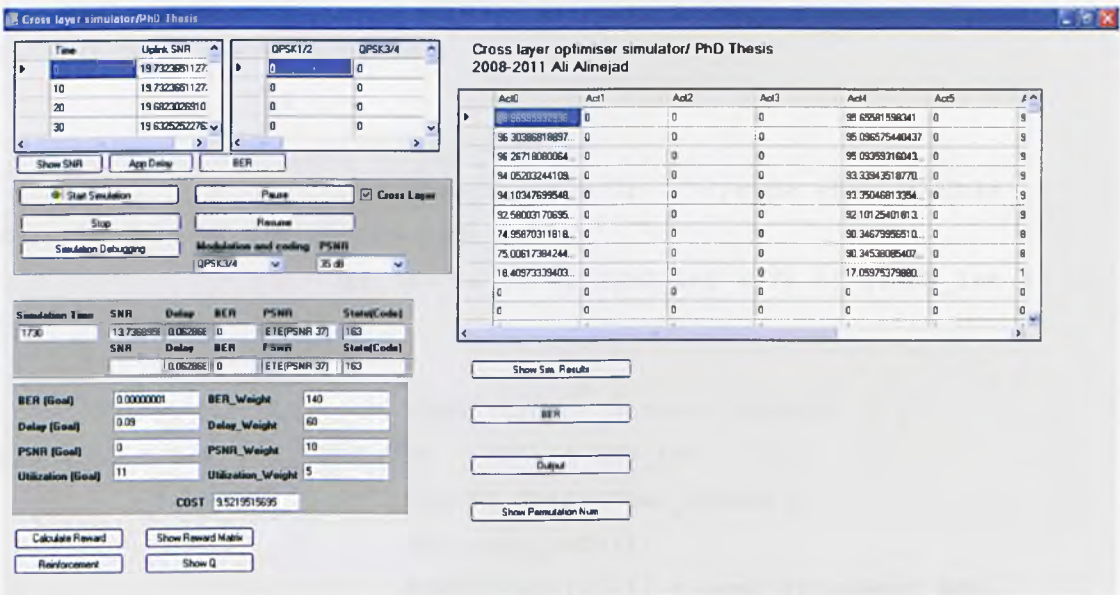


Figure A. 1 Cross layer emulator’s user interface

As discussed earlier in chapter 5, the formulation of the Reward matrix initialization is considered a critical part of the reinforcement algorithmic approach and it affects the performance of the learning process. The emulator provides the Initial-Reward matrix. The off-line process allows us to choose the best fitted parameters. However, the Initial-Reward matrix will be improved during the CLO operation as background process. The summary of initialization function is presented in the below codes.

```
//***** Reward Matrix initialing Function
public void Reward_Q_matrix_Initialize()
{
    // Initializing the Reward matrix to -1000
    for (int i = 0; i < 512; i++) //216
    {
        for (int j = 0; j < 9; j++) //J: 0)+MC/+P 1)+MC/-
P 2)-MC/+P 3)-MC/-P
        { // 4)MC/+P 5)MC/-P 6)MC/P
//7)+MC/P 8)-MC/P
            REWARD_Arr[i, j] = double.MinValue; //-Rew_Goal;
            if ( ( ( i & 15) <= 8) && ((i & 112) / 16 <= 7) &&
((i & 384) / 128 <= 2)) //SNR_int = (st & 15); MC_int = (st &
112) / 15;PSNR_int = (st & 384) / 127;
            {
                DECODE_State(i);
                int Next_State = 0; //code_state(double
SNR_in, double MC_in, double PSNR_in )
                if ((j == 0) && ((MC_int < 7) && (PSNR_int <
2)))
                {
                    Next_State = Convert.ToInt32 ( (
++PSNR_int * 128) + (++MC_int * 16) + SNR_int );
                    DECODE_State(Next_State);
                    Retrieve_info();
                    REWARD_Arr[i, j] = cost_func(Next_BER,
Next_delay, PSNR_int, Next_Util);
                }
            }
        }
    }
}
```

```

else if ((j == 1) && ((MC_int < 7) &&
(PSNR_int > 0)))
{
    Next_State = Convert.ToInt32((--PSNR_int *
128) + (++MC_int * 16) + SNR_int);
    DECODE_State(Next_State);
    Retrieve_info();
    REWARD_Arr[i, j] = cost_func(Next_BER,
Next_delay, PSNR_int, Next_Util);
}
else if ((j == 2) && ((MC_int > 0) &&
(PSNR_int < 2)))
{
    Next_State = Convert.ToInt32(++PSNR_int *
128) + (--MC_int * 16) + SNR_int);
    DECODE_State(Next_State);
    Retrieve_info();
    REWARD_Arr[i, j] = cost_func(Next_BER,
Next_delay, PSNR_int, Next_Util);
}
else if ((j == 3) && ((MC_int > 0) &&
(PSNR_int > 0)))
{
    Next_State = Convert.ToInt32((--PSNR_int *
128) + (--MC_int * 16) + SNR_int);
    DECODE_State(Next_State);
    Retrieve_info();
    REWARD_Arr[i, j] = cost_func(Next_BER,
Next_delay, PSNR_int, Next_Util);
}
else if ((j == 4) && (PSNR_int < 2))
{
    Next_State = Convert.ToInt32(++PSNR_int *
128) + (MC_int * 16) + SNR_int);
    DECODE_State(Next_State);
    Retrieve_info();
    REWARD_Arr[i, j] = cost_func(Next_BER,
Next_delay, PSNR_int, Next_Util);
}
else if ((j == 5) && (PSNR_int > 0))
{

```

```

        Next_State = Convert.ToInt32((--PSNR_int *
128) + (MC_int * 16) + SNR_int);
        DECODE_State(Next_State);
        Retrieve_info();
        REWARD_Arr[i, j] = cost_func(Next_BER,
Next_delay, PSNR_int, Next_Util);
    }
    else if (j == 6)
    {
        Next_State = Convert.ToInt32((PSNR_int *
128) + (MC_int * 16) + SNR_int);
        DECODE_State(Next_State);
        Retrieve_info();
        REWARD_Arr[i, j] = cost_func(Next_BER,
Next_delay, PSNR_int, Next_Util);
    }
    else if ((j == 7) && (MC_int < 7))
    {
        Next_State = Convert.ToInt32((PSNR_int *
128) + (++MC_int * 16) + SNR_int);
        DECODE_State(Next_State);
        Retrieve_info();
        REWARD_Arr[i, j] = cost_func(Next_BER,
Next_delay, PSNR_int, Next_Util);
    }
    else if ((j == 8) && (MC_int > 0))
    {
        Next_State = Convert.ToInt32((PSNR_int *
128) + (--MC_int * 16) + SNR_int);
        DECODE_State(Next_State);
        Retrieve_info();
        REWARD_Arr[i, j] = cost_func(Next_BER,
Next_delay, PSNR_int, Next_Util);
    }
}
Q_Arr[i, j] = 0; // Initializing the Q matrix
Q1[i, j] = Rew_Goal; //Convergence
}
}
}

```


Appendix – B

Rinicom Ltd – Mobile WiMAX devices

This appendix describes some of the technical specifications of the WiMAX system platform. The System is supplied by Rinicom Ltd., Lancaster, U.K.; the experimental testbed includes the following items:

- 1) 802.16e BS R8000 (Base station)
- 2) 802.16e CPE R8000 (Subscriber station)

Figure B.1 illustrates the device set-up. The network connection (RJ45) and serial connection (RS232) are used to configure and manage the BS and CPEs. The RJ45 connections are also used to transfer experimental data to these devices.

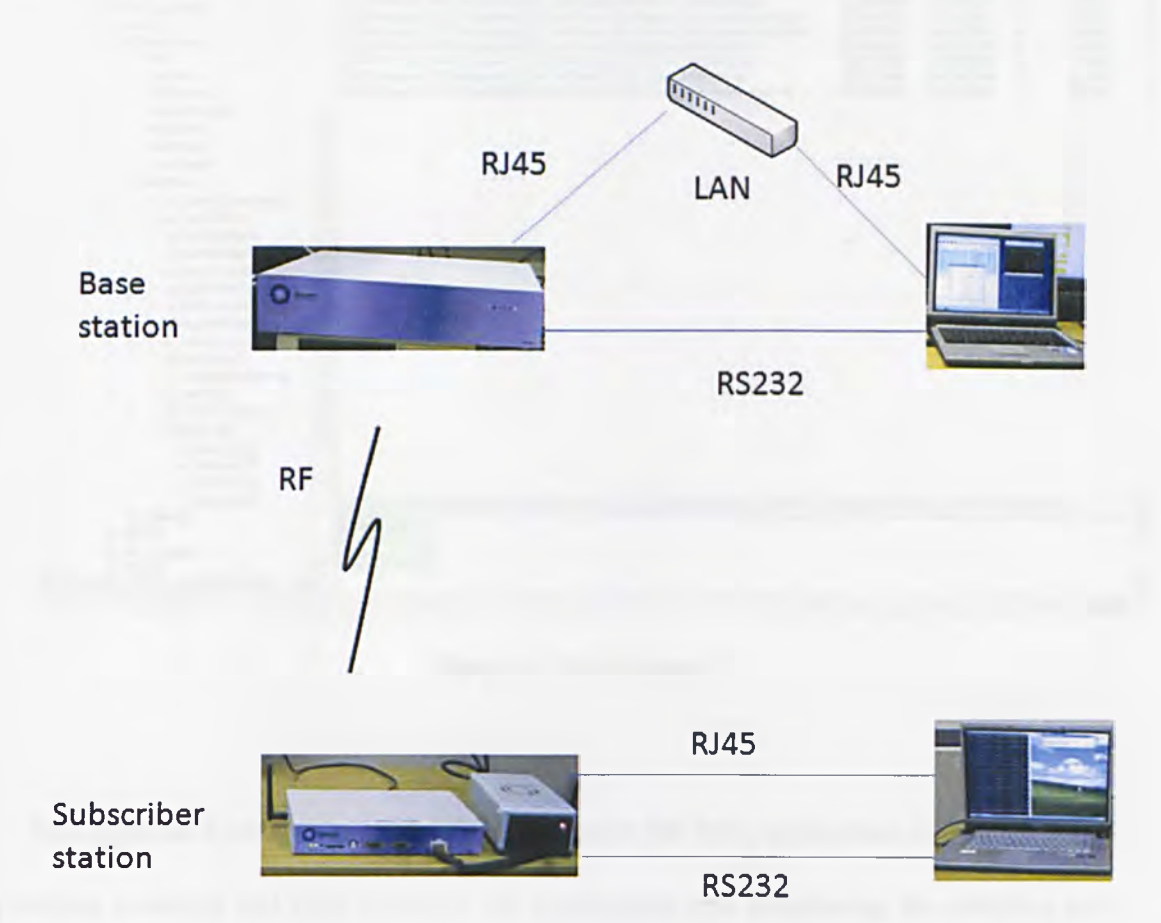


Figure B. 1 Experimental WiMAX device set-up

Hyper terminal application is used to set up initial configuration parameters such as the device IP and gateway IP.

Gdb browser is application that is used as PC front-end of Global Data Base on the target CPE and BS. The Gdb browser allows us to view and edit of WiMAX parameters, The Gdb browser is run through another application called Dispatcher. Figure B.2 shows some of the parameters that have been changed through Gdb browser. For example, the QoS class has been set to rtPS. And traffic priority is set to 7 through m-ServiceFlowSchedulingType and TrafficPriority parameters.

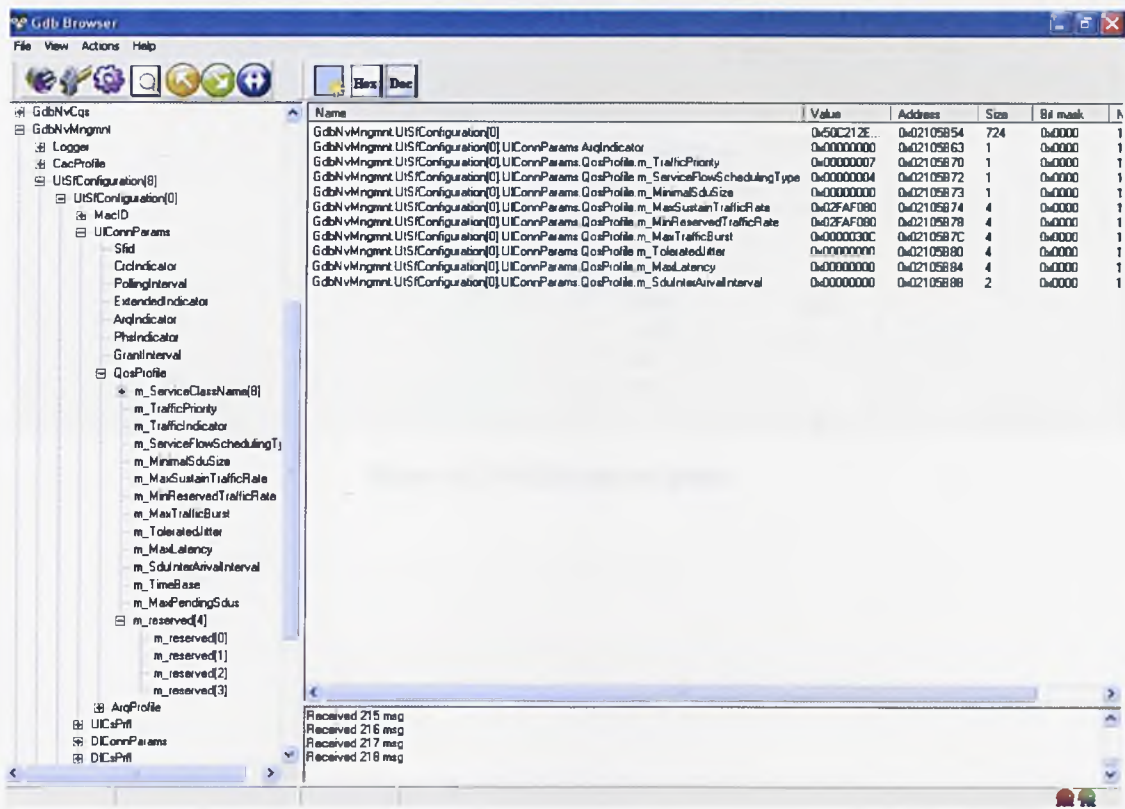


Figure B. 2 Gdb Browser

The Rinicom Configuration Management Script (RCMS) application is also used that provides a simple and clear interface for configuring and monitoring the statistics and

events of a base station. Figure B.3 shows the RCMS control panel. During the experimental work, this control panel is used specially for changing modulation and coding.

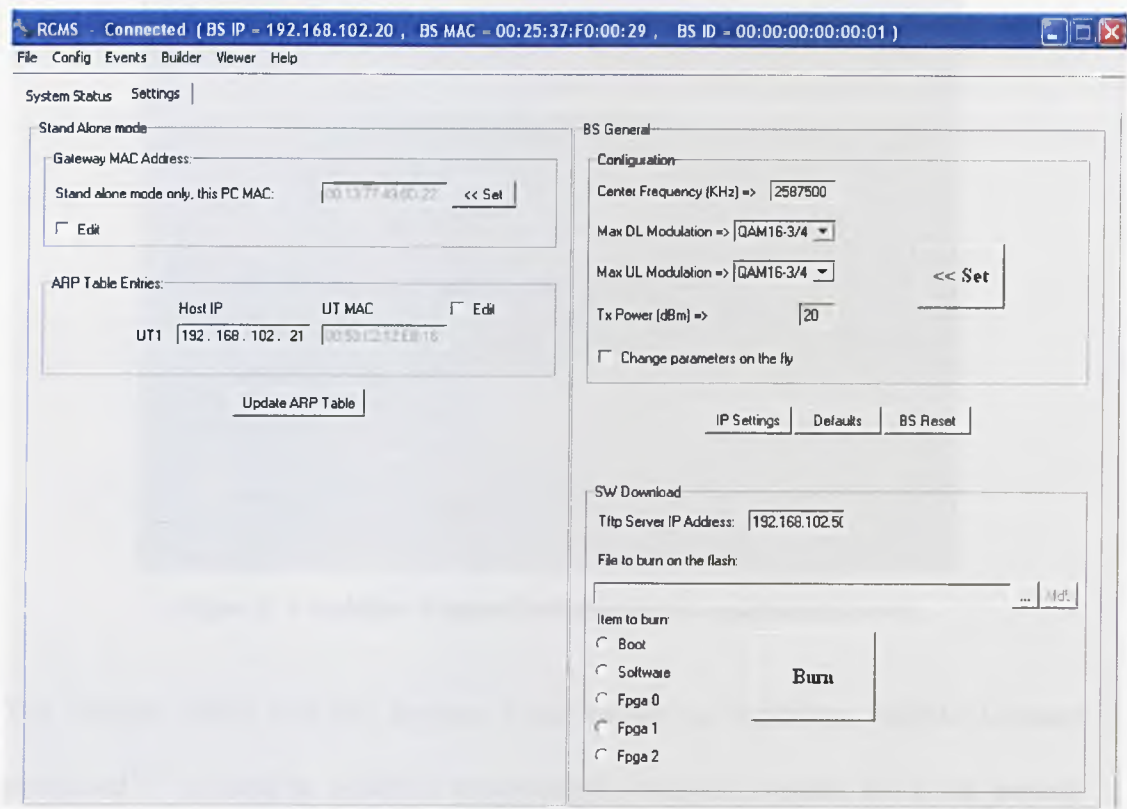


Figure B. 3 RCMS control panel

Appendix – C

Vodafone – Broadband Express Card



Figure C. 1 Vodafone ExpressCard used in the experimental work

The Huawei E870 HSUPA Express Card known as Vodafone Mobile Connect ExpressCard™ is used in HSUPA experimental analysis (Figure C.1). Its general features are as follows:

- HSUPA/HSDPA/UMTS 850/1900/2100MHz
- EDGE/GPRS/GSM 850/900/1800/1900MHz
- HSDPA Downlink 7.2Mbps;
- HSUPA Uplink 2Mbps
- SMS Service
- Plug and Play
- PCMCIA Card when adaptor equipped
- Express Card/54 or 34 slot, PCMCIA slot

Appendix – D

OPNET Modeler[®] introduction

OPNET Modeler[®] is the most popular network simulator package that contains a vast range of available models of network elements. OPNET Modeler[®] provides appropriate methods for analysis of simulation outputs [110]. I this research work, we use OPNET Modeler 15.0 [Figure D.1].

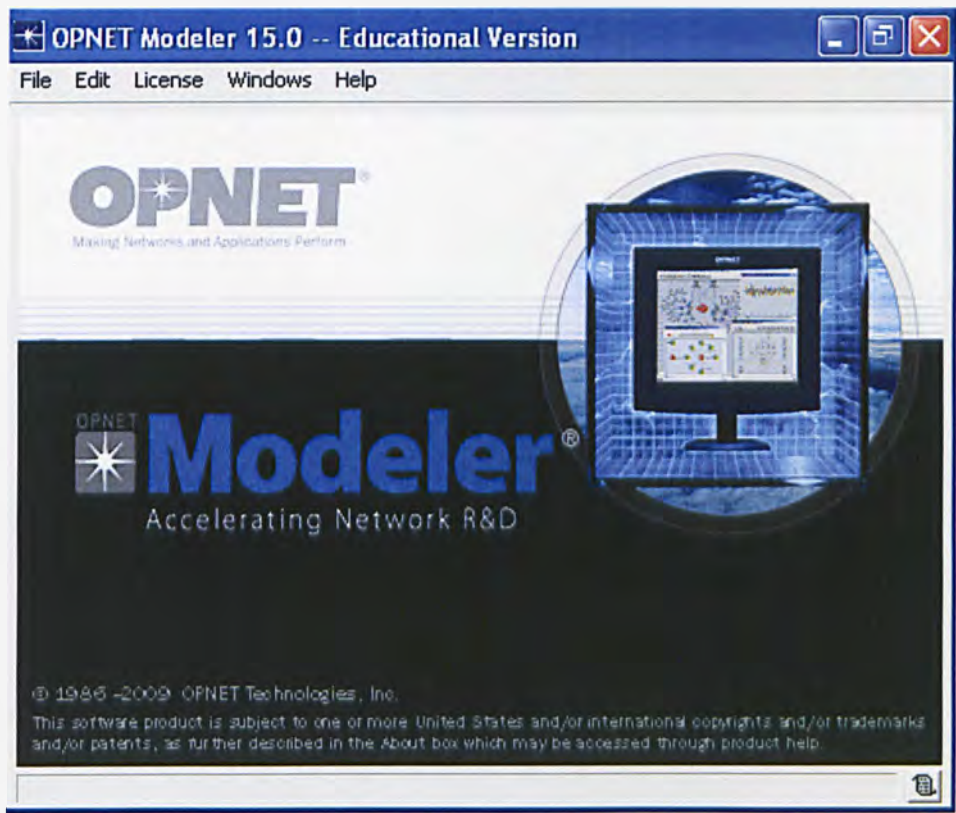


Figure D. 1 OPNET Modeler 15.0 start up

OPNET allows simulating a project with multiple scenarios and topology which is useful to compare the outputs of different scenarios with each other [110]. OPNET is a comprehensive simulation tools that benefits from a proper graphic user interface (GUI), a large library of network elements and protocols, source code of most of

network models and protocols, and proper tools for result analysis and presentation; therefore a complex network scenario with different hierarchical layers can be modeled efficiently [110, 111]. OPNET uses the discrete-event simulation approach to support realistic modeling of complex systems. In this approach, the system includes a sequence of events that each event can change the states in the system [111].